

ASTARTE

Assessment, Strategy And Risk Reduction for Tsunamis in Europe

Grant Agreement no: 603839
 Organisation name of lead contractor: IPMA
 Coordinator: Maria Ana Baptista

Deliverable 2.9

Recurrence rate of tsunamis of earthquake, volcanic and landslide origin

Due date of deliverable:	M14
Actual submission date:	M14
Start date of the project:	11/2013
Duration:	36 months

Work Package:	2 “Long Term Recurrence of Tsunamis”
Lead beneficiary of this deliverable:	FFCUL
Author(s):	Luis Matias
Revision:	V3

Project co-funded by the European Commission within the Seventh Framework Programme (2007-2013)	
Dissemination Level	
PU Public	X
PP Restricted to other programme participants (including the Commission Services)	
RE Restricted to a group specified by the consortium (including the Commission Services)	
CO Confidential, only for members of the consortium (including the Commission Services)	

TABLE OF CONTENTS

Executive summary	3
Document information	4
List of figures and tables	5
Abbreviations and Acronyms	7
CHAPTER 1: INTRODUCTION	8
CHAPTER 2: THE EARTHQUAKE CATALOGUE AND ZONATION	8
2.1 Tsunamis caused by earthquakes in the ASTARTE region	8
2.2 Building the ASTARTE working catalogue for earthquakes	9
2.3 Tsunamigenic earthquake zonation	9
CHAPTER 3: EARTHQUAKE ZONE PROPERTIES	11
3.1 Basic information	11
3.2 Division in sub-catalogues and completeness	12
3.3 Earthquake recurrence parameters for each zone	14
3.3.1. Methodology	14
3.3.2. Recurrence model parameters	17
3.3.3. Relationship with plate kinematics	23
CHAPTER 4: PROBABILITY OF A TSUNAMI CAUSED BY AN EARTHQUAKE	24
4.1 Earthquake frequency	24
4.2 Tsunami frequency	26
4.3 Consistency of information sources	29
CHAPTER 5: PROBABILITY OF A TSUNAMI CAUSED BY A VOLCANIC ERUPTION	29
CHAPTER 6: PROBABILITY OF A TSUNAMI CAUSED BY MASS MOVEMENT	30
CHAPTER 7: RECURRENCE OF TSUNAMI IMPACT	32
REFERENCES	33
Annex 1 – CUMULATIVE NUMBER OF EARTHQUAKES AND COMPLETENESS MAGNITUDE	
Annex 2 – RECURRENCE MODELS	
Annex 3 - TSUNAMI INTENSITY SCALES	

EXECUTIVE SUMMARY

This deliverable provides the initial support for the Probabilistic Tsunami Hazard Assessment studies where earthquake, volcanic and landslide sources are considered. For the earthquake tsunami sources we built upon the work by Sorensen et al. (2012) using the most updated version of earthquake and tsunami catalogues. The reference catalogue for tsunamis of all sources was the TRANSFER catalogue (Gallazzi et al., 2010).

As regards earthquake generation, we split the overall catalogue into two main periods, one defined as historical and the other as instrumental. The instrumental catalogue was further split into two catalogues with different completeness magnitudes to consider the evolution of the seismic network since 1900. To derive the earthquake recurrence distribution we used the HA2 algorithm (Kijko and Sellevoll, 1992) that combines in a Bayesian approach all information provided in the historical and instrumental catalogues. The maximum magnitude for each source zone in the Mediterranean was taken from Sorensen et al. (2012) and two new generation zones were added for the North-Eastern Atlantic, modified after Omira et al. (2014). For quality control the earthquake recurrence models were converted to kinematic velocities using a very simple single fault model.

The analysis of the TRANSFER tsunami catalogue with earthquake sources suggests that it is complete since 1700. Then we can infer that the ASTARTE study area (North-Eastern Atlantic, Mediterranean and Connected Seas) is affected by one tsunami caused by an earthquake every 2 years. Assuming that the tsunami catalogue is complete then we obtained the probability that an earthquake with a given magnitude can generate a tsunami of any amplitude.

The investigation of tsunami caused by volcanic eruptions relied on the TRANSFER catalogue information. Assuming that it is complete since year 1700 we can infer that the ASTARTE region is affected by one tsunami caused by a volcanic eruption every 34.5 years with intensity ≥ 2 in the Ambraseys (1962) scale. Applying the same procedure to tsunamis caused by some type of mass movement (coastal, submarine, rock-fall) we estimated the completeness year as 1900. Disregarding the trans-oceanic event of Grand Banks in 1929 we can infer that, on average, the ASTARTE region is affected by one tsunami generated by mass movement every 19 years with intensity ≥ 2 in the Ambraseys (1962) scale.

Considering all tsunami sources in the TRANSFER catalogue, we estimate that a damaging tsunami (intensity equal or greater than 6 in the Papadopoulos & Imamura, 2001, scale) may occur on average once every 12.6 years.

DOCUMENT INFORMATION

Project Number	FP7 - 603839	Acronym	ASTARTE
Full Title	Assessment, Strategy And Risk Reduction for Tsunamis in Europe		
Project URL	http://www.astarte-project.eu/		
Document URL			
EU Project Officer	Denis Peter		

Deliverable	Number	D2.9	Title	Recurrence rate of tsunamis of earthquake, volcanic and landslide origin
Work Package	Number	WP2	Title	Long Term Recurrence of Tsunamis

Date of Delivery	Contractual	M14	Actual	M14
Status	version 3.0		final <input type="checkbox"/>	
Nature	prototype <input type="checkbox"/> report <input checked="" type="checkbox"/> dissemination <input type="checkbox"/>			
Dissemination level	public <input checked="" type="checkbox"/> consortium <input type="checkbox"/>			

Authors (Partner)	Luis Matias (FFCUL)			
Responsible Author	Name	Luis Matias	E-mail	lmatias@fc.ul.pt
	Partner	FFCUL	Phone	+351-217500812

Abstract (for dissemination)	
Keywords	

Version Log

Issue Date	Rev. No.	Author	Change
1/12/2014	1.0	Luis Matias	First Version
13/12/2014	2.0	Luis Matias	Volcanic and Mass movement sources included. Recurrence of tsunami impact estimated.
31/12/2014	3.0	Luis Matias	Final version. Minor typing errors corrected.

LIST OF FIGURES AND TABLES

Figure 1: Location of all tsunamis caused by an earthquake. Source: TRANSFER tsunami catalogue (Gallazzi et al., 2010).

Figure 2: The ASTARTE earthquake working catalogue with $M_w \geq 4.5$ events represented.

Figure 3: Tsunami generation source zones considered overlain on the seismicity map ($M > 4.5$ events).

Figure 4: Tsunami generation source zones considered overlain on the seismicity map converted to equivalent M_w on each cell.

Figure 5: Tsunami generation source zones considered overlain on the TRANSFER catalogue for earthquake generated events.

Figure 6: Cumulated number of events for the ASTARTE catalogue.

Figure 7: Cumulated number of events for the ASTARTE catalogue restricted to events inside the source zones considered.

Figure 8: Cumulated number of events for the ASTARTE catalogue restricted to events inside the source zones considered for $M > 4.0$.

Figure 9: Evolution of the completeness magnitude for the ASTARTE zones catalogue.

Figure 10: Analysis of completeness magnitude for zone 18 with a large number of events in the catalogue (top) and for zone 04 with a reduced number of events (bottom).

Figure 11: Illustration of the different types of information that are considered by the HA2 method. The magnitude uncertainty is considered Gaussian with standard deviation (in Omira et al., 2014, modified from Kijko & Sellevoll, 1992).

Figure 12: Graphical representation of the earthquake recurrence models analysed for each source zone: (i) the HA2 results, in red; (ii) the truncated Gutenberg-Richter law of Sorensen et al. (2012), in black; the truncated Gutenberg-Richter law derived from the HA2 parameters, in magenta.

Figure 13: Single fault model used to compare the earthquake recurrence models with plate kinematics constrains.

Figure 14: Frequency of earthquakes (per 100 years) computed from the whole 24 source zones.

Figure 15: Cumulated frequency of earthquakes (per 100 years) computed from the whole 24 source zones.

Figure 16: Cumulative number of tsunamis from the TRANSFER catalogue.

Figure 17: Comparison between the estimated cumulative number of earthquakes and the cumulative number of tsunamis from the TRANSFER catalogue.

Figure 18: Comparison between the estimated cumulative number of earthquakes and the cumulative number of tsunamis from the TRANSFER catalogue after distributing the events with missing magnitude.

Figure 19: Estimated probability that an earthquake with magnitude $\geq M$ may generate a tsunami in the ASTARTE region.

Figure 20: Location of tsunamis caused by a volcanic eruption. Source: TRANSFER tsunami catalogue (Gallazzi et al., 2010).

Figure 21: Location of tsunamis caused by any type of mass movement. Source: TRANSFER tsunami catalogue (Gallazzi et al., 2010).

Figure 22: Determination of completeness magnitude, all sources in the TRANSFER catalogue combined since 1700.

Figure 23: Fit of a truncated Gutenberg-Richter law to the TRANSFER tsunami catalogue, all sources considered since 1700.

Table 1: Basic information on the earthquake catalogue for each source zone.

Table 2: Earthquake recurrence derived for each source zone and its comparison with Sorensen et al. (2021).

Table 3: Simplified fault model and average slip rate.

Table 4: Simplified description of the tsunamis caused by volcanic eruptions according to the TRANSFER catalogue.

Table 5: Simplified description of the tsunamis caused by mass movements according to the TRANSFER catalogue.

Table 6: Equivalence between Tsunami Intensity scales

ABBREVIATIONS AND ACRONYMS

EMEC - Euro-Mediterranean Earthquake Catalogue (Grünthal et al., 2012).

G-R - Gutenberg-Richter law for the recurrence of earthquakes.

HA2 - Matlab implementation of the methodology developed by Andrezej Kijko (Kijko and Sellevoll, 1992; Kijko, 2004) to derive earthquake recurrence models from all types of catalogues using a Bayesian approach.

ICG/NEAMTWS - Intergovernmental Coordination Group for the Tsunami Early Warning and Mitigation System in the North-eastern Atlantic, the Mediterranean and connected seas.

ISC - International Seismological Centre

PSHA - Probabilistic Seismic Hazard Assessment

PTHA - Probabilistic Tsunami Hazard Assessment

TRANSFER - Tsunami Risk AND Strategies For the European Region, EU Project no. 037058 (GOCE). It refers also the short name for the tsunami catalogue that resulted from that project.

ZMAP - A software package to analyse seismicity (Wiemer and Wyss, 2000).

CHAPTER 1: INTRODUCTION

This deliverable is intended to provide the initial support for the Probabilistic Tsunami Hazard Assessment studies where earthquake, volcanic and landslide sources are to be considered. For the earthquake tsunami sources we will build on the work by Sorensen et al. (2012) using the most updated version of earthquake and tsunami catalogues. Our reference catalogue for tsunamis of all sources is the TRANSFER catalogue (Gallazzi et al., 2010). It will be used to make a preliminary assessment of the probability of tsunamis occurring from volcanic and landslide origin.

For this investigation we consider that the area of interest is comprised between 30° and 48° N in latitude, and between 37°W and 38°W in longitude (ASTARTE region).

CHAPTER 2: THE EARTHQUAKE CATALOGUE AND ZONATION

2.1 Tsunamis caused by earthquakes in the ASTARTE region

Since we are interested only in earthquakes that may generate tsunamis we have to restrict our investigation to the most active seismic areas in the ASTARTE region that are offshore but that also penetrate slightly inland. The tsunamigenic earthquake source zones will be designed according to the observed seismicity and to regional geology, following Sorensen et al. (2012). The outcome of this exercise must be compared to the TRANSFER tsunami catalogue (Gallazzi et al., 2010). For this reason, we begin by presenting a brief summary of the TRANSFER catalogue contents.

The TRANSFER catalogue contains 244 tsunamis that are attributed to earthquakes (both local and regional). 8 events are attributed to local and basin wide landslides, while 13 are attributed to a volcanic source. 8 events are catalogued with a unidentified source. The first tsunami reported with an earthquake origin is the 1365 BC Levantine event. The most recent entry is the Boumerdes tsunami in 2003 that caused damaging waves in the Balearic Islands and Southern France (Figure 1).

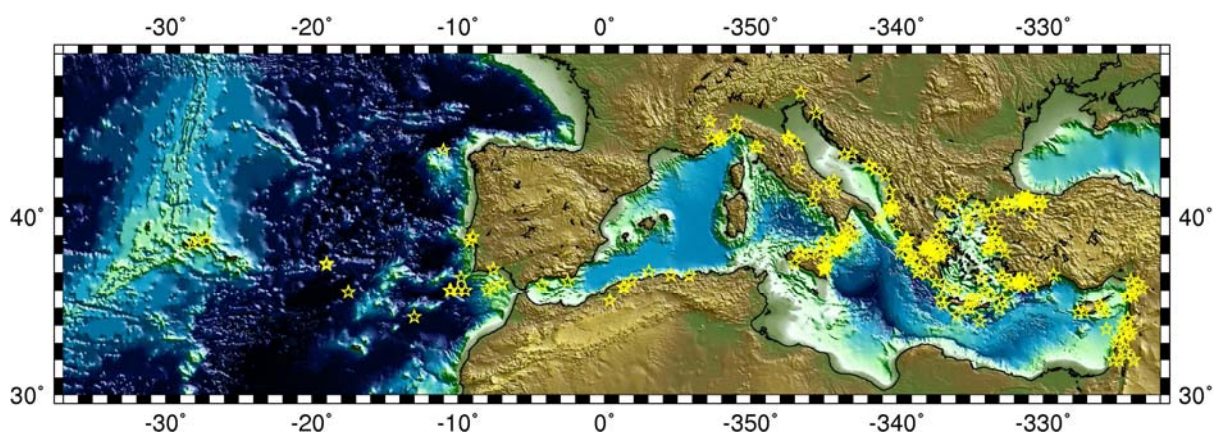


Figure 1: Location of all tsunamis caused by an earthquake. Source: TRANSFER tsunami catalogue (Gallazzi et al., 2010).

2.2 Building the ASTARTE working catalogue for earthquakes

The Euro-Mediterranean Earthquake Catalogue (EMEC, Grünthal et al., 2012) is a compilation of nearly 80 catalogues and over 100 special studies. Fake and duplicate events were identified and removed and a prioritization was considered inside each region. The catalogue spans from the year 1000 to the end of 2006 and comprises a total of 35,802 events with $M_w \geq 3.5$ inside the area of interest. EMEC catalogue entries for each event include the date, time, location (also focal depth if available), intensity I_0 (if given in the original catalogue), magnitude M_w (with uncertainty when given), and source (catalogue or special study). The moment magnitude was computed for all events using the methodology described in Grünthal et al., 2012. The fact that the catalogue is homogeneous in the study area makes it ideal for Probabilistic Tsunami Hazard Assessment studies.

To complete the EMEC up to 2014 we assessed the ISC bulletin online (ISC, 2012) and extracted all events inside the area of interest with a magnitude larger than 3.0. The ISC bulletin is a compilation of many contributor agencies that report very different locations and magnitudes for the same event. We accepted the main location as provided by ISC and made a multi-step process to determine the moment magnitude for each event. For each magnitude type published (including M_w) we took the first reference in the catalogue. Next, we ordered the available magnitudes by type, giving M_w and M_s the highest priority, followed by m_b , M_L and other less common magnitude types. Finally, if M_w was not available, we converted the highest priority magnitude value to M_w using the empirical relationships determined by Shapira (2007) for the ISC catalogue. In the end, when a M_w magnitude was available, we selected all events with $M_w \geq 3.5$. We obtained 16,039 earthquakes from 2007 to the end of October 2014.

Joining both catalogues, we obtained the ASTARTE working catalogue of earthquake for $M_w \geq 3.5$ with 51,839 events. Since it is considered that earthquakes with focal depth larger than 100 km are not likely to generate tsunamis (see the decision matrix established by the ICG/NEAMTWS, 2011), this catalogue was further restricted to hypocenters shallower than 100 km, resulting in 49,688 events (Figure 2).

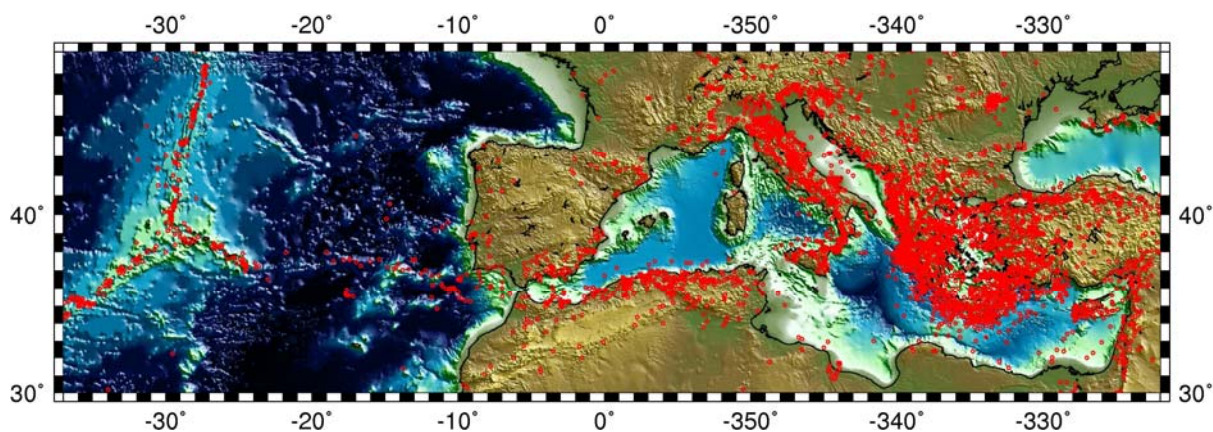


Figure 2: The ASTARTE earthquake working catalogue with $M_w \geq 4.5$ events represented.

2.3 Tsunamigenic earthquake zonation

We follow Sorensen et al. (2012) in attributing to the seismicity the main criteria for defining the zonation for the tsunamigenic earthquakes. *"These sources are chosen to be small enough to represent regions of relatively homogeneous earthquake activity rates and faulting regimes while at*

the same time being sufficiently large that the earthquake catalogue contains enough events within each zone to perform a stable statistical analysis for the source zone characteristics."

The zonation presented by these authors clearly considers also the regional geologic framework and we adopt it for the whole Mediterranean area, comprising 21 different zones. For the North-East Atlantic we consider that the main tsunami sources can be included in two additional zones, one for the South-west Iberia and another one for the Gloria Fault. Figure 3 shows the contours of the zones considered, overlain on the seismicity map.

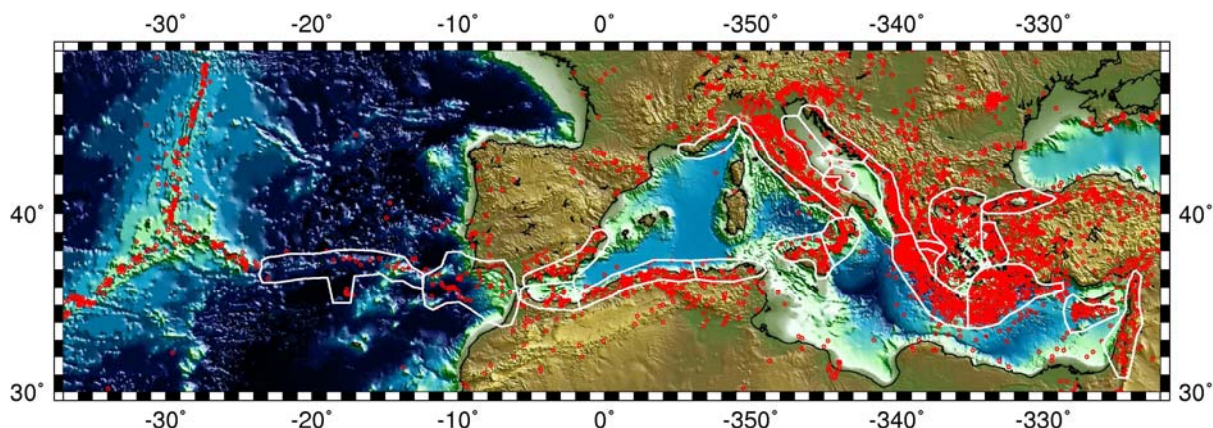


Figure 3: Tsunami generation source zones considered overlain on the seismicity map ($M > 4.5$ events).

To have a better image of the seismic energy release, we computed on each grid cell the total seismic moment released as given by the working catalogue and then converted it to moment magnitude. This map is shown in Figure 4 with the seismic zonation overlain.

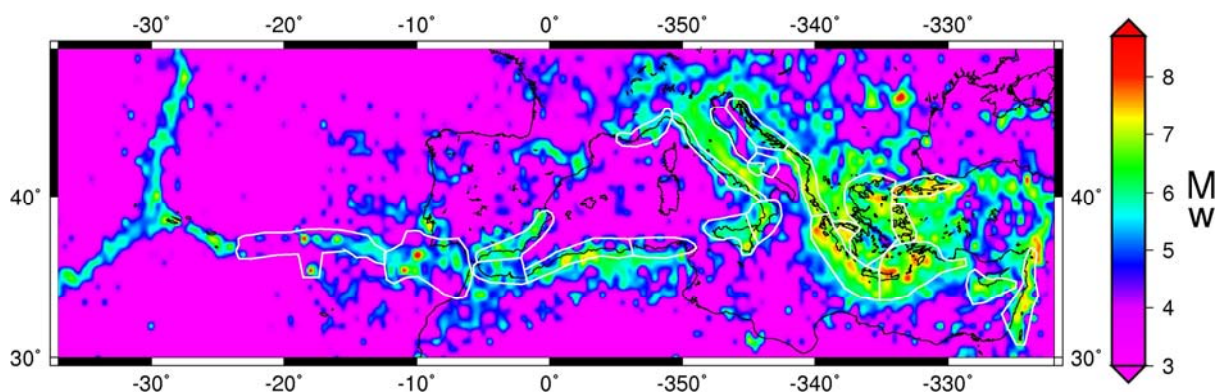


Figure 4: Tsunami generation source zones considered overlain on the seismicity map converted to equivalent M_w on each cell.

Finally we check if the zonation proposed includes all the tsunamis generated by earthquakes that are given in the TRANSFER catalogue (Figure 5).

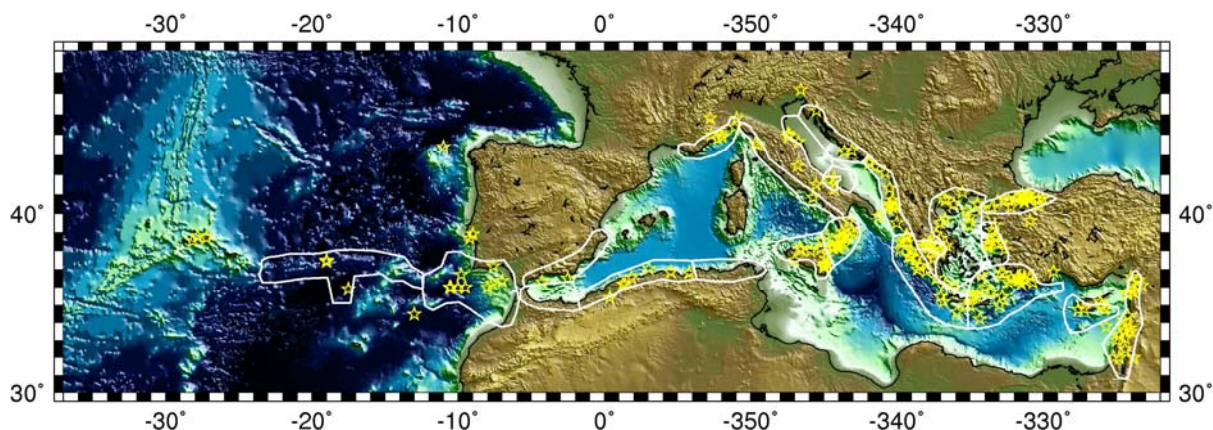


Figure 5: Tsunami generation source zones considered overlain on the TRANSFER catalogue for earthquake generated events.

Looking into Figure 5 we note that several tsunami events were left out in the seismic zonation. In the NE Atlantic our zonation does not include:

- The Galicia tsunami (16/11/1755). It is supported by historical evidence (Baptista et al., 2009) but there is no relevant seismic activity connected to the source area.
- Two tsunamis occurring in the Tagus River close to Lisbon (ibid.). These are in-land events.
- The Coral patch tsunami (31/3/1761). It is very close to one of the source zones considered.
- Four tsunamis in the Azores archipelago (9/7/1757, 26/7/1691, 2/6/1800 and 1/1/1980). We consider that the Azores archipelago cannot generate basin-wide tsunamis, following the methodology of Omira et al. (2004) to make a PTHA for the NE Atlantic. $M=7.2$

In the Mediterranean, the zonation proposed by Sorensen et al. (2012) and followed here only leaves out a set of tsunami events in the TRANSFER catalogue that are very close to some zone considered. Since the zones proposed are consistent with the known seismicity, we did not find necessary to change the initial zonation to include these events¹.

CHAPTER 3: EARTHQUAKE ZONE PROPERTIES

3.1 Basic information

Our first evaluation of the earthquake zonation considers a few basic parameters: number of events available, date of the first event reported, maximum magnitude present in each zone and its date. The results are shown in Table 1 that also defines the names used for each zone, which follow the ones proposed by Sorensen (2012) for the Mediterranean. In red we outline the values that differ more than 0.2 from those of Sorensen (2012) with the later values between (). We remark that most of the catalogue values obtained in this report are significantly different from the ones previously published.

¹ 1808-4-2 16:43 Liguria-Cote d'Azur, Flux and reflux at Marseilles, $I_{max}=8.0$, $M=5.7$
 1511-3-26 14:30 North Adriatic, Large sea level rise at Trieste, $I_{max}=9.0$, $M=6.5$
 1743-2-20 16:30, Apulia, Sea withdrawal in Brindisi, $I_{max}=9.5$, $M=6.9$
 1703-2-2 11:5, Latium, Sea withdrawal at the Tiber mouth, $I_{max}=10.0$, $M=6.7$
 1805-7-26 21: , Campania, Sea rise in the Gulf of Naples, $I_{max}=10.0$, $M=6.6$
 1928-5-2 21:54:32, North Aegean, $I_{max}=8$, $M=6.2$
 303-4-2, Levantine, $I_{max}=8.5$, $M=7.1$

Table 1: Basic information on the earthquake catalogue for each source zone.

N.	Name	N. of events	1st event	M _{max}	M _{max} date	N.	Name	N. of events	1st event	M _{max}	M _{max} date
1	Southeastern Spain	406	1-1-1048	6.8 (7.8)	9-10-1680	13	Western Albania	8758	1-1-1246	7.5 (7.0)	27-8-1886
2	Northern Morocco	314	21-10-1578	6.7	13-1-1804	14	Western Hellenic Arc	264	10-11-1002	7.4 (8.3)	18-5-1156
3	Northern Algeria	1551	3-1-1365	7.3	2-1-1867	15	Gulf of Corinth	455	6-3-1032	7.0	6-3-1032
4	Northern Tunisia	62	15-8-1182	6.3 (7.0)	23-2-1887	16	Aegean Sea	7330	8-8-1303	8.0 (7.5)	8-8-1303
5	Ligurian coast	208	27-1-1091	5.8 (6.3)	20-11-1836	17	Marmara Sea	1509	6-8-1383	7.1 (7.5)	14-2-1672
6	Western Italy	334	7-6-1125	7.4 (5.9)	11-1-1693	18	Western Anatolia	738	8-1-1010	7.5 (7.1)	23-9-1063
7	Sicily	284	24-5-1184	7.1 (7.4)	28-12-1908	19	Eastern Hellenic Arc	3279	1-1-1321	7.5 (8.0)	8-11-195
8	Calabria	107	1-9-1296	6.1 (7.2)	16-08-1916	20	Cyprus	1142	1-6-1402	7.0 (7.3)	1-6-1402
9	Eastern Italy	297	15-4-1178	6.5	6-6-1280	21	Dead Sea Fault area	524	1-1-1758	7.0 (7.5)	1-1-1758
10	Western Croatia	78	1-1-1223	6.7	30-7-1627	22	Southwest Iberia	717	1-1-1079	8.7	1-11-1755
11	Gargano, onshore	47	1-1-1414	5.8 (6.7)	1-1-1414	23	Gloria Fault	354	21-10-1930	8.3	25-11-1941
12	Gargano, offshore	1553	1-1-1153	7.0 (5.8)	5-2-1786						

3.2 Division in sub-catalogues and completeness

Earthquake catalogues can be divided between the historical and instrumental period. In the instrumental period we expect that a larger number of events is detected when a significant improvement of the seismic network is observed. The separation between historical and different instrumental periods is revealed by the plot of the cumulative number of events in the catalogue over time. We restrict this analysis to dates larger than year 1800. Figure 6 shows the evolution of the cumulative number of events for the full working catalogue, while Figure 7 shows an analogous plot restricted to the events inside the tsunamigenic source areas defined above.

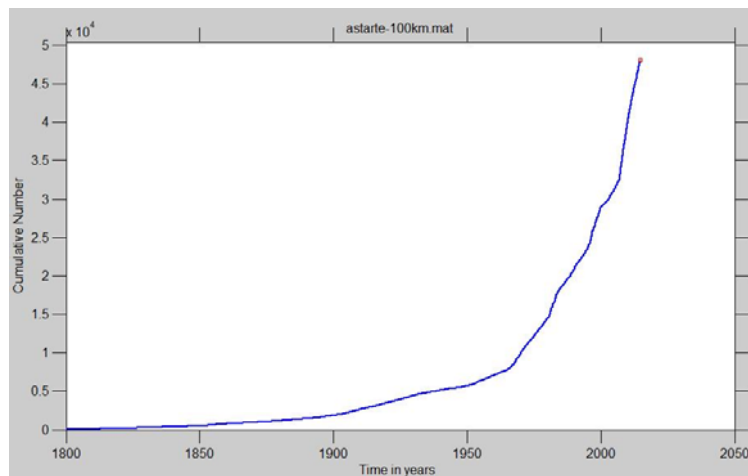


Figure 6: Cumulated number of events for the ASTARTE catalogue.

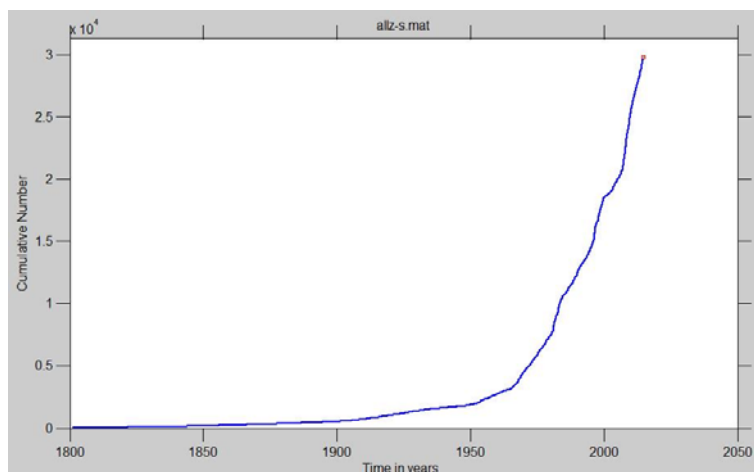


Figure 7: Cumulated number of events for the ASTARTE catalogue restricted to events inside the source zones considered.

Both plots show three kinks, marking significant changes in the catalogue. The kink at ~ 1900 is interpreted as the limit between the historical and instrumental periods. The kink at ~ 1960 marks a significant change to the seismic monitoring networks while the kink at 2007 marks the merge of the two catalogues used to build our working catalogue. The 2007 kink shows that the two catalogues are not consistent for magnitudes larger than 3.5. However, the 2007 kink disappears when we consider a larger magnitude threshold, $M \geq 4.0$ as shown in Figure 8.

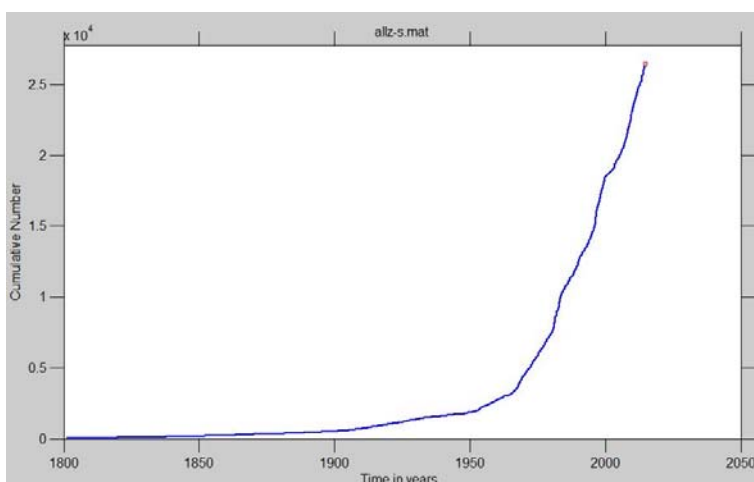


Figure 8: Cumulated number of events for the ASTARTE catalogue restricted to events inside the source zones considered for $M > 4.0$.

These considerations suggest that we may divide the working catalogue in 3 periods: (i) the historical catalogue up to 1900; (ii) the first instrumental catalogue, between 1900 and 1960; (iii) the second instrumental catalogue, after 1960.

Next, we used the ZMAP analysis tool (Wiemer and Wyss, 2000) to estimate the completeness magnitude over time. The result is shown in Figure 9. We note that during the historical period the completeness magnitude is consistently estimated to be ~ 6.1 , with a large uncertainty, between 1900 and 1960 it is ~ 4.8 and it is between 4.2 and 4.4 in the second instrumental period, after 1960. The completeness analysis confirms the proposition made before of splitting the whole catalogue into 3 periods, one historical and two instrumental.

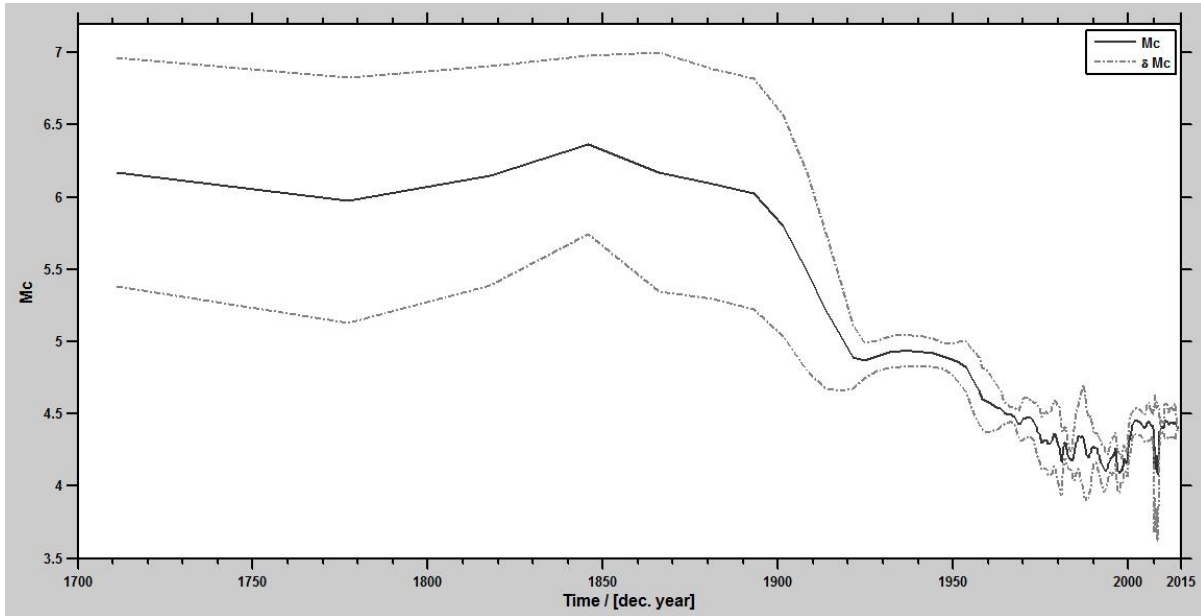


Figure 9: Evolution of the completeness magnitude for the ASTARTE zones catalogue.

The same analysis of the cumulative number of events and completeness magnitude over time was performed for each of the source zones considered. The full set of graphic results is provided in Annex-1. Some of the zones did not have a number of events allowing the evaluation of the completeness magnitude over time. For these zones we considered the full instrumental catalogue and estimated a single value for M_C . As an example, Figure 10 displays the results for a zone with a large number of events (Z19, Eastern Hellenic Arc) compared with a zone with only a few events (Z04, Northern Tunisia).

3.3 Earthquake recurrence parameters for each zone

3.3.1. Methodology

In Probabilistic Seismic and Tsunami Hazard Assessment (PSHA, PTHA) the earthquake generation in each source area considered is given by the function $\dot{N}(m)$, that is, the average number of earthquakes that are expected to occur every year with magnitude greater or equal to m . In time independent PSHA we assume that the occurrence of main shocks follow a Poisson distribution, that is, each event is independent from the previous ones. If m_{\min} is the minimum magnitude of interest, then the Poisson distribution will be completely characterized by the annual frequency of earthquakes with $m \geq m_{\min}$, $\lambda_{m_{\min}}$ or simply λ .

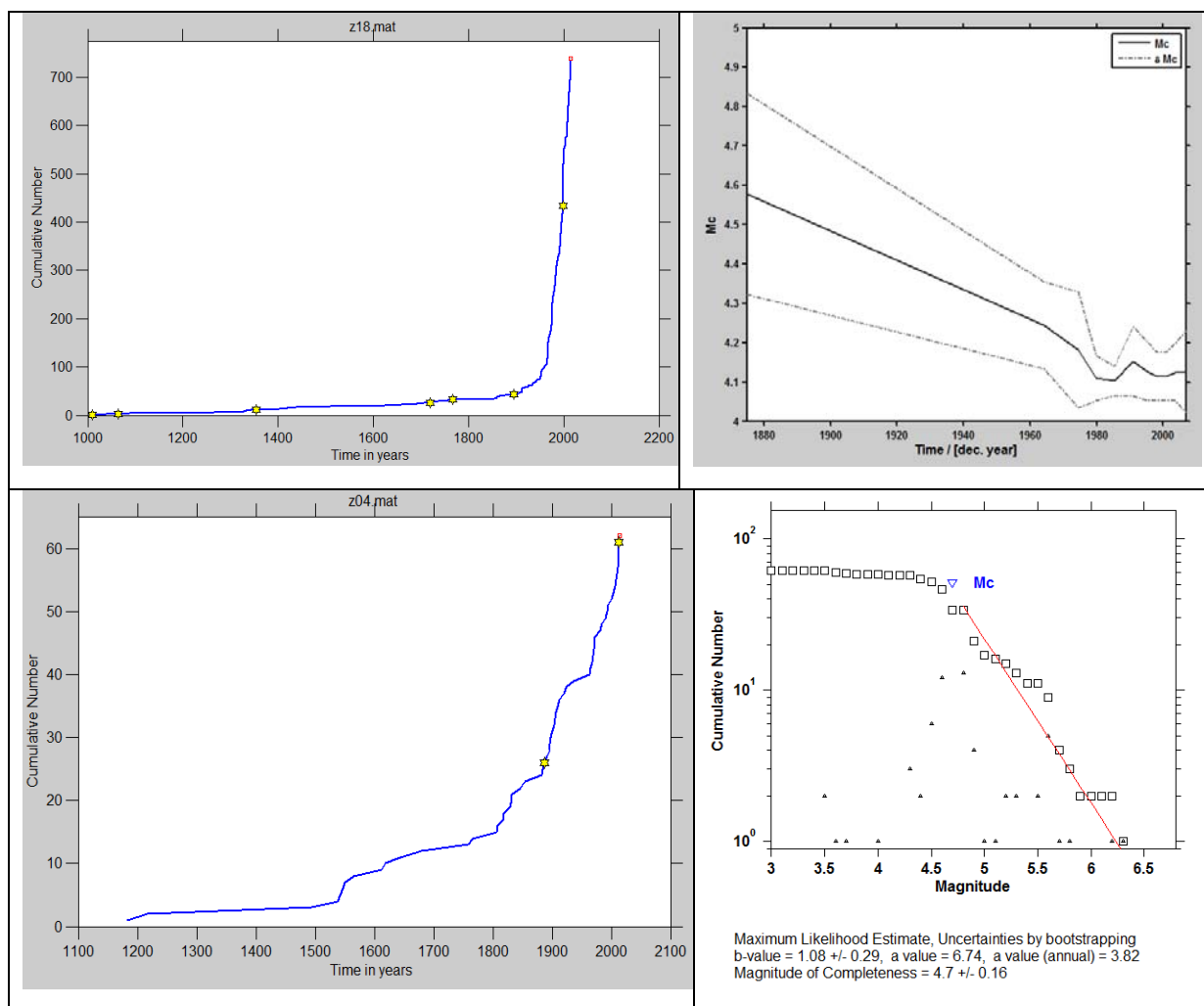


Figure 10: Analysis of completeness magnitude for zone 18 with a large number of events in the catalogue (top) and for zone 04 with a reduced number of events (bottom).

The next assumption we use in PSHA and PTHA is that the number of earthquakes with a given magnitude follows the truncated Gutenberg-Richter law, characterized by the distribution function given by the following equation:

$$F_M(m | m_{\min}, m_{\max}) = \begin{cases} 0 & m < m_{\min} \\ \frac{1 - \exp[-\beta(m - m_{\min})]}{1 - \exp[-\beta(m_{\max} - m_{\min})]}, & m_{\min} \leq m \leq m_{\max} \\ 1 & m > m_{\max} \end{cases}$$

This distribution has three free parameters, λ , m_{\min} and m_{\max} .

When $F_M(m | m_{\min}, m_{\max})$ and λ are known, then the average annual frequency of earthquakes with magnitude equal or larger to m , $\dot{N}(m)$, is given by the equation:

$$\dot{N}(m) = \lambda [1 - F_M(m | m_{\min}, m_{\max})]$$

In this work, we use the application HA2 built in Matlab by Andrezej Kijko (Kijko and Sellevoll, 1992; Kijko, 2004) to derive the three main parameters that characterize the generation of tsunamigenic earthquakes in the Caribbean region, λ , β and m_{\max} .

One of the main advantages of the HA2 method is that it combines, using maximum likelihood, many sorts of information in one go, paleo-seismic catalogues, where the time and magnitude are uncertain, historical catalogues that are not complete and have a large magnitude uncertainty, and instrumental catalogues with different completeness magnitudes, different periods and different magnitude uncertainties. In this report we only consider historical and instrumental catalogues (see figure 11).

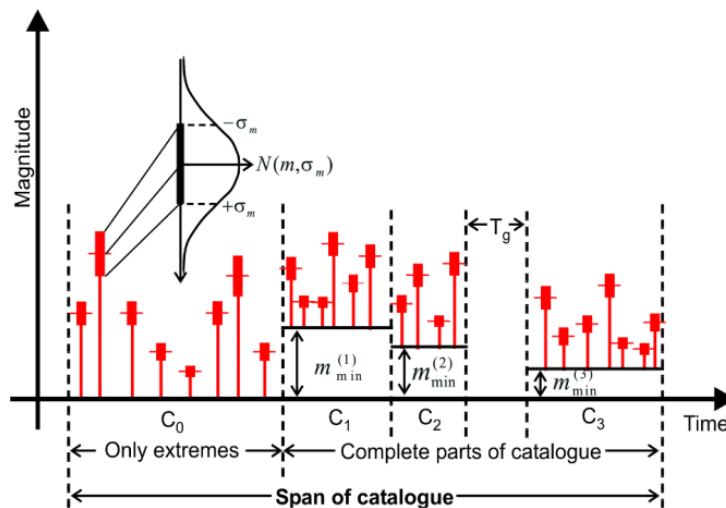


Figure 11: Illustration of the different types of information that are considered by the HA2 method.

The magnitude uncertainty is considered Gaussian with standard deviation σ_m (in Omira et al., 2014, modified from Kijko & Sellevoll, 1992).

For each instrumental period m_{\min} is simply the completeness magnitude derived from the catalogue. The magnitude uncertainty is considered to follow a Gaussian distribution characterized by the standard deviation σ_m , which is typical of each period (figure 11). The historical catalogue is not considered complete but the HA2 method assumes that it reports the extreme events that occurred in the period of time since the last event. Each historical earthquake can have its own uncertainty in magnitude.

The HA2 method includes all uncertainties present in each catalogue in a Bayesian model. It applies a Poisson-Gamma distribution for the time occurrence of events, and an exponential-Gamma distribution for the magnitudes. The parameters λ and β are derived by maximum likelihood while m_{\max} is obtained by an iterative method. The maximum magnitude can also be imposed by geological or geodynamic constrains. Both approaches will be examined in this report.

The HA2 method has the advantage to incorporate possible variations in time with the earthquake frequency (parameter λ) and magnitude (parameter β) as long as these variations are random. This feature is particularly relevant for areas where the instrumental and historical catalogues are insufficient to characterize the occurrence of extreme events with very large return periods.

3.3.2. Recurrence model parameters

For each tsunamigenic source zone we seek to obtain the recurrence model parameters using the maximum earthquake information as possible. However, we find that the instrumental and historical catalogues are not always consistent and we remark some differences between the two instrumental catalogues considered. For this reason we apply the H2A methodology to four possible combinations that are identified by one letter that is appended to the code of the zone: (a) all three catalogues are considered; (b) only the two instrumental catalogues are used; (c) the instrumental catalogues are merged into a single one and the historical catalogue is also included; (d) only a single instrumental catalogue is used.

The recurrence model parameters derived are presented in Table-2 and compared with the ones derived by Sorensen et al. (2012) for the same source zones. The maximum magnitude for each zone is taken from this work and compared with the one estimated by the HA2 method. The maximum magnitude for zones Z22 (Southwest Iberia) and Z23 (Gloria Fault) are taken from Omira et al. (2014). All graphical results are given in Annex-2.

For the Gloria Fault source area, we have no historical information and instrumental catalogues are clearly incomplete and cannot help us to define an adequate G-R law for the earthquake generation. Instead, we use a semi-empirical approach where we fit a fracture zone typical scaling law (e.g. Wells and Coppersmith, 1994) to the known plate movement along the Gloria Fault (~ 5 mm/year, e.g. Fernandes et al., 2003). Imposing a maximum magnitude of 9.0 we can uniquely derive the parameters λ and β required.

Examining Table 2 we note that the HA2 method was successful in 21/23 of the zones. The two failures are a consequence of the reduced number of events present in the catalogues. On these 21 we were able to use the historical catalogue more than half of the time (12 zones). The other zones showed a very large inconsistency between the historical and instrumental periods, as evaluated by the HA2 method. In 5 zones it was preferable to use a single instrumental catalogue instead of the two initially proposed.

When we compare the results derived in this report with the ones presented before by Sorensen et al. (2012) we see a considerable discrepancy between the $\lambda(M=5)$ and β parameters. One of the reasons for this discrepancy lies in the fact that the HA2 method derives a statistical distribution for $\lambda(m)$ that is not forced to follow a truncated Gutenberg-Richter law as was done by Sorensen et al. (2012). The β value refers to the initial slope of the $\lambda(m)$ and does not reflect the full $\lambda(m)$ variation. A more realistic comparison is provided in Figure 12 where we plot the $\lambda(m)$ distribution derived by HA2 together with the linear truncated G-R law from the parameters estimated by HA2 and the truncated G-R law proposed by Sorensen et al. (2012).

Table 2: Earthquake recurrence derived for each source zone and its comparison with Sorensen et al. (2021).

N.	Name	K	$\beta \pm \sigma$	β^S	$\lambda(M=5) \pm \sigma$	λ^S	$M_{max} \pm \sigma$	M_{max}^{obs}	M_{max}^{HA2}	Notes
1	Southeastern Spain	b	3.45	1.89	0.261±0.050	0.23	8.0±0.4	6.10	6.4	Historical catalogue is not consistent with instrumental
2	Northern Morocco	b	3.45	2.46	0.155±0.029	0.12	7.5±1.8	6.4	8.1	Historical catalogue is not consistent with instrumental
3	Northern Algeria	b	2.79±0.09	2.42	1.26±0.23	0.82	8.0±0.4	7.1	7.4	Historical catalogue is not consistent with instrumental
4	Northern Tunisia	x	2.49±0.67	2.03	0.026	0.16	7.5	6.3	---	Reduced number of earthquakes in catalogue
5	Ligurian coast	a	3.45	2.16	0.114±0.012	0.06	7.5±0.3	5.8	5.8	Instrumental catalogues slightly inconsistent
6	Western Italy	b	3.45	2.23	0.326±0.066	0.17	7.5±0.5	6.3	6.8	Historical catalogue is not consistent with instrumental
7	Sicily	d	2.72±0.38	2.19	0.224±0.063	0.28	8.0	7.1	---	Very inconsistent instrumental and historical catalogues
8	Calabria	d	3.17±0.59	2.05	0.105±0.032	0.31	7.5±1.0	6.1	7.1	Very inconsistent instrumental and historical catalogues
9	Eastern Italy	d	2.57±0.42	3.11	0.171±0.50	0.10	7.5±0.4	6.1	6.4	Very inconsistent instrumental and historical catalogues
10	Western Croatia	a	1.81±0.23	1.73	0.097±0.024	0.21	7.5±0.3	6.7	6.8	
11	Gargano, onshore	c	2.57±0.36	2.69	0.030±0.009	0.12	7.5±0.3	5.8	5.9	Too few events. Only a single instrumental catalogue was possible
12	Gargano, offshore	c	2.76±0.11	2.23	0.874±0.120	0.04	7.5±0.3	7.0	7.1	Instrumental catalogues slightly inconsistent
13	Western Albania	a	3.45	1.93	8.392±1.052	1.45	7.5±0.3	7.5	7.6	
14	Western Hellenic Arc	a	1.83±0.12	1.84	0.292±0.044	3.85	8.5±0.3	7.4	7.5	
15	Gulf of Corinth	a	2.62±0.13	1.70	0.391±0.068	0.51	7.5±0.3	7.0	7.1	
16	Aegean Sea	c	3.22±0.12	1.84	6.63±1.38	2.20	8.0±0.3	8.0	8.2	Single instrumental catalogue performs better
17	Marmara Sea	c	2.27±0.17	1.73	0.982±0.232	0.83	8.0±0.3	7.1	7.2	Single instrumental catalogue performs better
18	Western Anatolia	a	2.41±0.09	2.19	1.661±0.326	1.16	7.5±0.3	7.5	7.6	
19	Eastern Hellenic Arc	a	3.17±0.07	2.44	2.761±0.396	5.77	8.5±0.3	7.5	7.6	
20	Cyprus	a	2.70±0.09	1.98	1.278±0.219	0.22	7.5±0.3	7.0	7.1	
21	Dead Sea Fault area	d	3.18±0.41	1.66	0.203±0.057	0.28	8.0±0.3	5.8	5.9	Historical catalogue is not consistent with instrumental. Single instrumental catalogue performs better
22	Southwest Iberia	d	2.92±0.13	---	0.415±0.105	---	8.8	8.0	---	Historical catalogue is not consistent with instrumental. Single instrumental catalogue performs better. G-R dominated by a single large event
23	Gloria Fault	y	2.07		0.95		9.0	8.3	---	Computed using plate tectonics constraints

K - Methodology/set of catalogues used to derive the recurrence parameters

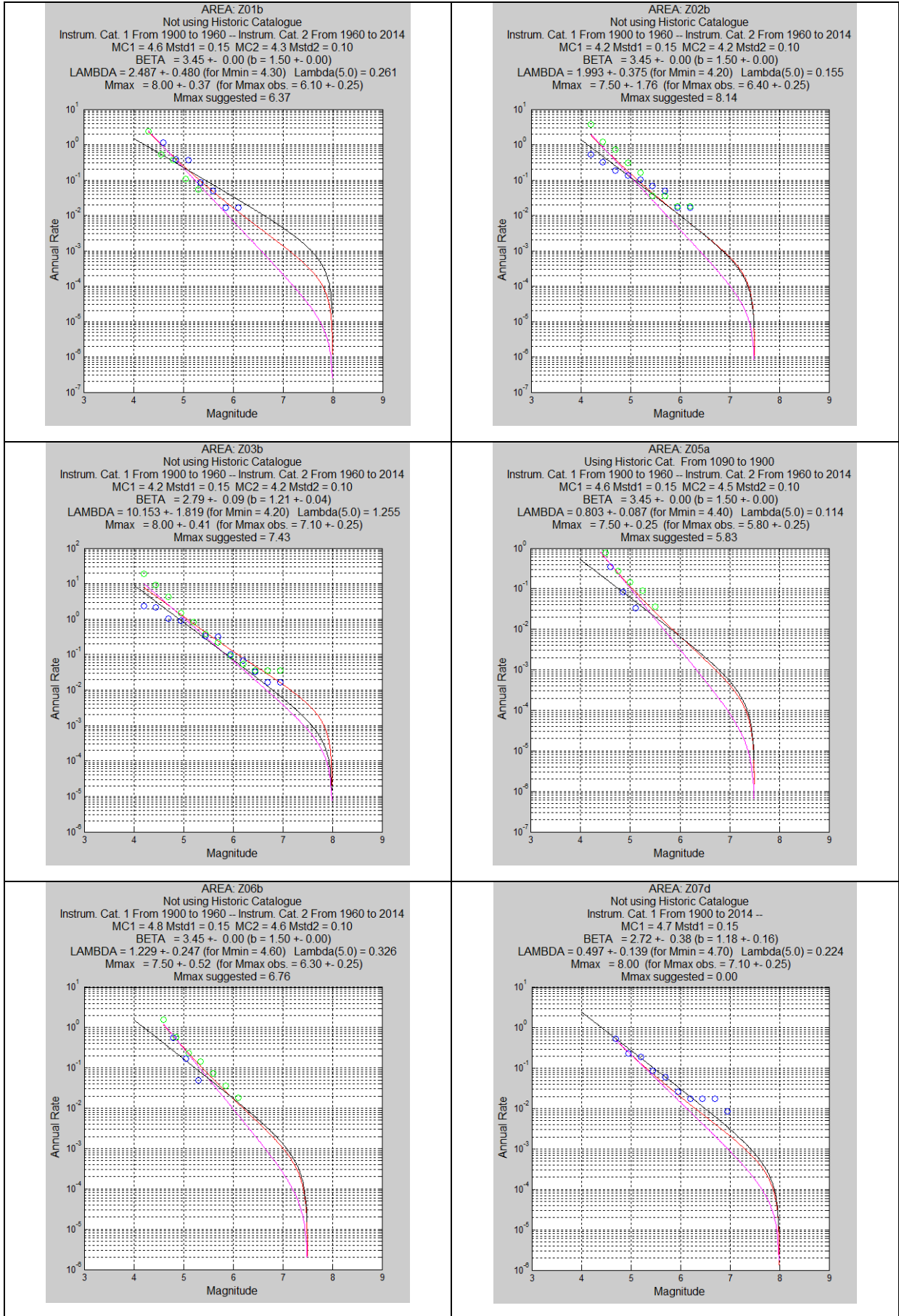
β^S, λ^S - Values by Sorensen et al., 2012

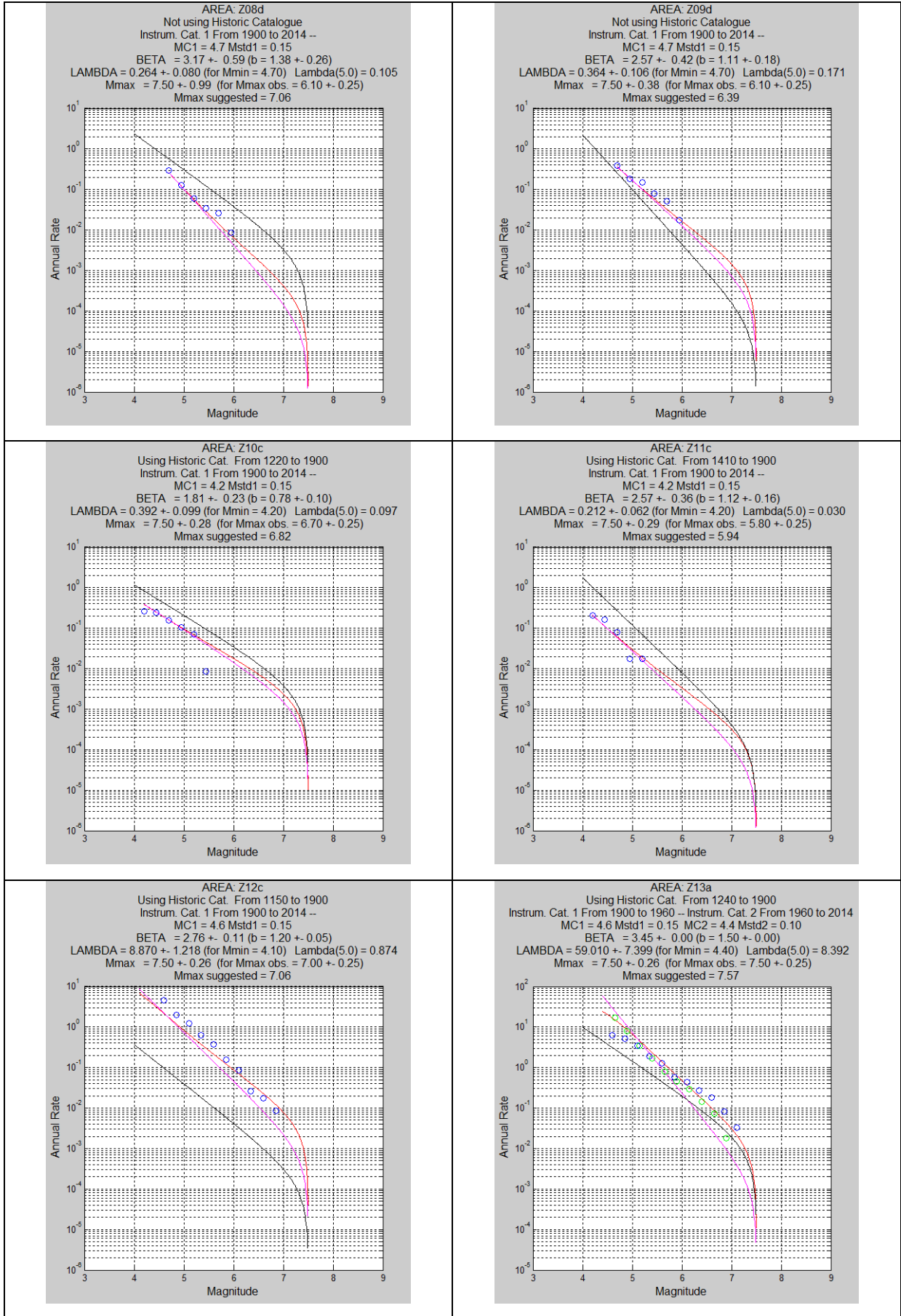
M_{max}^{HA2} - Maximum magnitude suggested by the HA2 method

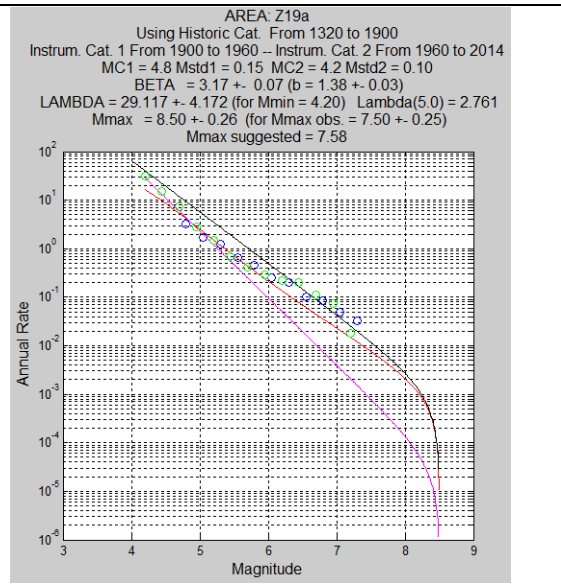
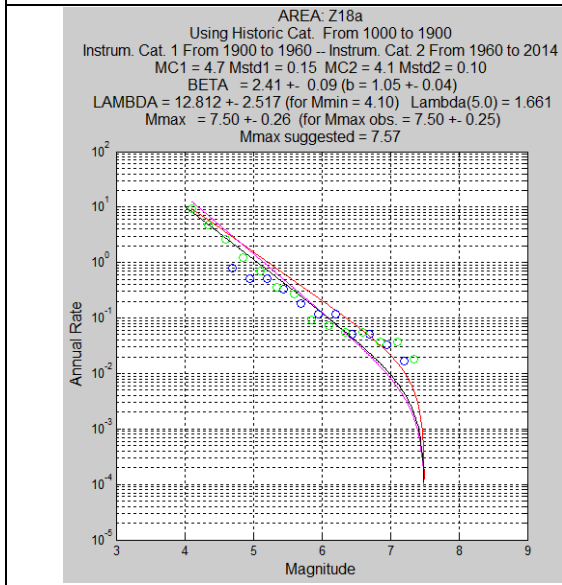
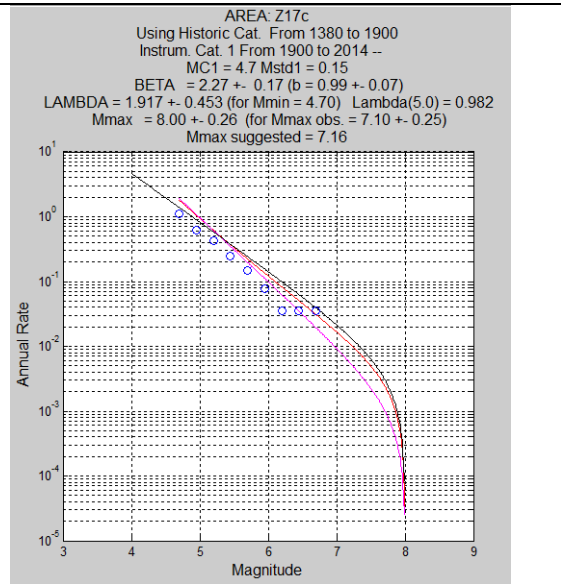
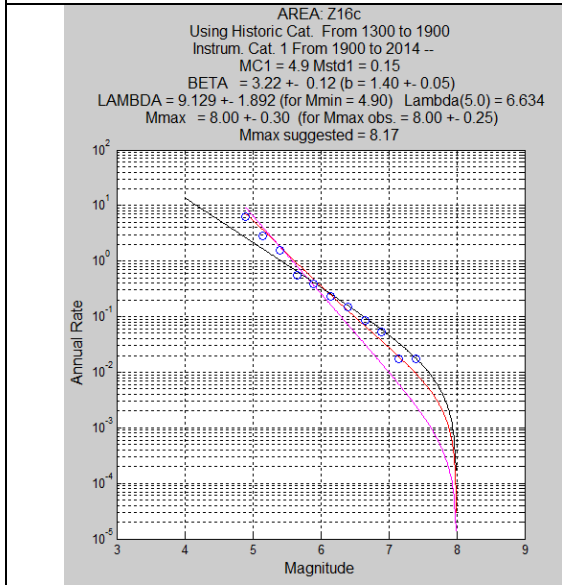
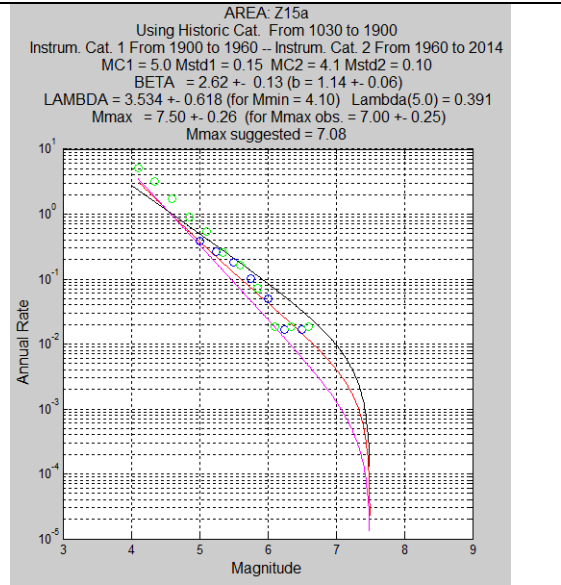
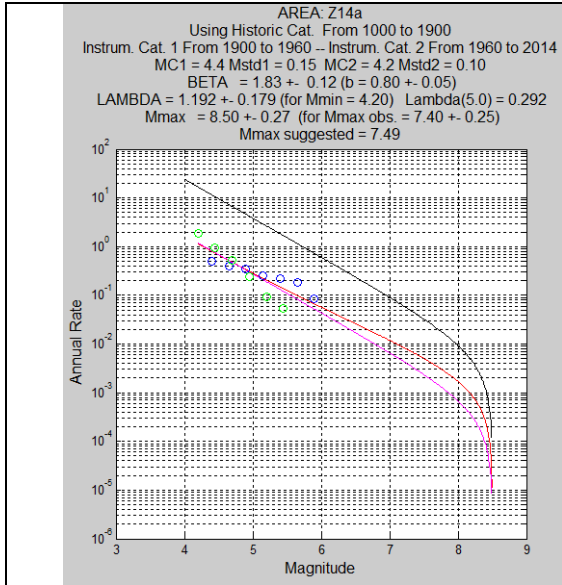
M_{max}^{obs} - Maximum magnitude observed in the used catalogues

x - Values computed from the completeness analysis

Y - Values derived from plate tectonic constraints. See text.







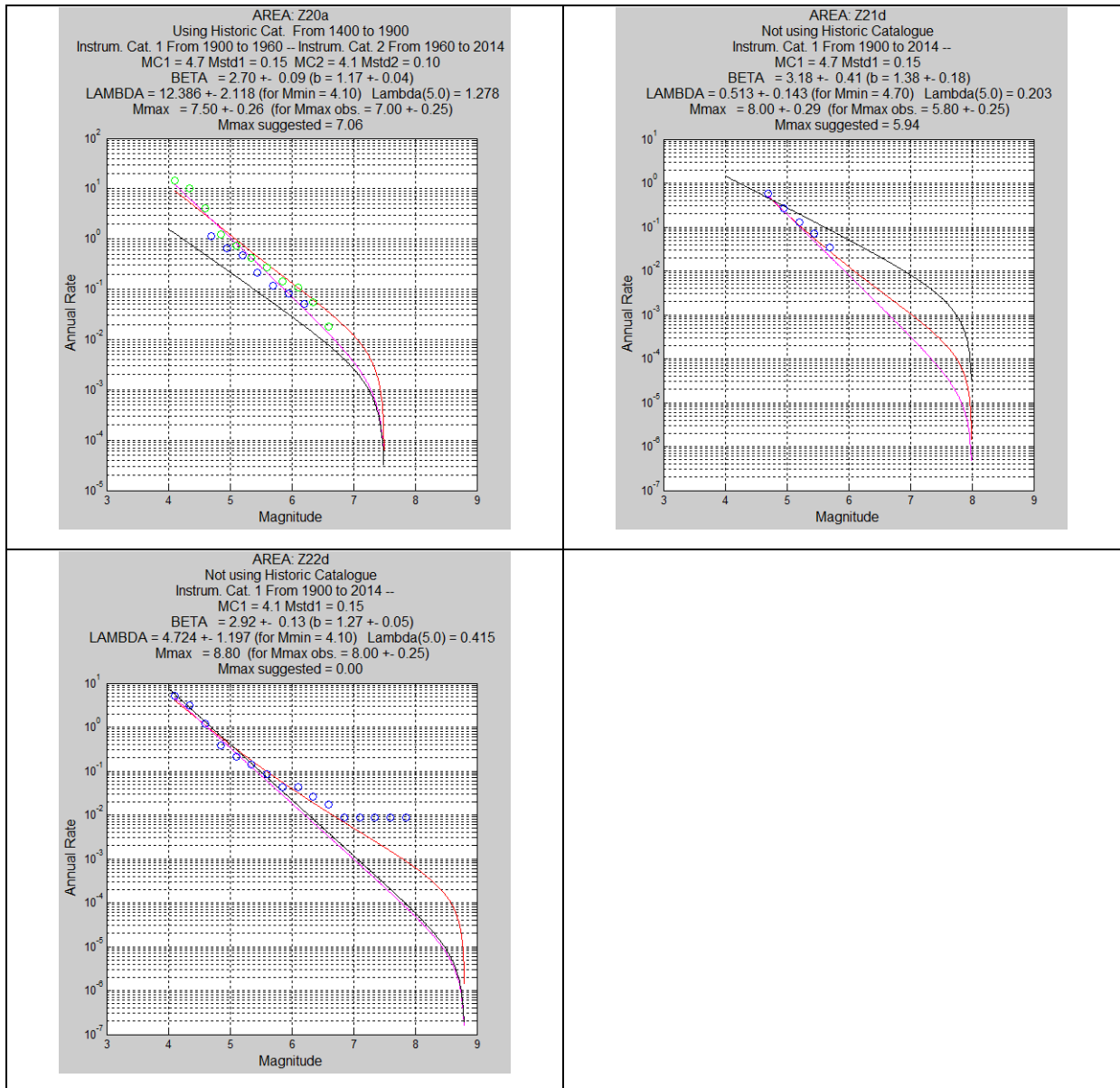


Figure 12 (this and previous pages): Graphical representation of the earthquake recurrence models analysed for each source zone: (i) the HA2 results, in red; (ii) the truncated Gutenberg-Richter law of Sorensen et al. (2012), in black; the truncated Gutenberg-Richter law derived from the HA2 parameters, in magenta.

Examining the earthquake recurrence laws presented in Figure 12 we remark that in general the HA2 method does not derive a simple truncated G-R law. In fact, we observe that the larger magnitudes have a larger frequency than would be expected from the extrapolation of the small magnitude tendency. This makes the HA2 results similar to the ones proposed by Sorensen et al. (2012) for the large magnitude earthquakes, but they necessarily differ for smaller magnitude events.

However, larger discrepancies between the two recurrence laws persist for many of the zones considered, despite the fact that the zones are identical and the earthquake catalogue is identical for its larger part. The major discrepancies are observed for zones Z08, Z09, Z12, Z13, Z14, Z20 and Z21. Looking into the earthquake frequencies presented in figure 12 we see that the HA2 results are

clearly consistent with the catalogues analysed and so the reason for these discrepancies remains unknown.

3.3.3. Relationship with plate kinematics

Given the very long recurrence of large events in the ASTARTE study area, the earthquake recurrence law has to be inferred from historical and instrumental catalogues which are either incomplete or do not cover a complete earthquake cycle. Since earthquake generation is driven by plate tectonics, it is desirable to compare the recurrence models with tectonic plate kinematics. This consistency test is often neglected in the applications of PSHA and PTHA with the consequence that the seismicity rate can be grossly overestimated or underestimated in some of the considered source zones.

To compare the magnitude frequency law derived in the previous section with the plate kinematic constrain, we will consider a very simple model in which all the seismic energy is released on a single fault with length L , width W (area A), dip α , slip angle λ (Figure 13). H is the lithosphere brittle thickness.

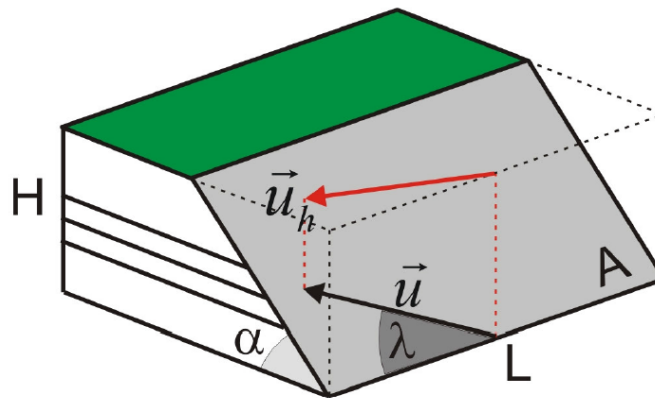


Figure 13: Single fault model used to compare the earthquake recurrence models with plate kinematics constrains.

Using this model, the average slip rate on the fault can be computed by summing the moment released by all possible earthquakes as

$$\Delta \dot{u} = F_1 \sum \frac{M_0}{\mu A T} = F_1 \sum \frac{M_0}{\mu L W T} = F_2 \sum \frac{M_0}{\mu L H T}$$

T is the total time-span considered while F_1 and F_2 are scaling factors that depend on the geometry of the fault and the slip angle. To simplify the computation we will assume that the representative fault in each zone will be a pure reverse fault, a pure normal fault or a pure strike-slip fault. For a pure dip-slip fault the scaling factor is given by $F_2 = \sin \alpha \cos \alpha$. For a strike-slip fault the scaling factor is unity.

To apply this simple model to the ASTARTE source areas we measure the representative length on a map and use the lithosphere brittle thickness proposed by Sorensen et al. (2012). From this work we take also the representative dip of the model fault. The shear modulus used is for most of the zones

one that is typical of continental crust. It is higher for zones Z22 and Z23 where old oceanic lithosphere is rupturing. The complete set of results is shown in Table 3.

Table 3: Simplified fault model and average slip rate

N.	Name	L (km)	H (km)	α	μ ($\times 10^{10}$ Pa)	$\Delta \dot{u}$ (mm/year)
1	Southeastern Spain	550	40	35°	4.0	0.19
2	Northern Morocco	310	25	30°	4.0	0.18
3	Northern Algeria	700	25	30°	4.0	2.15
4	Northern Tunisia	400	25	30°	4.0	0.03
5	Ligurian coast	350	10	25°	4.0	0.23
6	Western Italy	700	12	30°	4.0	0.27
7	Sicily	270	18	30°	4.0	1.12
8	Calabria	230	15	20°	4.0	0.18
9	Eastern Italy	330	8	30°	4.0	0.91
10	Western Croatia	400	22	15°	4.0	0.22
11	Gargano, onshore	60	25	90°	4.0	0.80
12	Gargano, offshore	130	25	90°	4.0	9.46
13	Western Albania	480	14	30°	4.0	9.95
14	Western Hellenic Arc	640	60	30°	4.0	1.93
15	Gulf of Corinth	160	31	28°	4.0	1.29
16	Aegean Sea	370	34	45°	4.0	7.09
17	Marmara Sea	350	20	90°	4.0	14.04
18	Western Anatolia	230	26	45°	4.0	6.53
19	Eastern Hellenic Arc	600	56	45°	4.0	3.92
20	Cyprus	320	30	45°	4.0	2.46
21	Dead Sea Fault area	650	16	90°	4.0	0.64
22	Southwest Iberia	490	60	35°	6.5	0.92
23	Gloria Fault	980	40	90°	6.5	5.00

Using this table as a diagnostic, we note that the earthquake recurrence models for zones 12, 13 and 18 may need a more detailed investigation, not done in this report. We also note that the average fault slip should reflect the plate kinematics constrain multiplied by a seismic coupling factor that is less than 1. We further notice that the ASTARTE zone catalogue is restricted to the tsunami generation zones and so additional seismic deformation must occur outside.

CHAPTER 4: PROBABILITY OF A TSUNAMI CAUSED BY AN EARTHQUAKE

4.1 Earthquake frequency

In the previous chapter we derived an earthquake recurrence model for each source zone that can be expressed as the number of earthquakes that may be expected to occur in a single zone belonging to a magnitude class. For the sake of investigating tsunamigenic earthquakes we will consider only events with magnitude larger than 5.0 and each magnitude class of width 0.2.

Summing the contribution of all 24 source zones we obtain the earthquake frequency presented in Figure 14, expressed as the number of earthquakes predicted in 100 year period. Figure 15 represents the same results expressed as the cumulative number of earthquakes, that is, the number of earthquakes occurring with a magnitude $\geq M$.

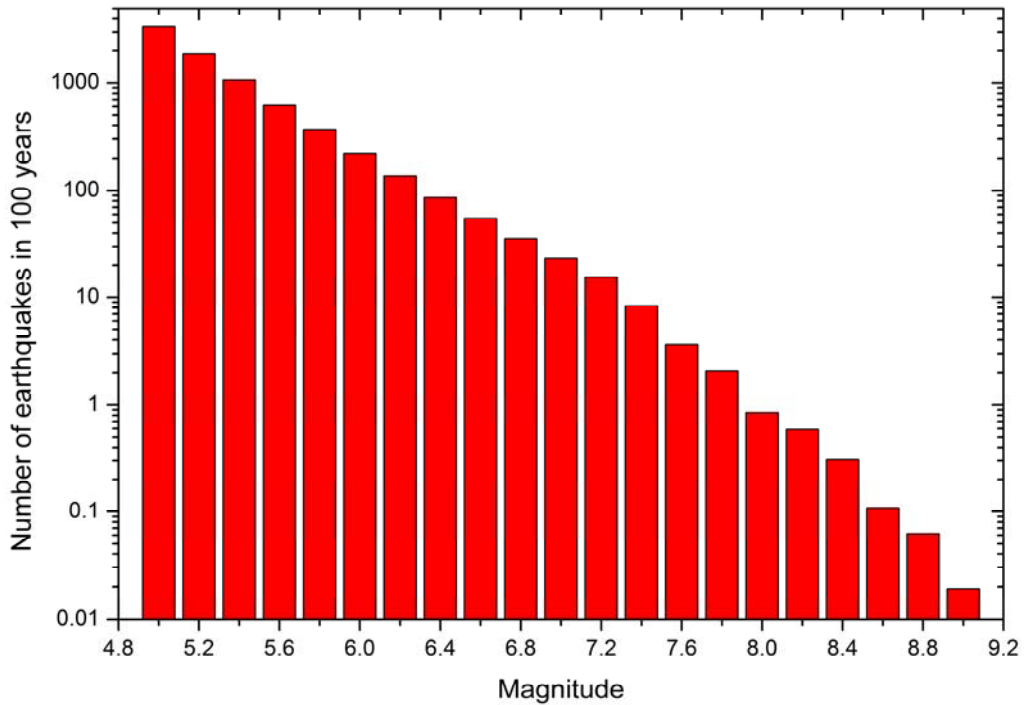


Figure 14: Frequency of earthquakes (per 100 years) computed from the whole 24 source zones.

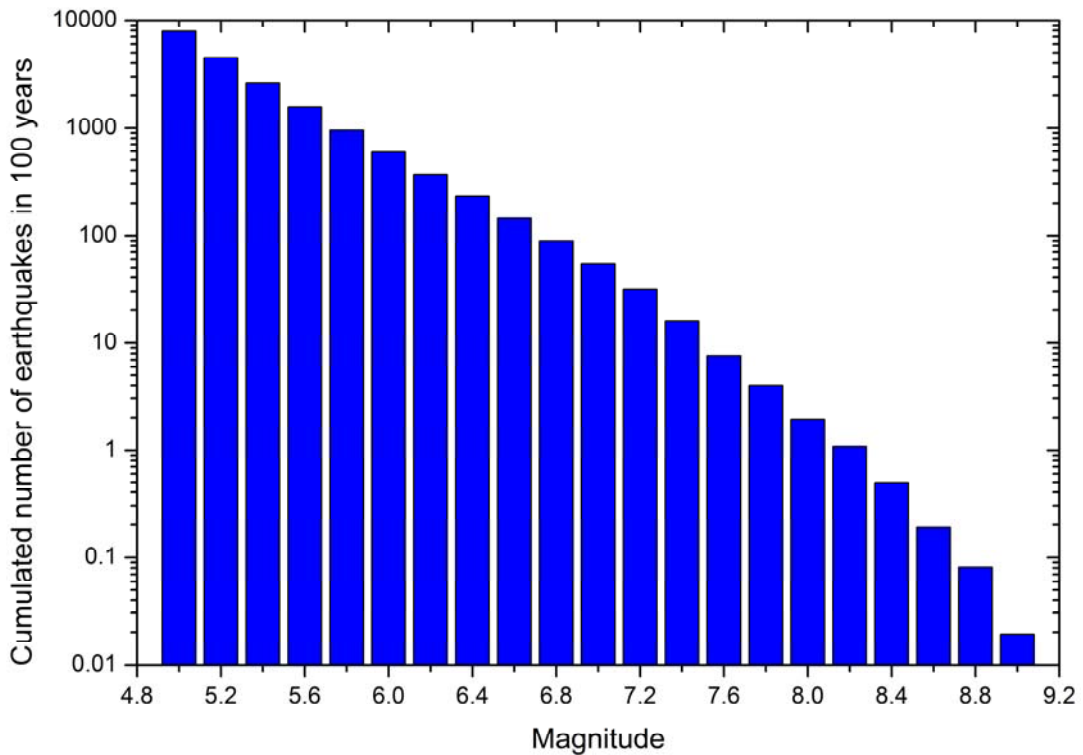


Figure 15: Cumulated frequency of earthquakes (per 100 years) computed from the whole 24 source zones.

We note that the frequency-magnitude relation expressed in Figures 14 and 15 resembles a G-R recurrence law with several slopes that result from the consideration of different maximum magnitudes on each source zone.

Since not all earthquakes in the source zones generate a tsunami we need to ascribe a probability that an event may cause a tsunami by comparing the earthquake recurrence model with the TRANSFER tsunami catalogue. This probability should be a function of the magnitude.

4.2 Tsunami frequency

The TRANSFER catalogue (Gallazzi et al., 2010) contains 274 tsunami events ascribed to an earthquake origin. Of these events, 188 have one magnitude value and the other 56 do not have a magnitude. Eight earthquake tsunamis have a magnitude smaller than 5.0. The smallest tsunami caused by an earthquake has $M=3.1$.

We begin by examining all tsunamis caused by an earthquake and plot the cumulative number of events in Figure 16. It is remarkable to verify that after 1700 we have a steady increase in the number of events which suggests that the tsunami catalogue may be complete after this year. The rate of tsunami events estimated from this plot is 0.50/year. Every two years we should expect a tsunami event caused by an earthquake of any magnitude in the ASTARTE region.

If we assume that the tsunami catalogue is complete from 1700 onwards, then we may use this information to find the frequency of tsunamigenic earthquake as a function of the magnitude. In this period we have 35 events without magnitude ascribed and 8 events with a magnitude smaller than 5.0. 116 events have a magnitude reported ≥ 5.0 .

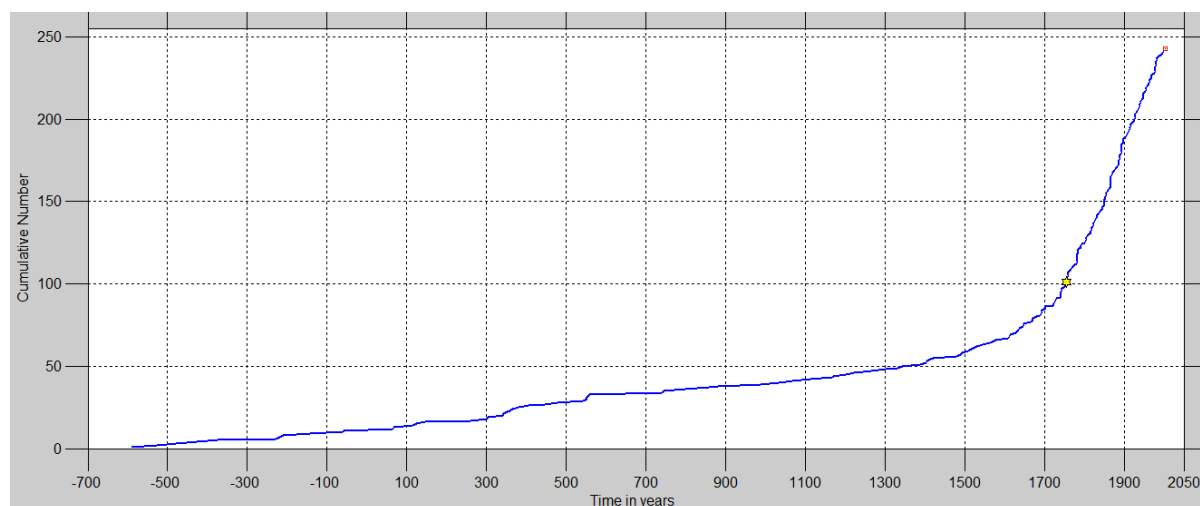


Figure 16: Cumulative number of tsunamis from the TRANSFER catalogue.

We may use the information on the complete period of the TRANSFER catalogue (1700 to 2014) to estimate the cumulative number of events and compare it to the earthquake generation model estimated before. This comparison is presented in Figure 17. Outside of this plot remain 8 events with a reported magnitude smaller than 5.0

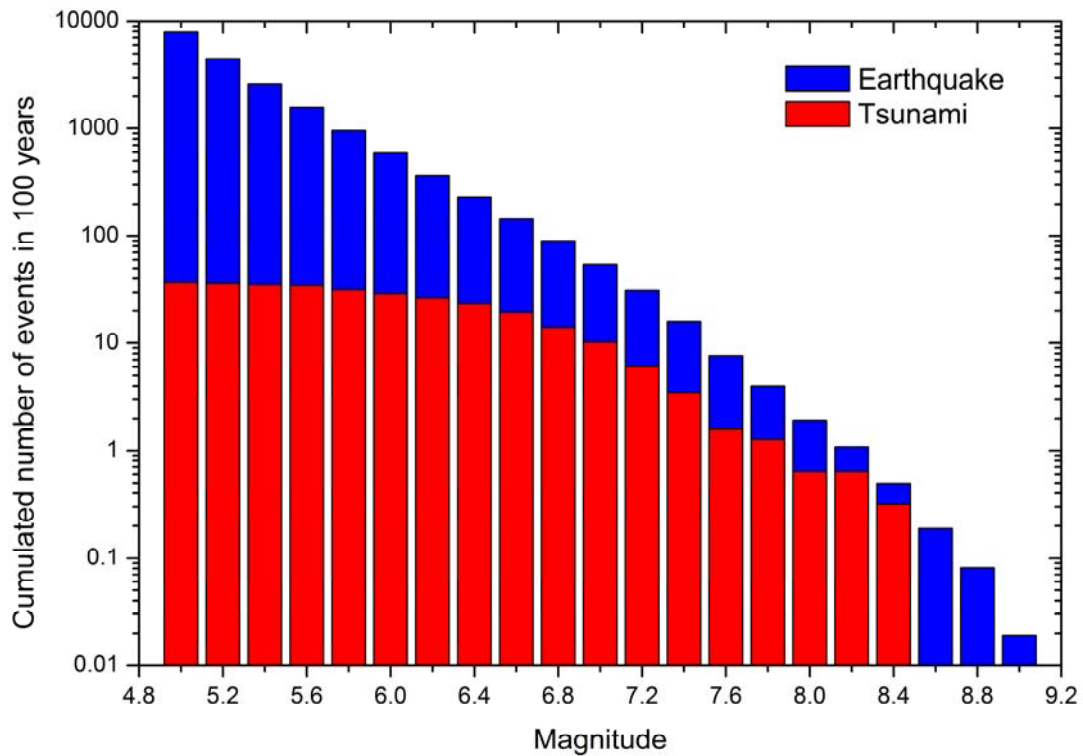


Figure 17: Comparison between the estimated cumulative number of earthquakes and the cumulative number of tsunamis from the TRANSFER catalogue.

Recalling that the TRANSFER catalogue also contains 35 events without a reported magnitude for the period 1700 to 2014, we may distribute these events according to the previous dataset and obtain a corrected plot presented in Figure 18. During this period we estimate that ~10 earthquakes with $M < 5.0$ may have generated a tsunami.

We remark a good agreement between the "causes", the earthquake generation, and the "consequences", the tsunami, as shown in Figure 18. Given that the very large magnitude earthquakes may generated with nearly 100% probability a tsunami, the slight disagreement in Figure 18 may reflect a small over-estimation of large magnitude earthquakes in our recurrence model.

Comparing the two cumulative frequencies, we may estimate the probability that an earthquake of magnitude $\geq M$ may generate a tsunami. The result of this computation is shown in Figure 19. By visually smoothing the trend we estimate that 70% of $M \geq 8.0$ earthquakes do generate a tsunami. This probability reduces to 25% for $M \geq 7.0$ and it reduces again to 7% for a $M \geq 6.0$ earthquake.

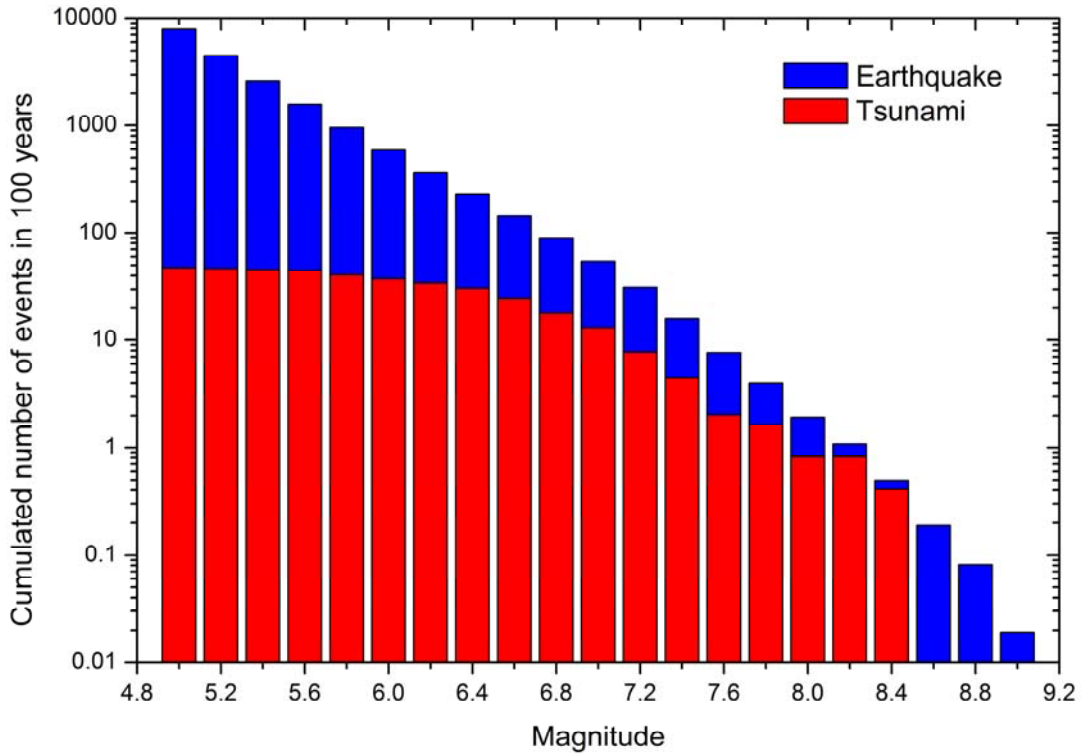


Figure 18: Comparison between the estimated cumulative number of earthquakes and the cumulative number of tsunamis from the TRANSFER catalogue after distributing the events with missing magnitude.

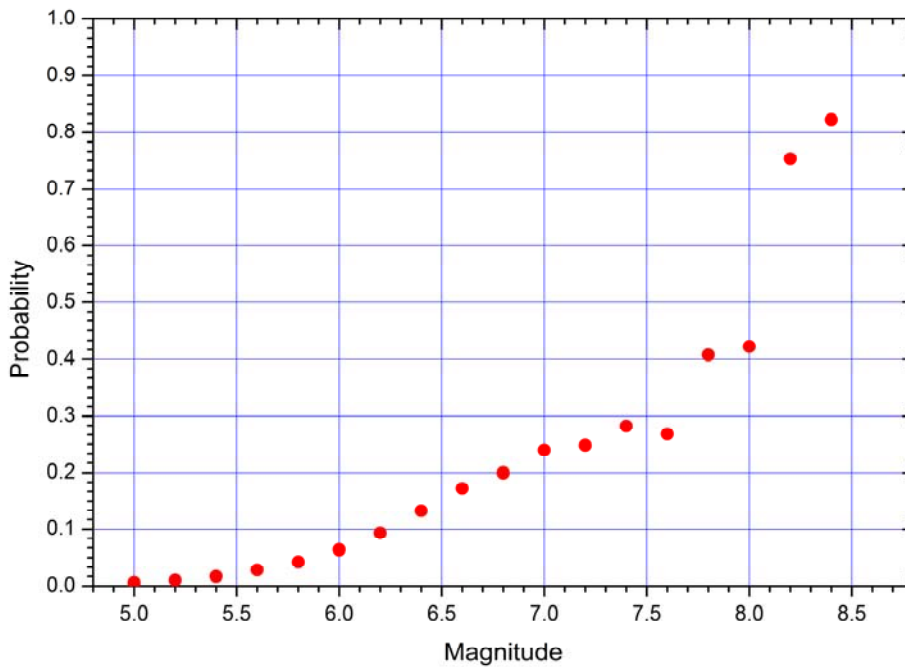


Figure 19: Estimated probability that an earthquake with magnitude $\geq M$ may generate a tsunami in the ASTARTE region.

4.3 Consistency of information sources

The TRANSFER tsunami catalogue provides a series of information regarding the earthquakes that generated a particular event that can be compared with the working catalogue we built for years greater than 1000. For years earlier than this, we also used the historical earthquake catalogue of Grünthal and Wahlström (2012) that spans from 303 to 1000 for a restricted area inside the ASTARTE domain (latitude $\leq 40^{\circ}\text{N}$ and longitude $\geq 10^{\circ}\text{E}$). The results of this comparison are summarized below.

The TRANSFER catalogue reports 274 tsunamis ascribed to an earthquake origin, of which 56 do not have a magnitude defined. We found 20 of these events on the ASTARTE earthquake catalogue. This information could be used to amend the tsunami catalogue. After year 303 we also found 20 tsunami events with an earthquake magnitude that could not be found on the ASTARTE earthquake catalogue (spanning between year 342 and year 1898). Overall, we found that the TRANSFER catalogue contains 66 events that could not be found in the earthquake catalogues investigated, most of them without a magnitude defined. A couple of events could not be associated due to insufficient information on the dates.

For those earthquakes appearing in both catalogues, TRANSFER and ASTARTE, we also compared the date and time, the location and the magnitudes reported (M_w for ASTARTE, unknown for TRANSFER). 34 events showed a magnitude difference greater than 0.2, 12 events presented a time difference greater than 2 hours and 7 events had a location difference greater than 1 degree. It is our view that the differences that are noted between both catalogues do not hinder the major analysis and conclusions presented in the previous sections.

CHAPTER 5: PROBABILITY OF A TSUNAMI CAUSED BY A VOLCANIC ERUPTION

For the investigation of tsunamis generated by volcanic sources our single source of information is the TRANSFER tsunami catalogue. In this catalogue there are 13 tsunami events with a source identified as a volcanic eruption. The first one dates back to 1630 BC in South Aegean (Santorini) and the last one occurred in Stromboli in December 2002. A summary of the most relevant parameters found in TRANSFER catalogue are reproduced in the Table-4 below. The tsunami impact is evaluated according to two tsunami intensity scales. These are given for reference in Annex-3. The location of the tsunami source areas is shown in Figure 20. All but one event occurred in the Eastern Mediterranean. The single event in the Atlantic was reported in the Canary islands which is outside the area plotted in the figure.

The tsunami intensities reported range from 2 (light according to Ambraseys, 1962) to 6 (disastrous in the Ambraseys, 1962, scale). Considering that after year 1600 the catalogue is complete for this type of tsunamis, then in the ASTARTE study area we should expect, on average, a tsunami caused by a volcanic eruption every 34.5 years, with intensity 2 or greater on the Ambraseys (1962) scale.

Table 4: Simplified description of the tsunamis caused by volcanic eruptions according to the TRANSFER catalogue.

#	Date	Zone	Short description	RU ¹	Ia ²	Ip ³
1	1630 BC	South Aegean		90	6	
2	79/8/24	Campania	Sea retreat in the Gulf of Naples		2	
3	1329/6/28	Eastern Sicily	Boats carried to the sea		3	
4	1631/12/17	Campania	Sea withdrawal in Gulf of Naples		2	4
5	1650/9/29	South Aegean		50	6	10
6	1698/5/14	Campania	Sea oscillations in Gulf of Naples		2	
7	1706/5/5	Canary Islands	Sea retreat/flooding at Garachico		4	
8	1714/6/30	Campania	Sea withdrawals in Gulf of Naples		2	
9	1813/5/17	Campania	Sea withdrawal in Gulf of Naples		2	
10	1906/4/4	Campania	Sea oscillations in Naples Gulf		2	3
11	1919/5/22	Aeolian Islands	Sea retreat/flooding at Stromboli		3	5
12	1930/9/11	Aeolian Islands	Strong sea retreat/flood Stromboli	2.5	3	4
13	1944/8/20	Aeolian Islands	Sea flooding. House destroyed		4	6

¹RU - Tsunami run-up (m)

²Ia - Tsunami Intensity according to the Ambraseys scale (1962) (see Annex-3)

³Ip - Tsunami Intensity according to the Papadopoulos & Imamura scale (2001) (see Annex-3)

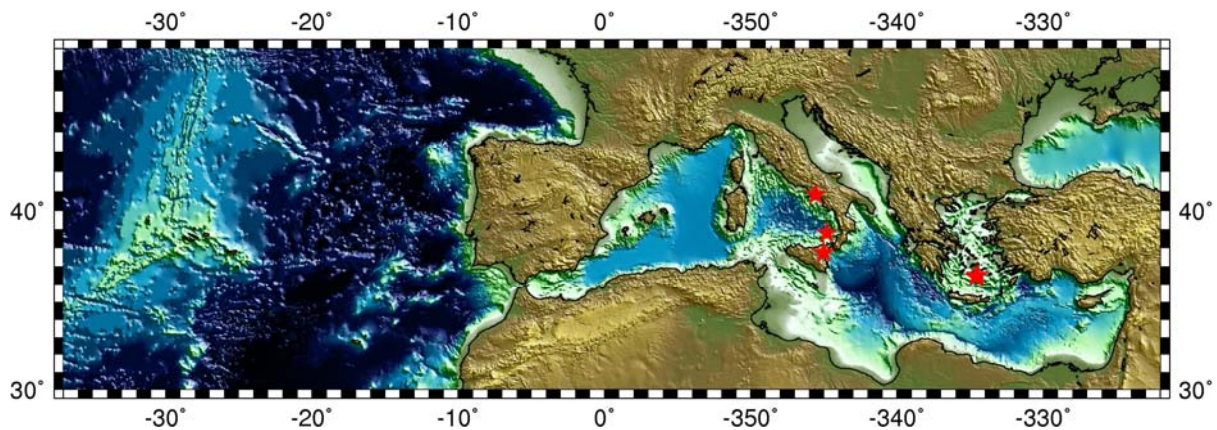


Figure 20: Location of tsunamis caused by a volcanic eruption. Source: TRANSFER tsunami catalogue (Gallazzi et al., 2010).

CHAPTER 6: PROBABILITY OF A TSUNAMI CAUSED BY MASS MOVEMENT

For the investigation of tsunamis generated by mass movement our single source of information is the TRANSFER tsunami catalogue. The mass movement source includes coastal landslides, submarine landslides and rock falls. In the TRANSFER catalogue there are 8 tsunami events with a source identified as resulting from some type of mass movement. The first event is dated year 1783 and occurred in the Messina Straits. A summary of the most relevant parameters found in TRANSFER catalogue are reproduced in the Table-5 below. The tsunami impact is evaluated according to two

tsunami intensity scales. These are given for reference in Annex-3. The location of the tsunami source areas is shown in Figure 21. One of the tsunamis was caused by the Grand Banks slide in 1929, which is out of the area plotted in the figure. This was a transoceanic tsunami with its source outside the ASTARTE study area.

The tsunami intensities reported range from 1 (very light according to Ambraseys, 1962) to 4 (strong on the Ambraseys, 1962, scale) or 8 (heavily damaging on the Papadopoulos & Imamura, 2001, scale). Considering that after year 1900 the catalogue is complete for this type of tsunami sources, then in the ASTARTE study area (excluding the Grand Banks event) we should expect, on average, one tsunami caused by some type of mass movement every 19 years, with intensity 2 or greater on the Ambraseys (1962) scale (3 or greater on the Papadopoulos & Imamura (2001) scale).

Table 5: Simplified description of the tsunamis caused by mass movements according to the TRANSFER catalogue.

#	Date	Zone	Short description	RU ¹	Ia ²	Ip ³
1	1783/3/24	Messina Straits	Capsizing of a boat. 1 man killed		3	
2	1929/11/18	Grand Banks	Tide gauge records in Ponta Delgada and Leixões		1	2
3	1930/3/4	Madeira Island	Enormous wave at Vigario beach	>5	4	8
4	1963/2/7	Corinthiakos-Patras Gulf		5	4	7
5	1979/10/16	Liguria-Côte d'Azur	3 m high waves at Antibes	3	3	4
6	1988/4/20	Aeolian Islands	Small waves in Vulcano and Lipari		2	3
7	1996/1/1	Corinthiakos-Patras Gulf			3	5
8	2002/3/24	Dodecanese Islands			2	5

¹RU - Tsunami run-up (m)

²Ia - Tsunami Intensity according to the Ambraseys scale (1962) (see Annex-3)

³Ip - Tsunami Intensity according to the Papadopoulos & Imamura scale (2001) (see Annex-3)

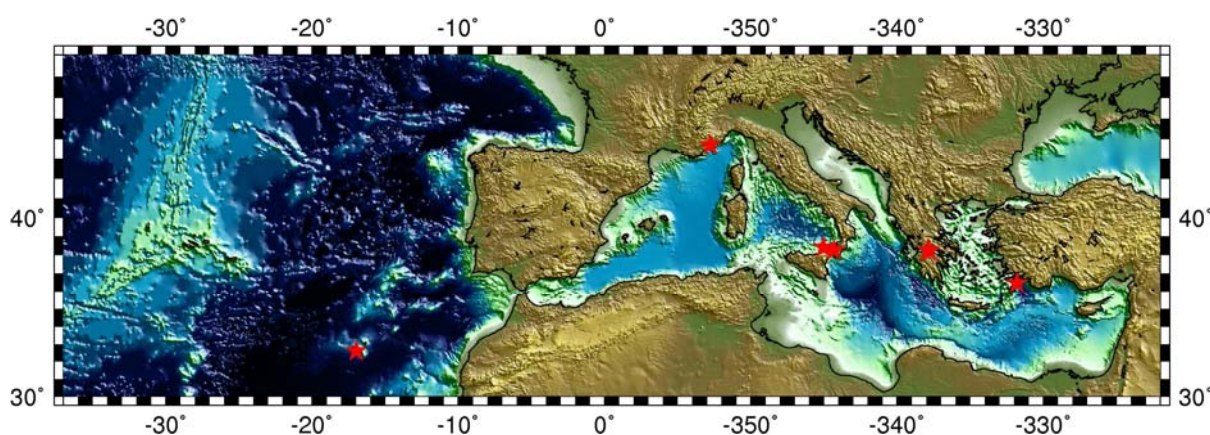


Figure 21: Location of tsunamis caused by any type of mass movement. Source: TRANSFER tsunami catalogue (Gallazzi et al., 2010).

CHAPTER 7: RECURRENCE OF TSUNAMI IMPACT

We saw in the two previous chapters that the TRANSFER catalogue characterizes the tsunami impact by several parameters, namely the run-up and tsunami intensity on two scales (Ambraseys, 1962 and Papadopoulos & Imamura, 2001). For simplicity these two scales will be identified as TIA and TIPI respectively. Since tsunami run-up is not reported for most of the events we will use the tsunami intensity as a measure of the tsunami impact, regardless of its origin.

We verified that 34 events do not have any type of tsunami intensity reported, while 33 have TIA but not TIPI and 15 have TIPI but no TIA. In order to complete as much as possible the tsunami intensity field, we looked for the best equivalence between both scales, using the common reported values. The adopted equivalence values are presented in Table-6.

TIA to	TIPI	TIPI to	TIA
1	2	3	2
2	3 (3.2±0.5)	4	2.5 (2.7±0.5)
3	5 (4.8±0.8)	5	3 (3.1±0.3)
4	7 (6.8±1.2)	7	4 (4.1±0.6)
5	8 (8.1±1.1)		
6	9 (9.3±0.5)		

Since the TIPI has a larger number of degrees, we choose this parameter for evaluation of tsunami impact. We used the ZMAP analysis tool (Wiemer and Wyss, 2000) to find that the completeness tsunami intensity for the TRANSFER catalogue since 1700 (all sources combined) is 3 (Figure 22).

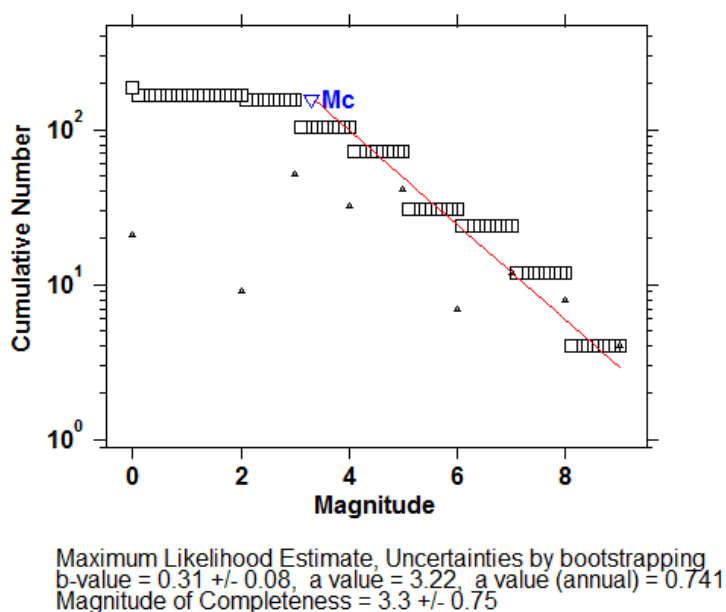


Figure 22: Determination of completeness magnitude, all sources in the TRANSFER catalogue combined since 1700.

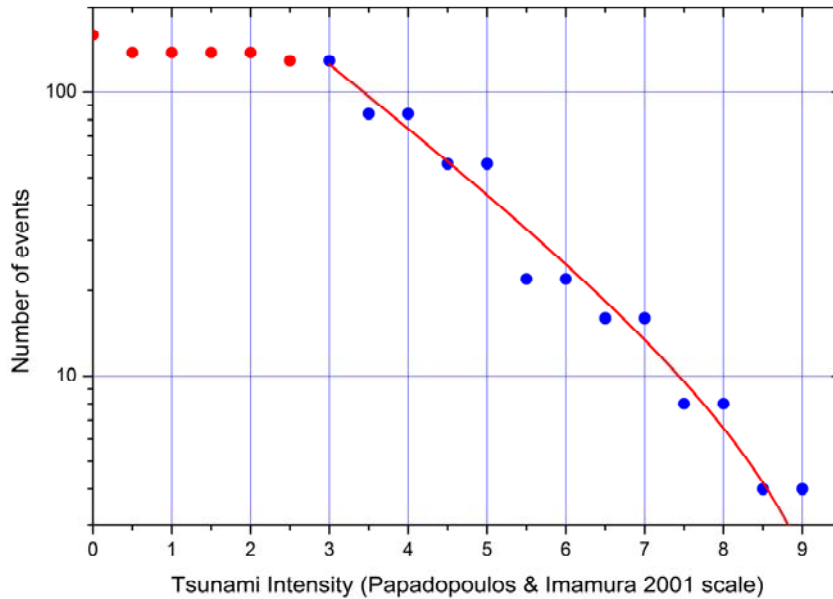


Figure 23: Fit of a truncated Gutenberg-Richter law to the TRANSFER tsunami catalogue, all sources considered since 1700.

We finally fit a truncated Gutenberg-Richter law to the TRANSFER tsunami catalogue, all sources considered since 1700. The parameters obtained were, $\lambda=125.4\pm 6.5$ (for 314 year time span); $\beta=0.501\pm 0.05$; $M_{\max}=9.9\pm 2.5$; for $M_{\min}=3.0$. Here the meaning of magnitude has to be replaced by the tsunami intensity in the Papadopoulos & Imamura (2001) scale. In this scale we expect damages for degrees equal or greater than 6. The estimated annual exceedance rate for this level of impact is 0.0796, implying a return period of 12.6 years.

REFERENCES

- Ambraseys, N.N., 1962. Data for the Investigation of the Seismic Sea-waves in the Eastern Mediterranean. *Bull. Seismol. Soc. Am.* 52, 895–913.
- Baptista, M.A., Miranda, J.M., 2009. Revision of the Portuguese catalog of tsunamis. *Nat. Hazards Earth Syst. Sci.* 9, 25–42.
- Gallazzi, S.C., Tinti, S., Armigliato, A., Alessandra Maramai, A., Antonio Patera, A., 2010. A GIS interface to the new Euro-Mediterranean Tsunami Catalogue produced by the TRANSFER Project, *Geophysical Research Abstracts*, Vol. 12, EGU2010-8406.
- Grünthal, G., Wahlström, R., 2012. The European-Mediterranean Earthquake Catalogue (EMEC) for the last millennium. *J. Seismol.* 16, 535–570. doi:10.1007/s10950-012-9302-y
- ICG/NEAMTWS, 2011. Interim Operational Users Guide for the Tsunami Early Warning and Mitigation System in the North-eastern Atlantic, the Mediterranean and Connected Seas (NEAMTWS), Version 2.00, Approved by ICG/NEAMTWS-VIII (Santander, 22-24 November 2011).
- ISC, 2012. International Seismological Centre, On-line Bulletin, <http://www.isc.ac.uk>, Internat. Seis. Cent., Thatcham, United Kingdom.

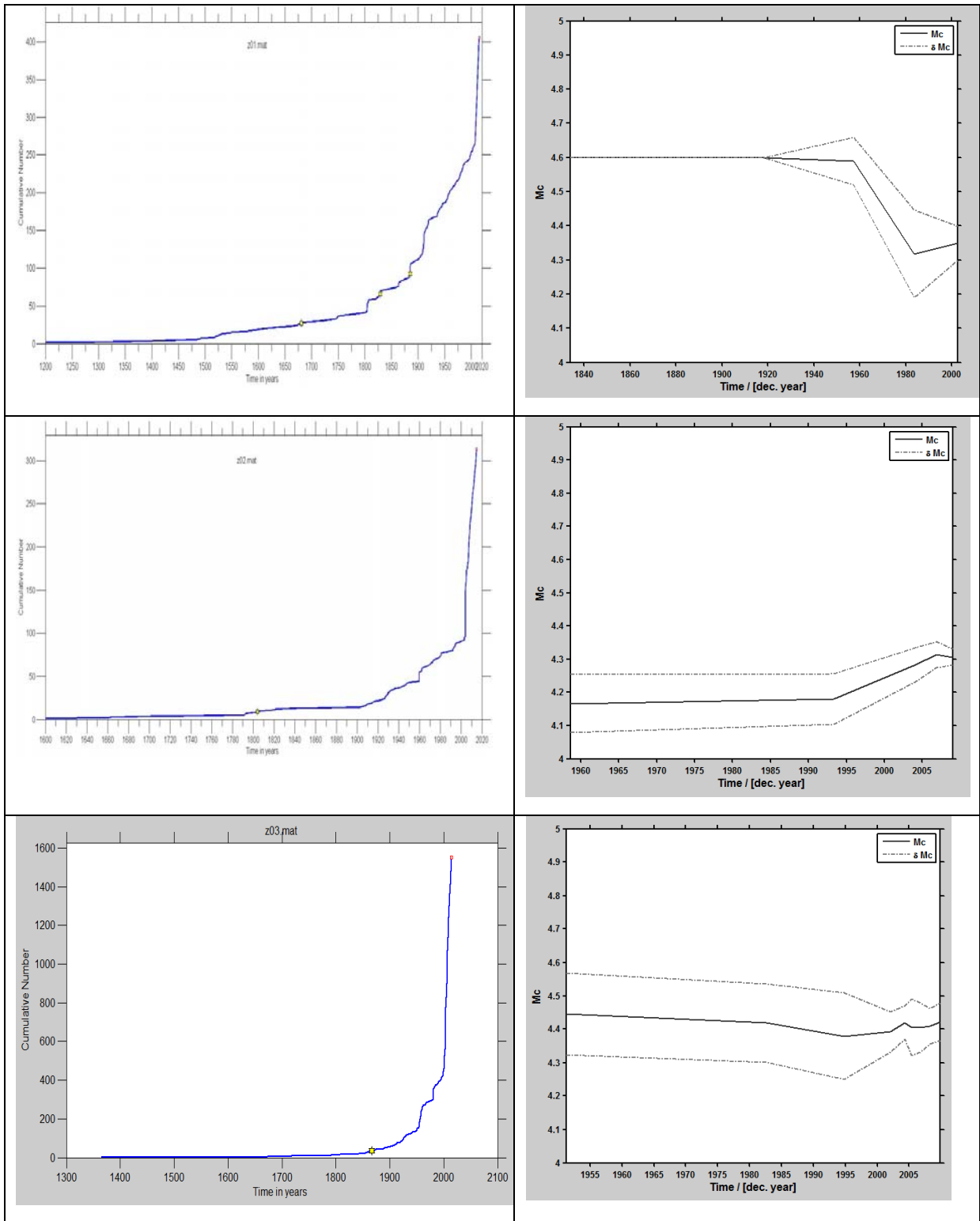
- Kijko, A., 2004. Estimation of the Maximum Earthquake Magnitude, m_{max} . *Pure Appl. Geophys.* 161, 1–27. doi:10.1007/s00024-004-2531-4
- Kijko, A., Sellevoll, M.A., 1989. Estimation of Earthquake Hazard Parameters from Incomplete Data Files. Part I. Utilization of Extreme and Complete Catalogs with Different Threshold magnitudes. *Bull. Seismol. Soc. Am.* 79, 645–654.
- Kijko, A., Sellevoll, M.A., 1992. Estimation of Earthquake Hazard Parameters from Incomplete Data Files. Part II. Incorporation of Magnitude Heterogeneity. *Bull. Seismol. Soc. Am.* 82, 120–134.
- Papadopoulos, G.A., Imamura, F., 2001. A proposal for a new tsunami intensity scale. *ITS Proc.* 569–577.
- Parsons, T., Geist, E.L., 2014. The 2010–2014.3 global earthquake rate increase. *Geophys. Res. Lett.* 41, 4479–4485. doi:10.1002/2014GL060513. Received
- Shapira, A., 2007. ISC Magnitude relationships, RELEMR meeting, Madrid.
- Sørensen, M.B., Spada, M., Babeyko, A., Wiemer, S., Grünthal, G., 2012. Probabilistic tsunami hazard in the Mediterranean Sea. *J. Geophys. Res.* 117, B01305. doi:10.1029/2010JB008169
- Wiemer, S., Wyss, M., 2000. Minimum Magnitude of Completeness in Earthquake Catalogs: Examples from Alaska, the Western United States, and Japan. *Bull. Seismol. Soc. Am.* 90, 859–869.

www.astarte-project.eu

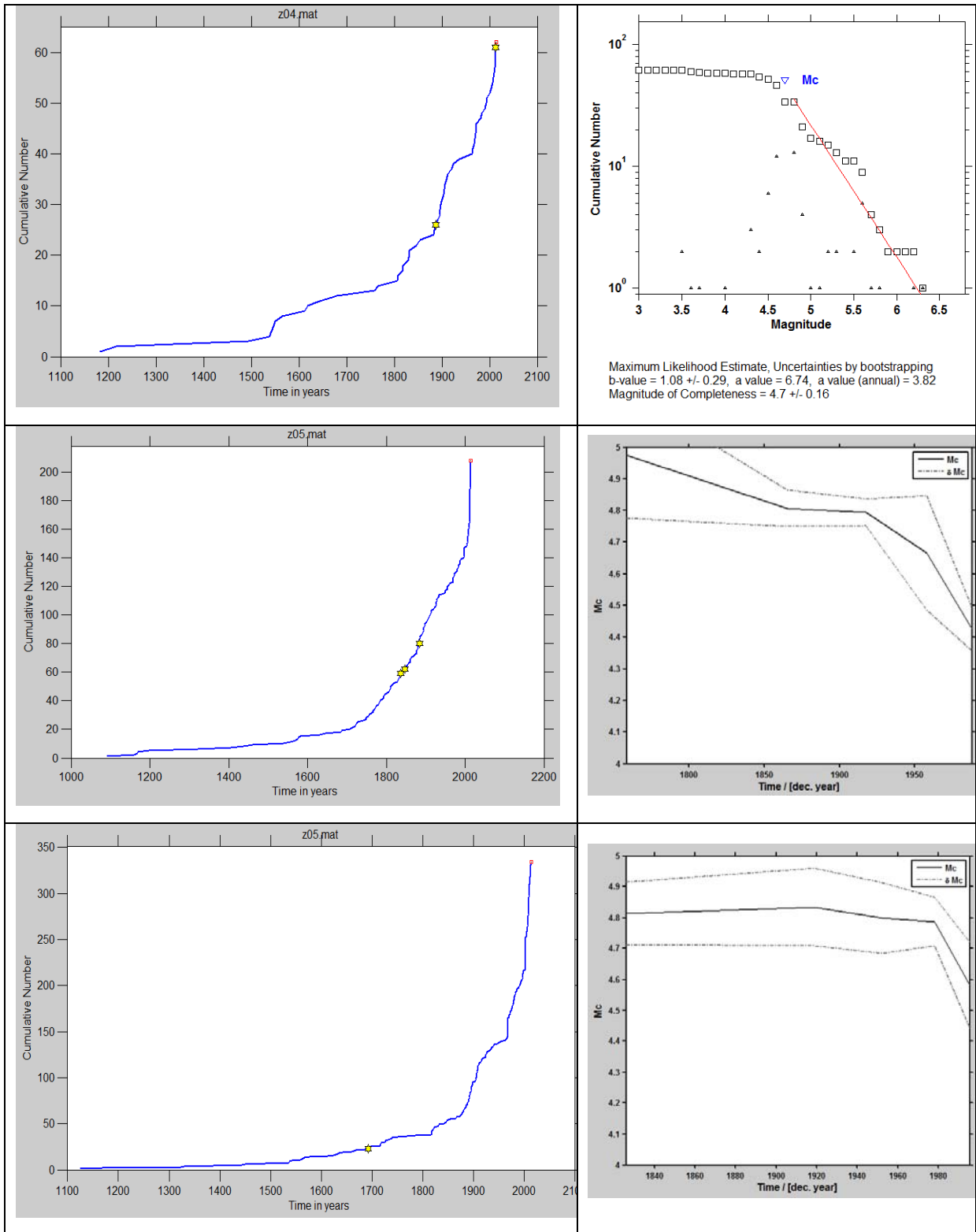
ANNEX 1

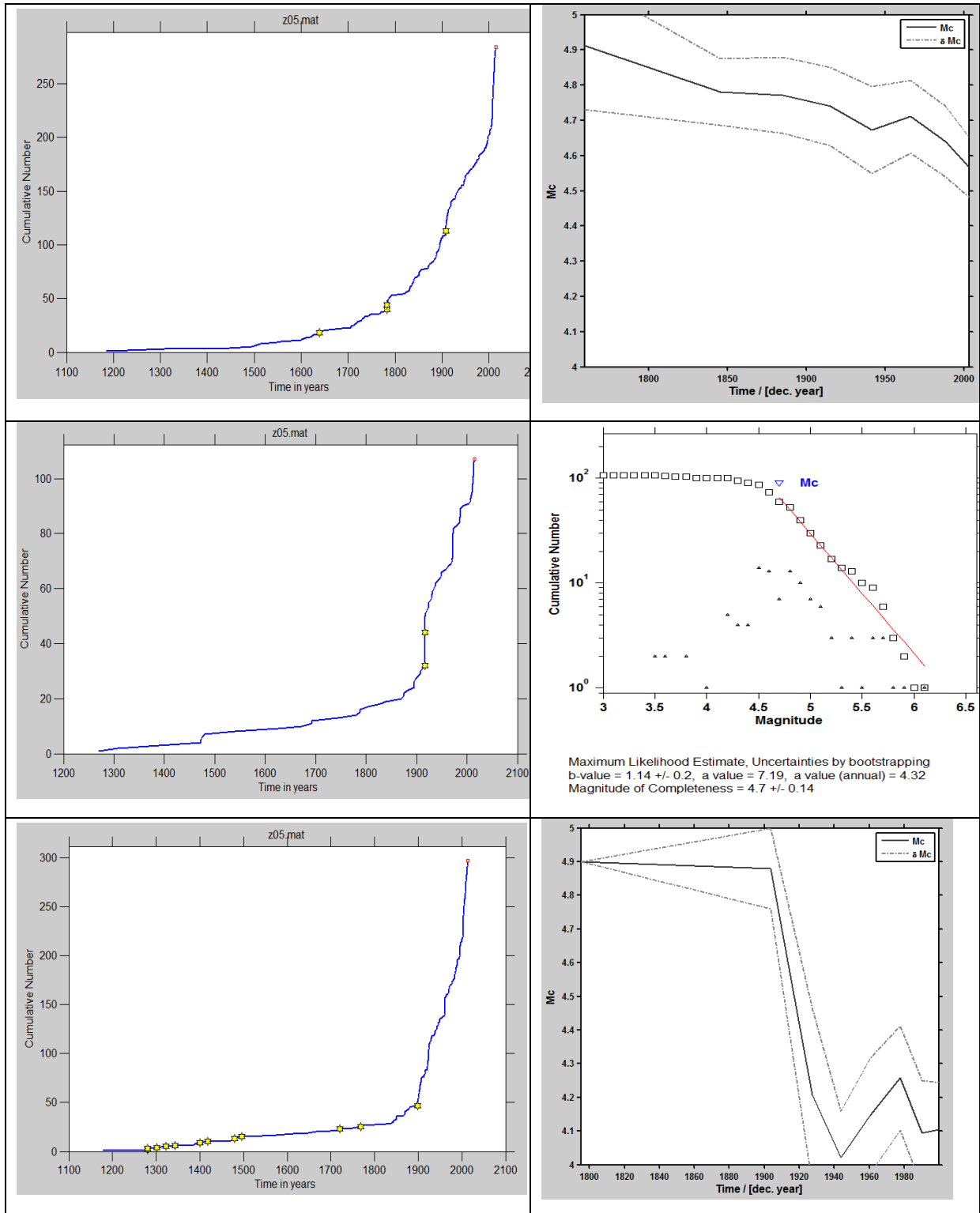
CUMULATIVE NUMBER OF EARTHQUAKES AND COMPLETENESS MAGNITUDE

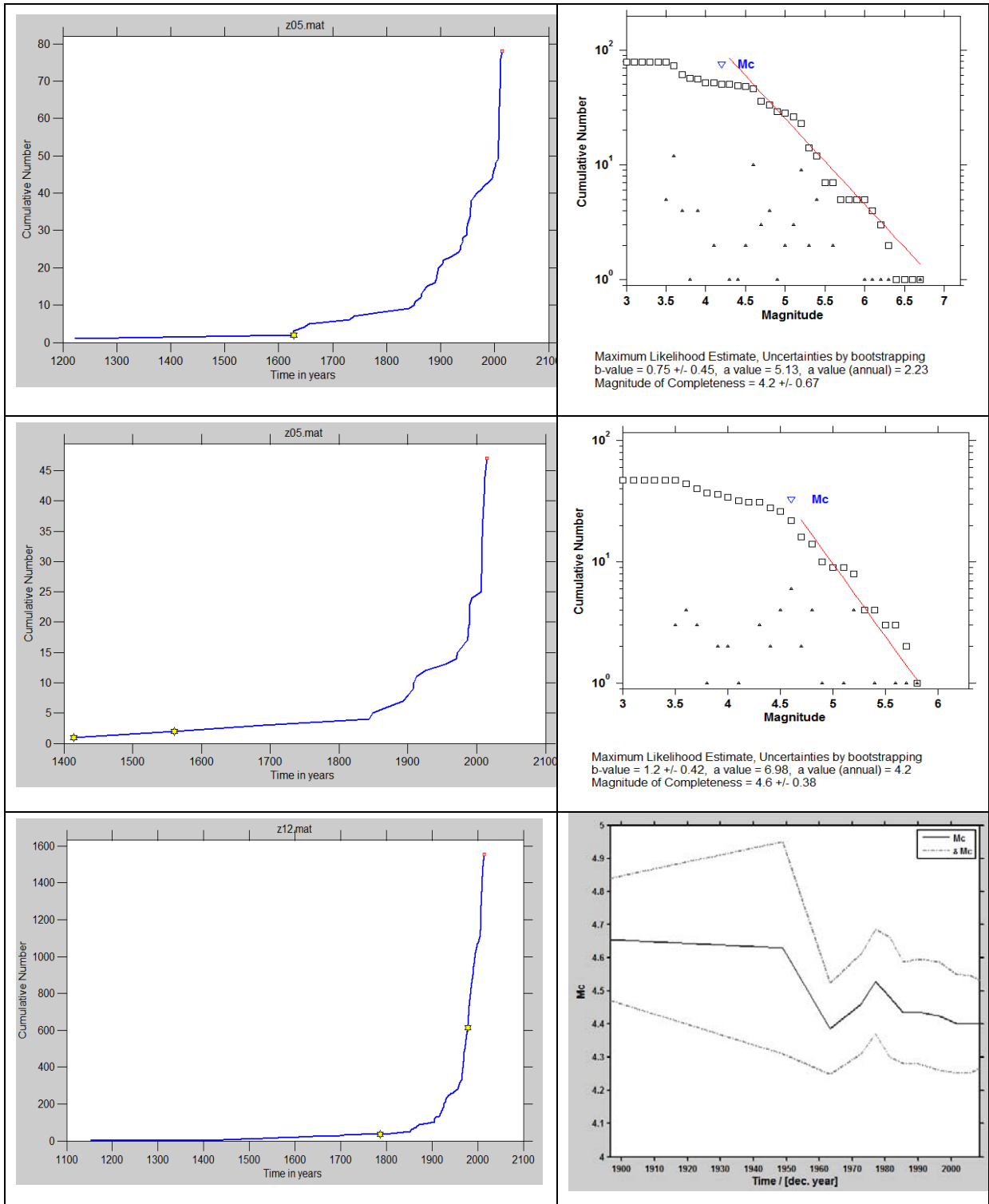
ASTARTE [603839] – Deliverable 2.9 - Annex 1

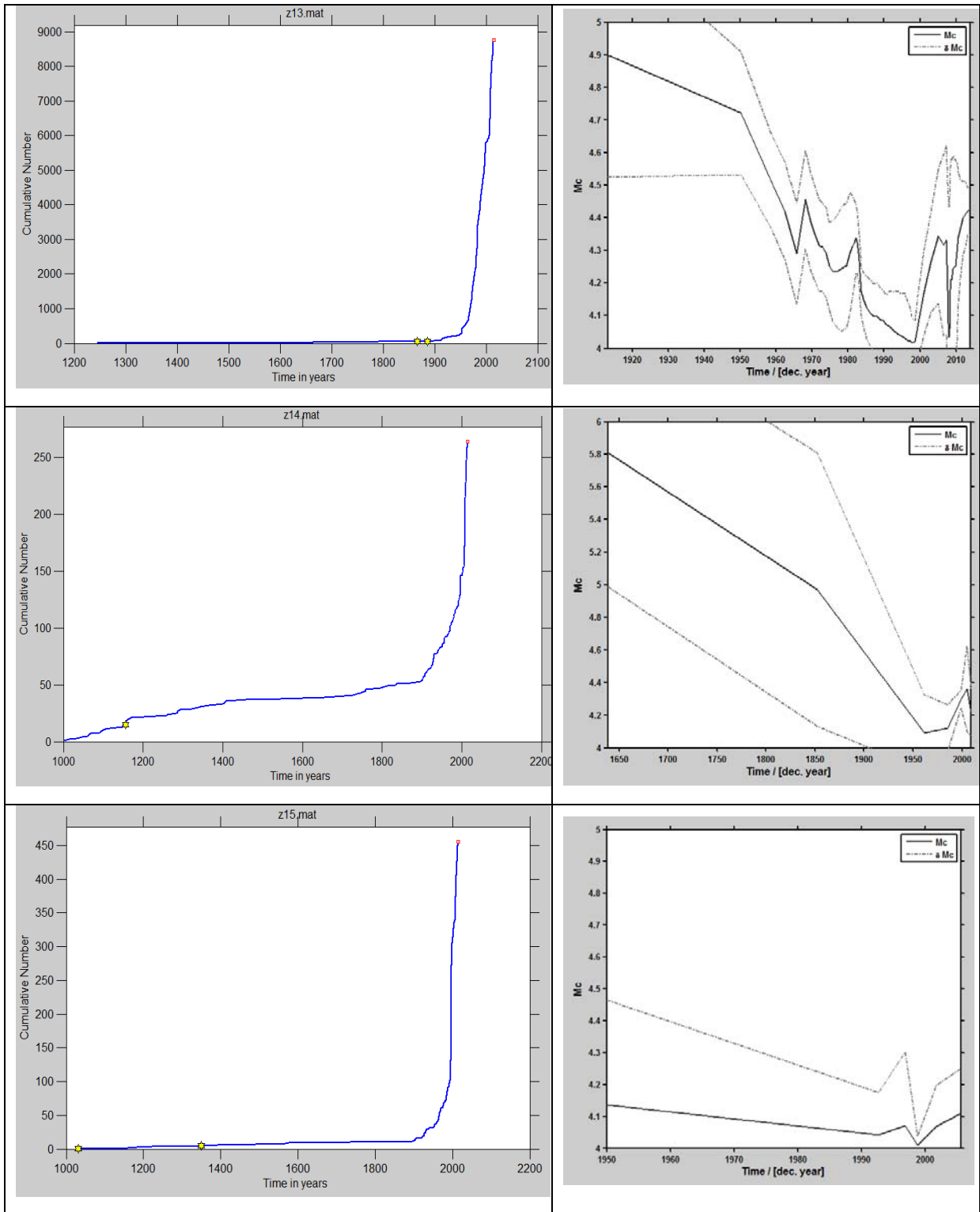


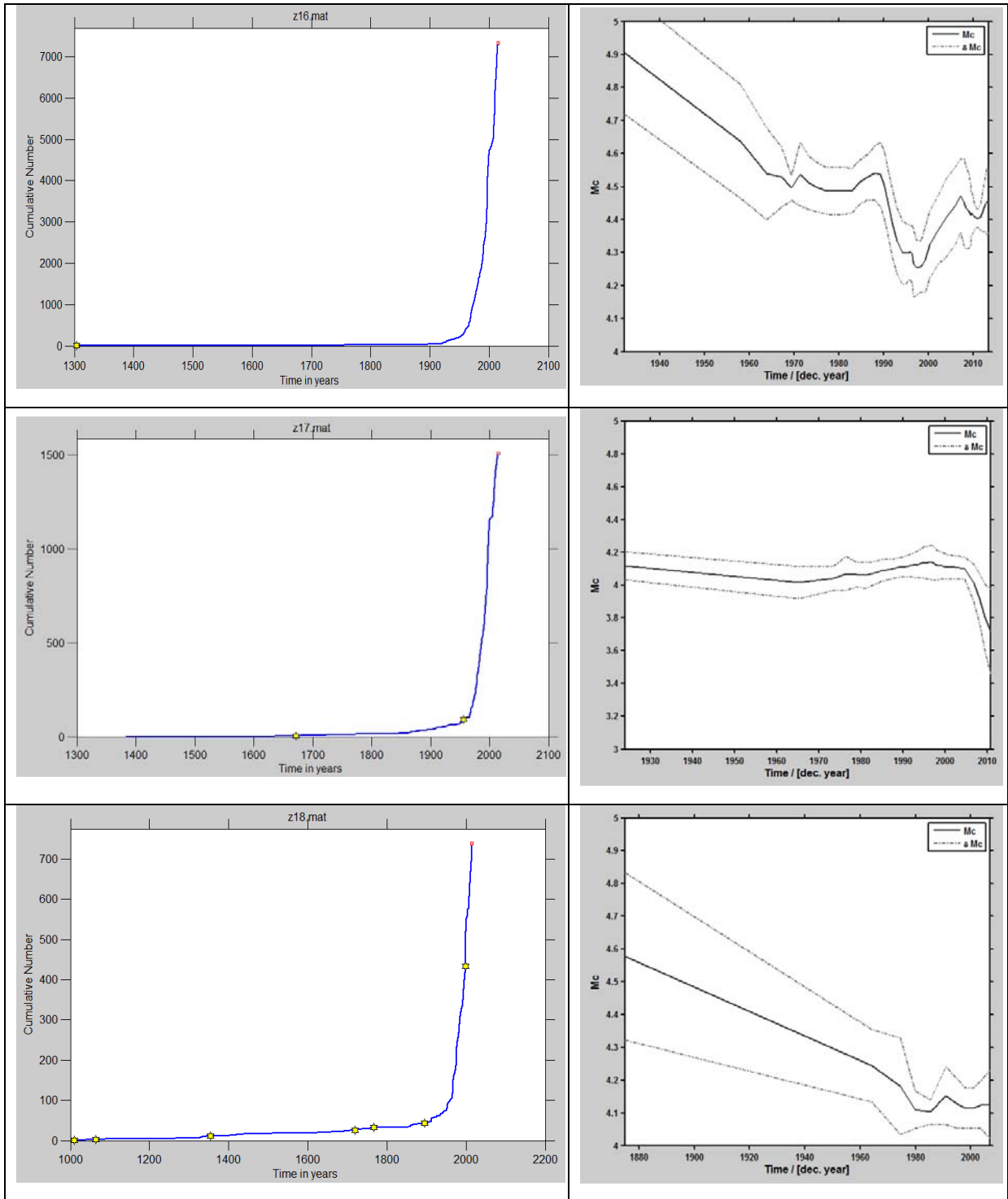
ASTARTE [603839] – Deliverable 2.9 - Annex 1

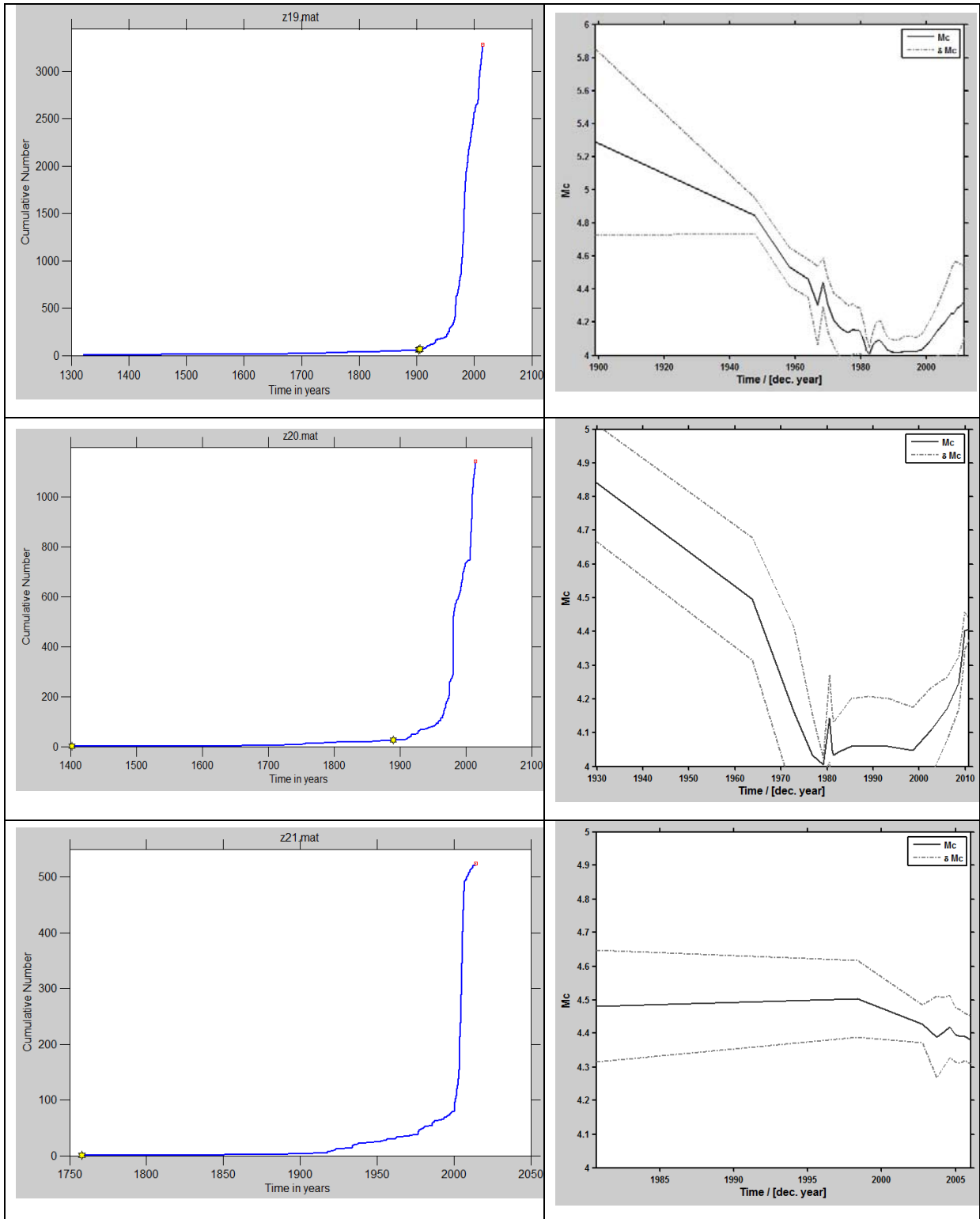


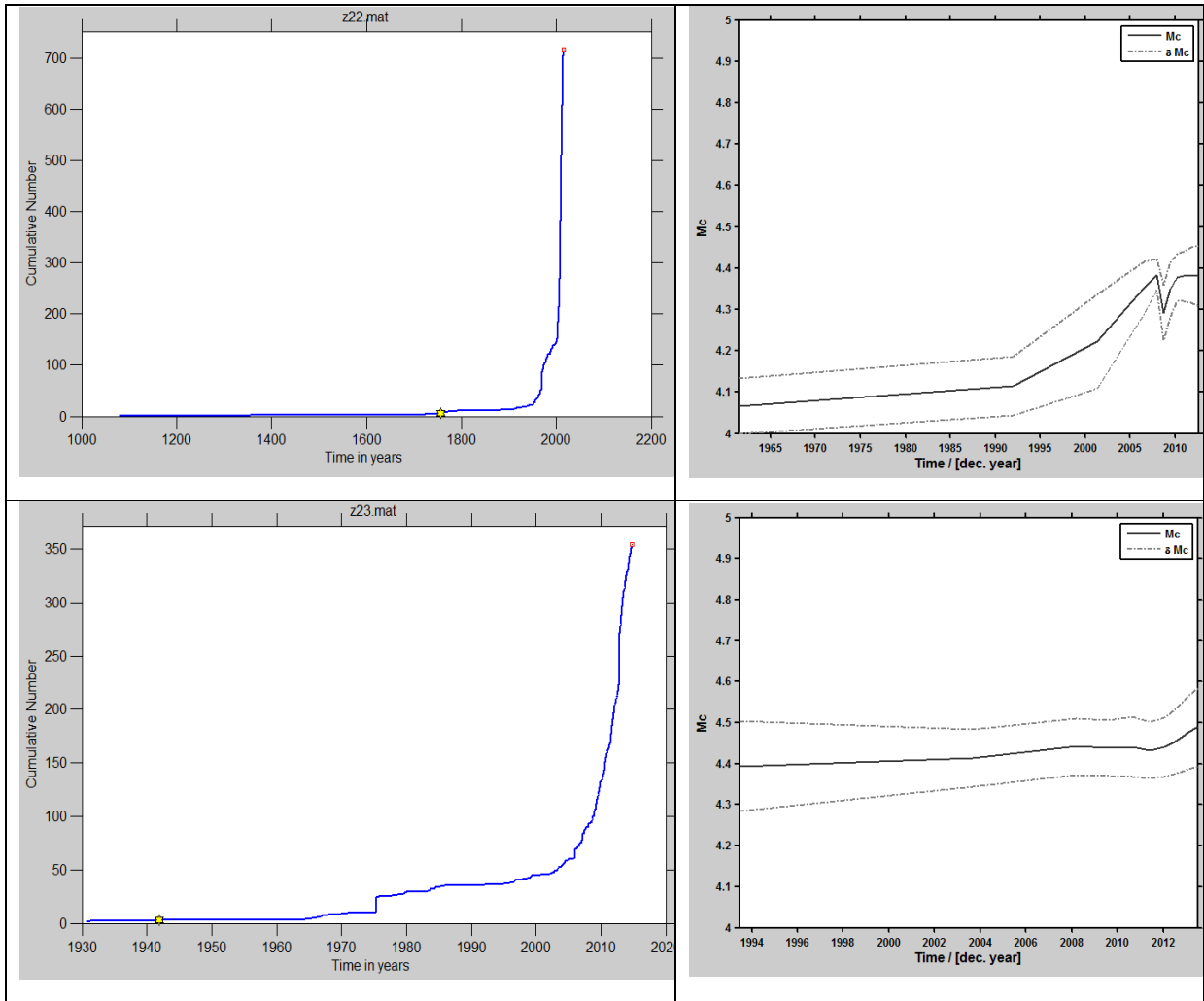






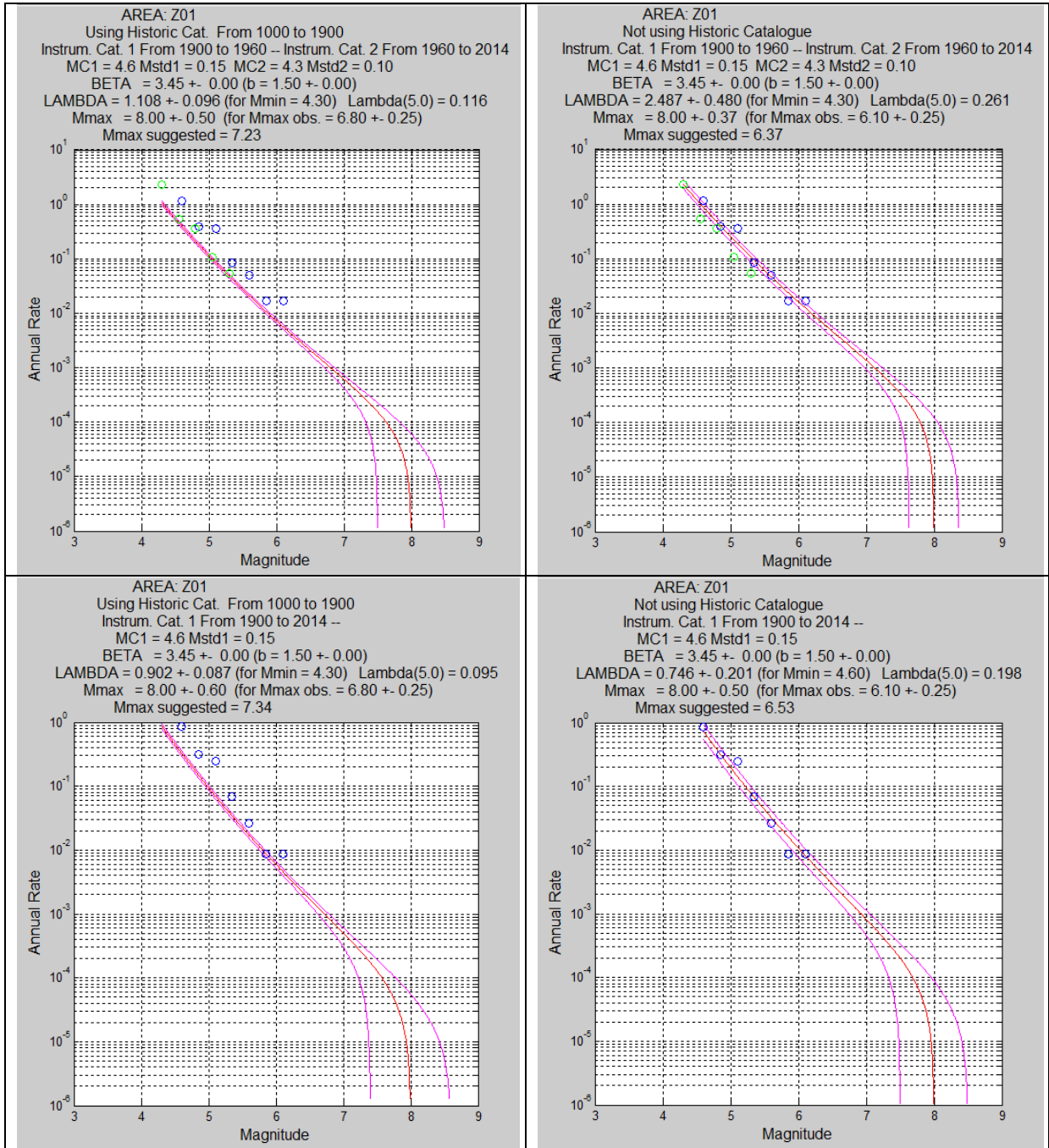


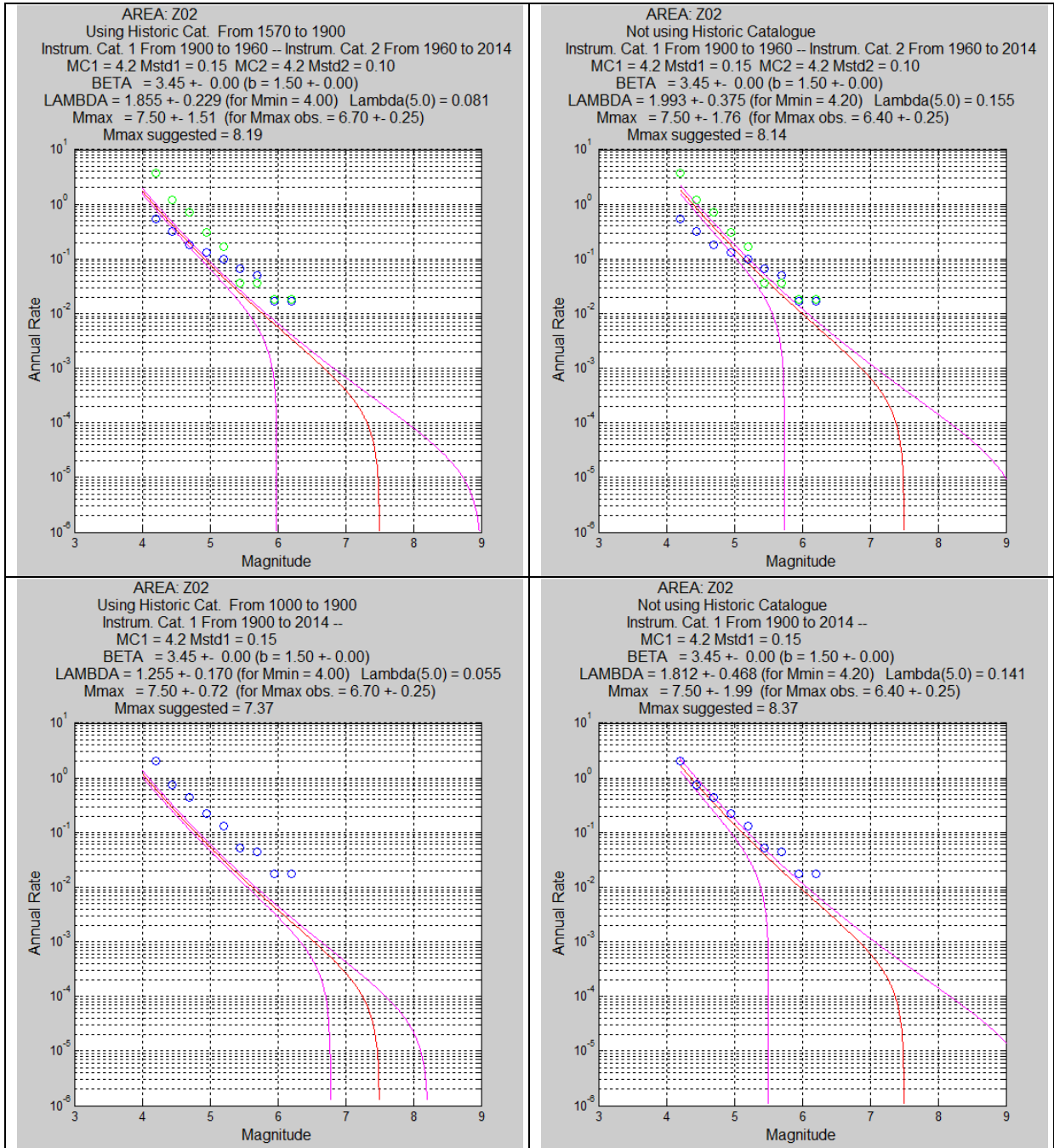


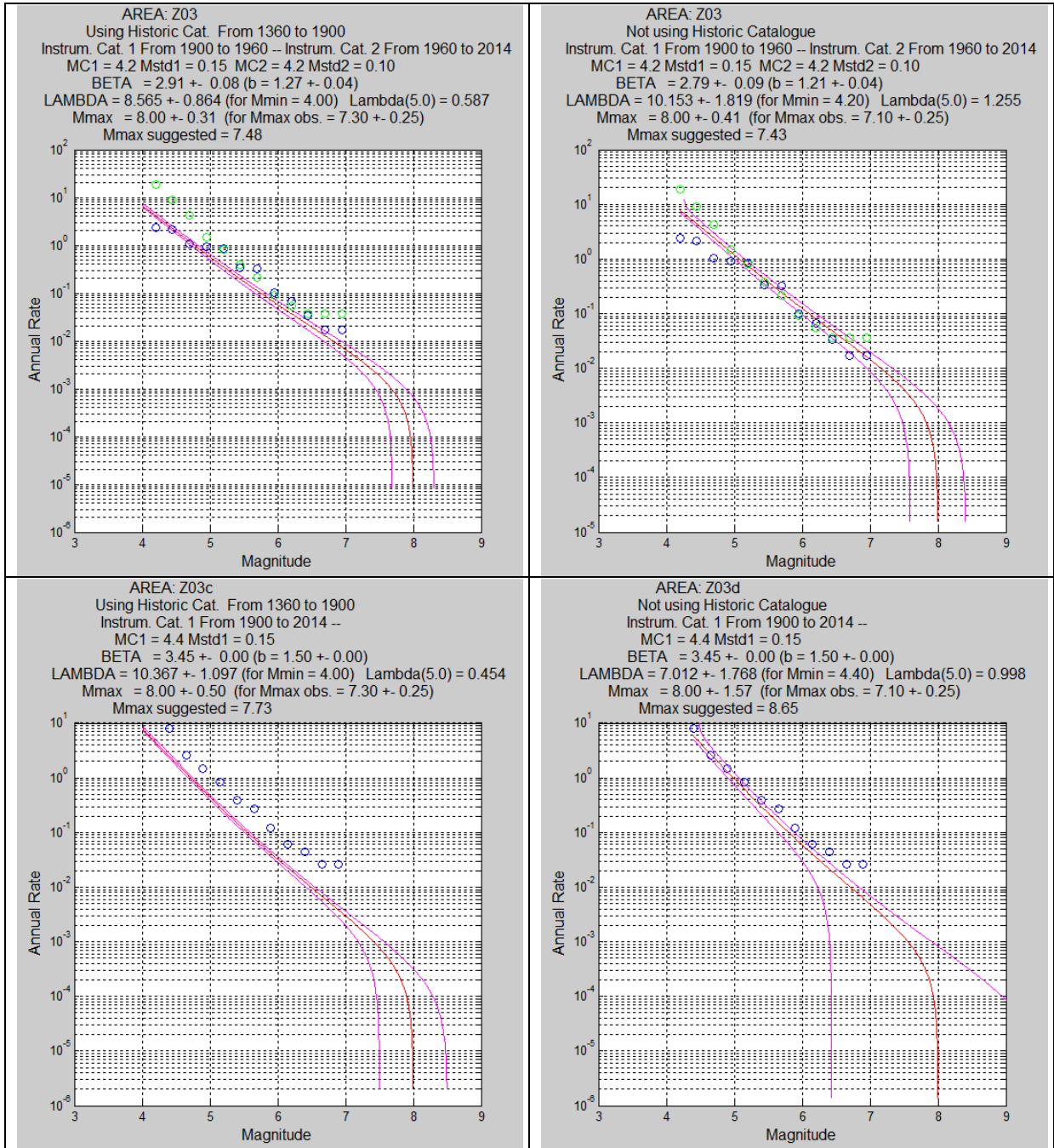


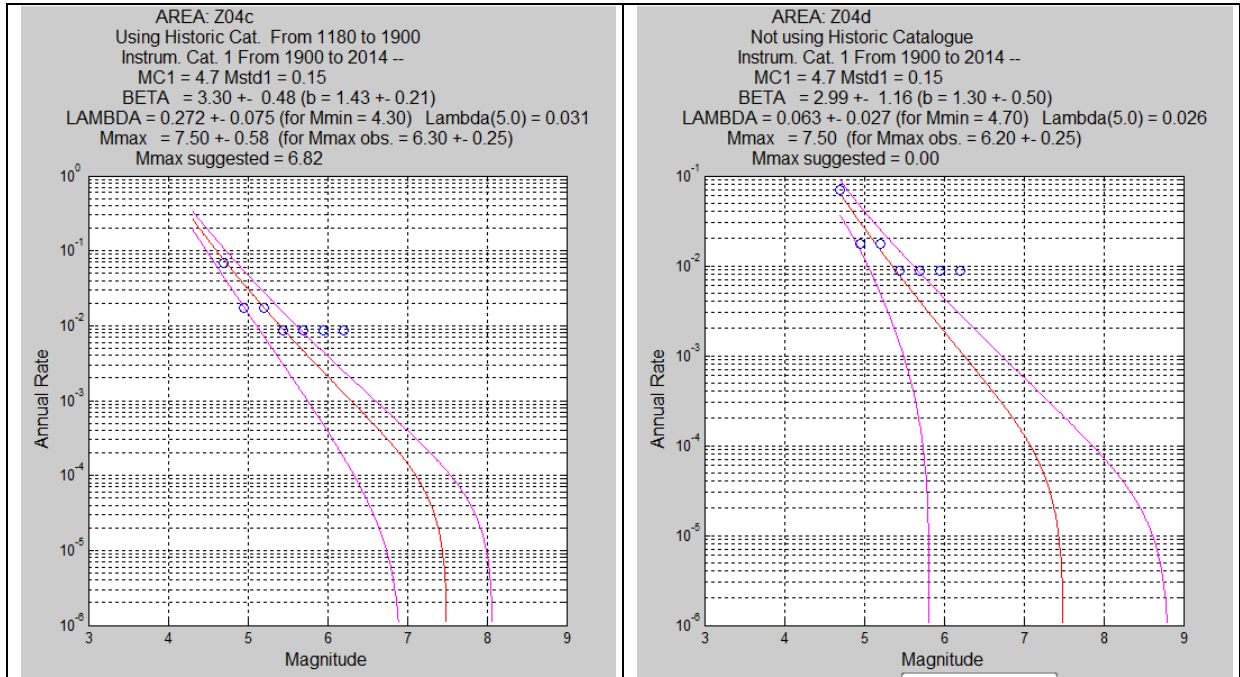
ANNEX 2

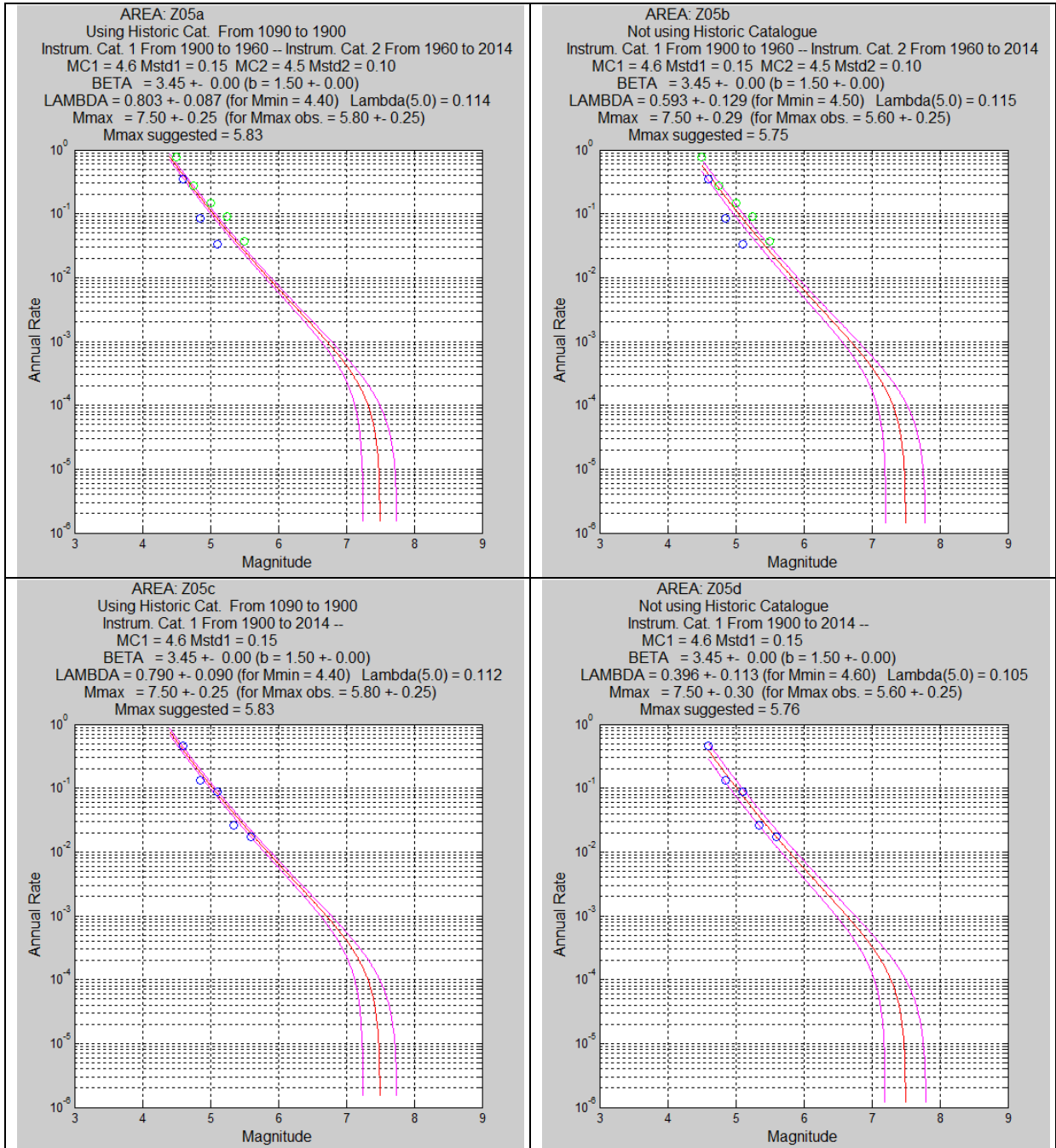
RECURRENCE MODELS

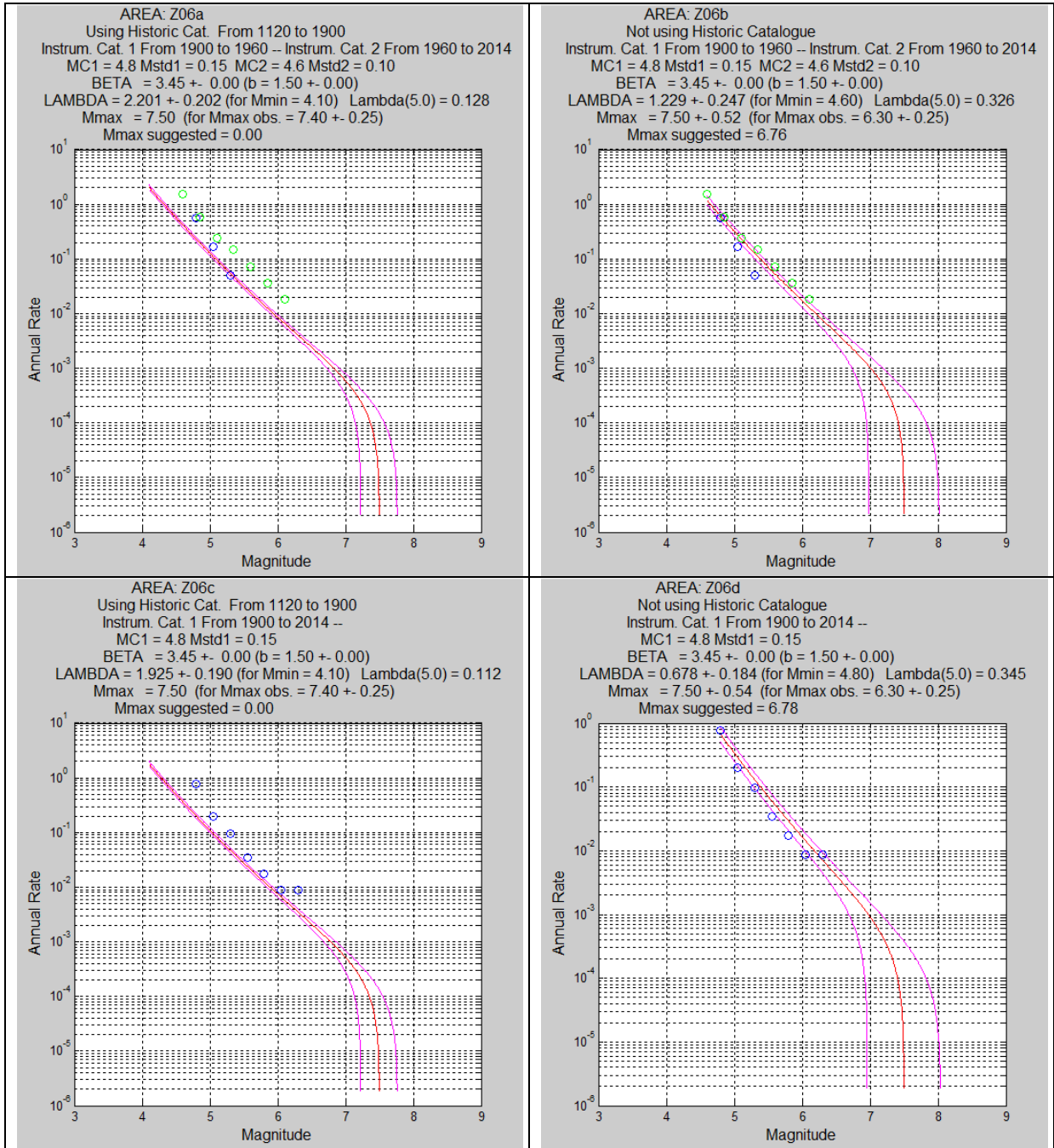


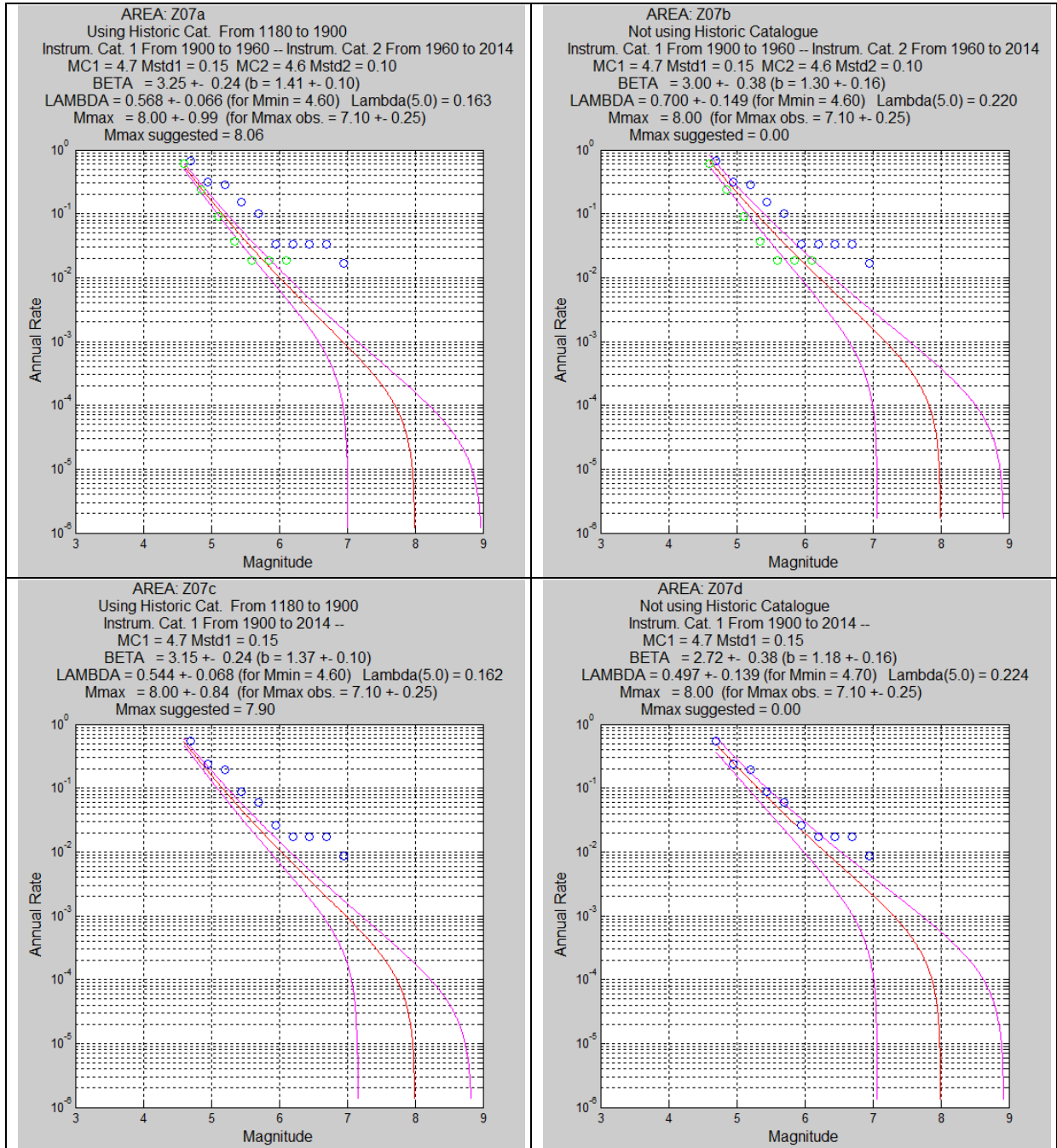


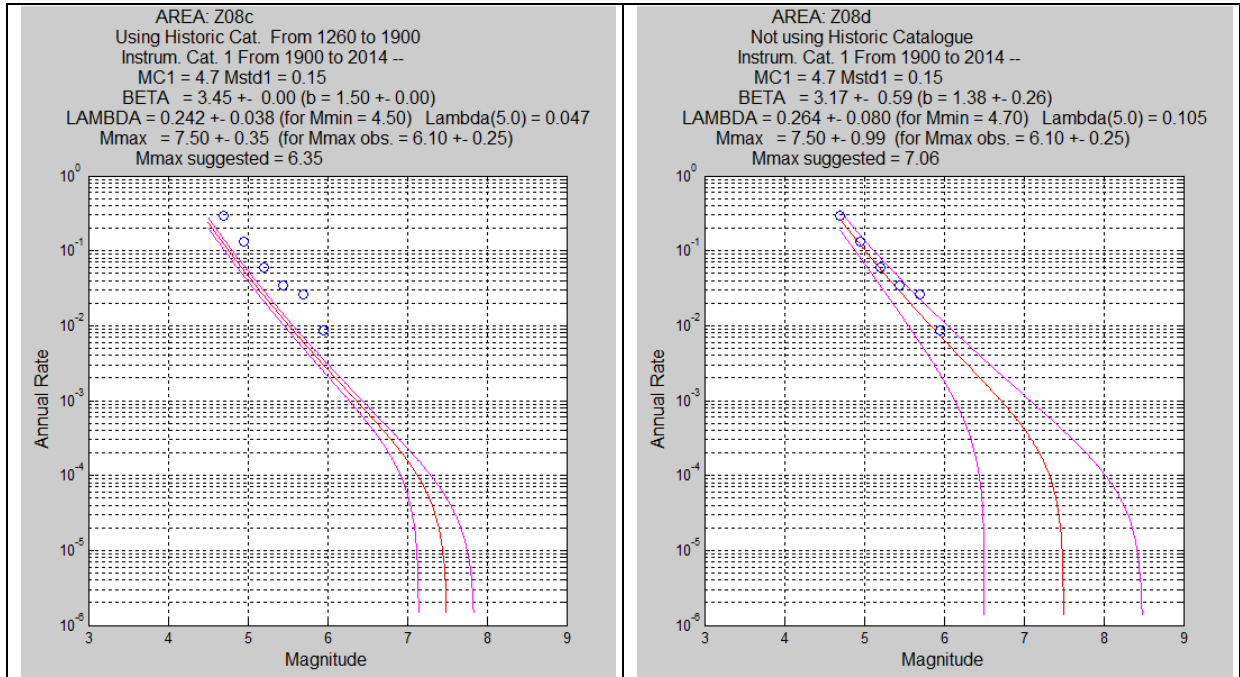


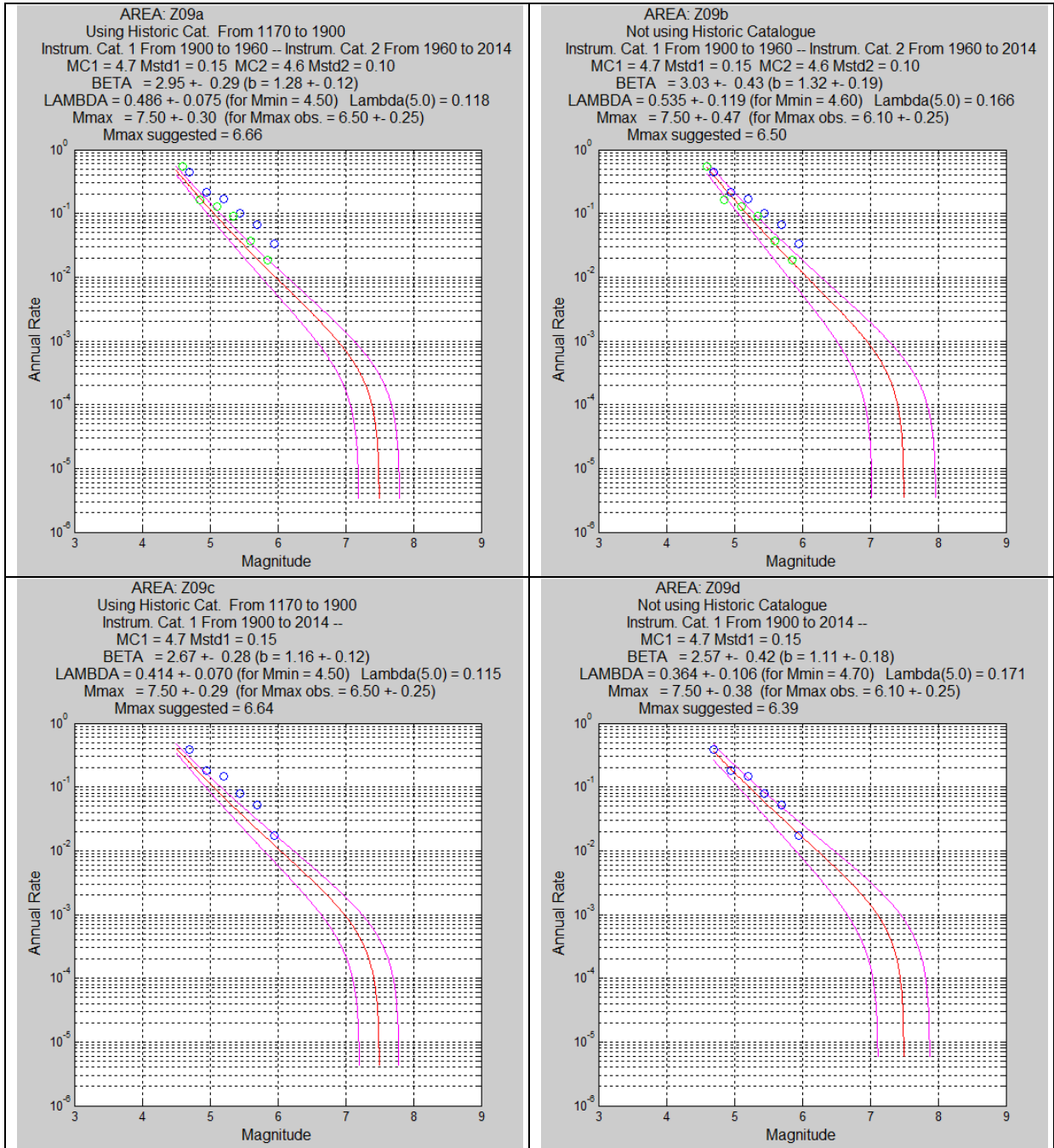


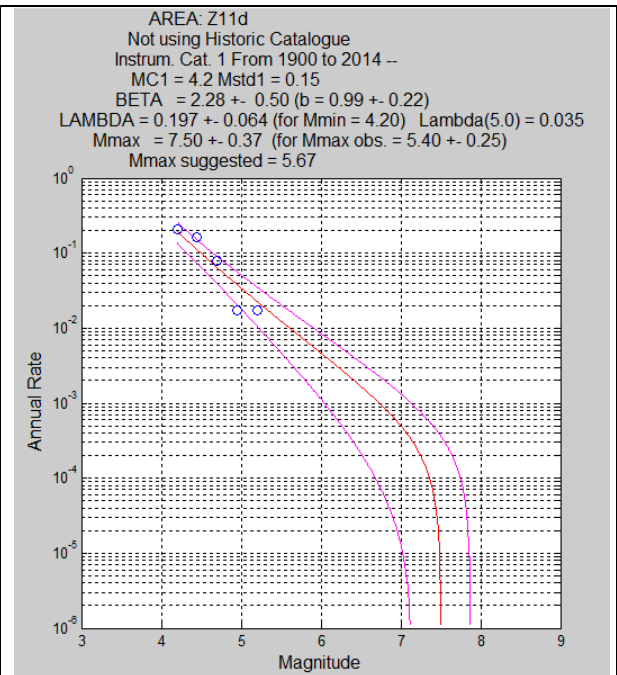
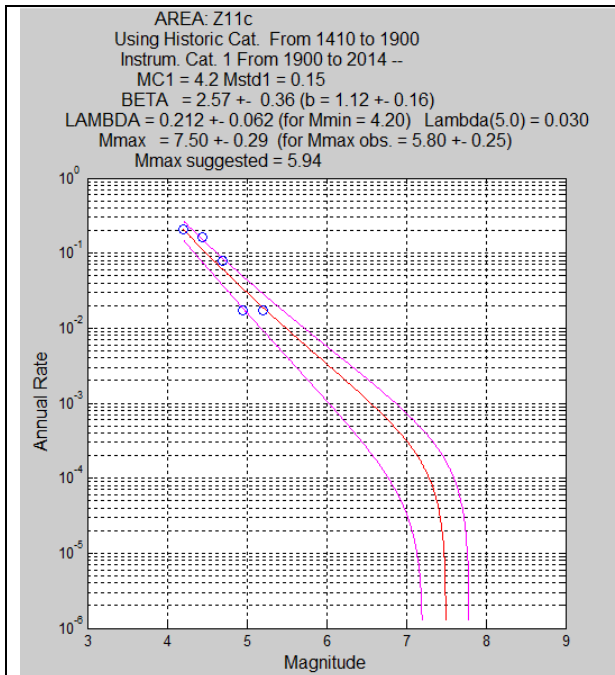
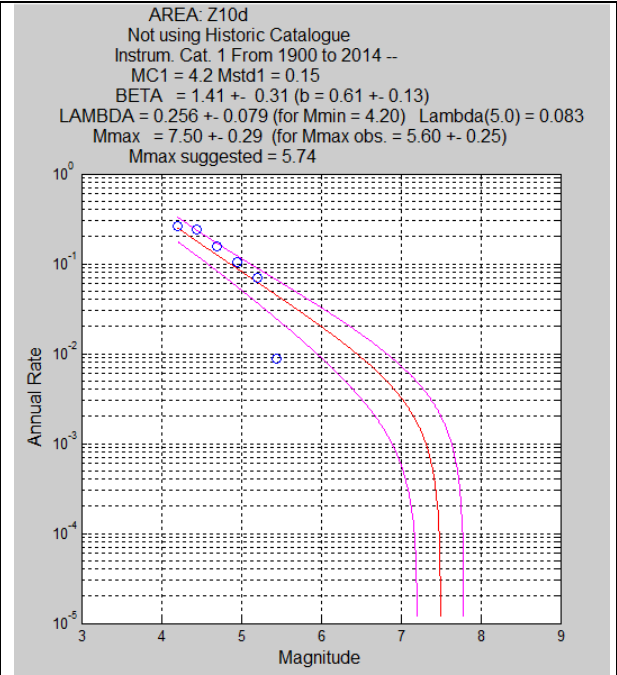
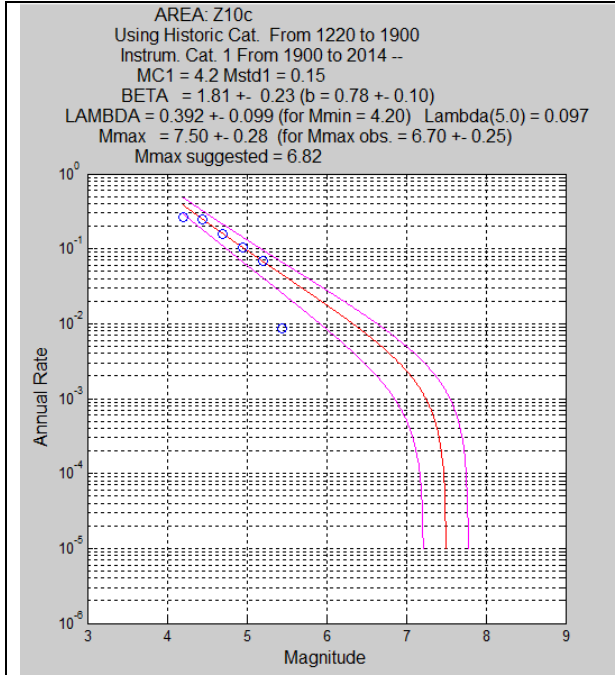


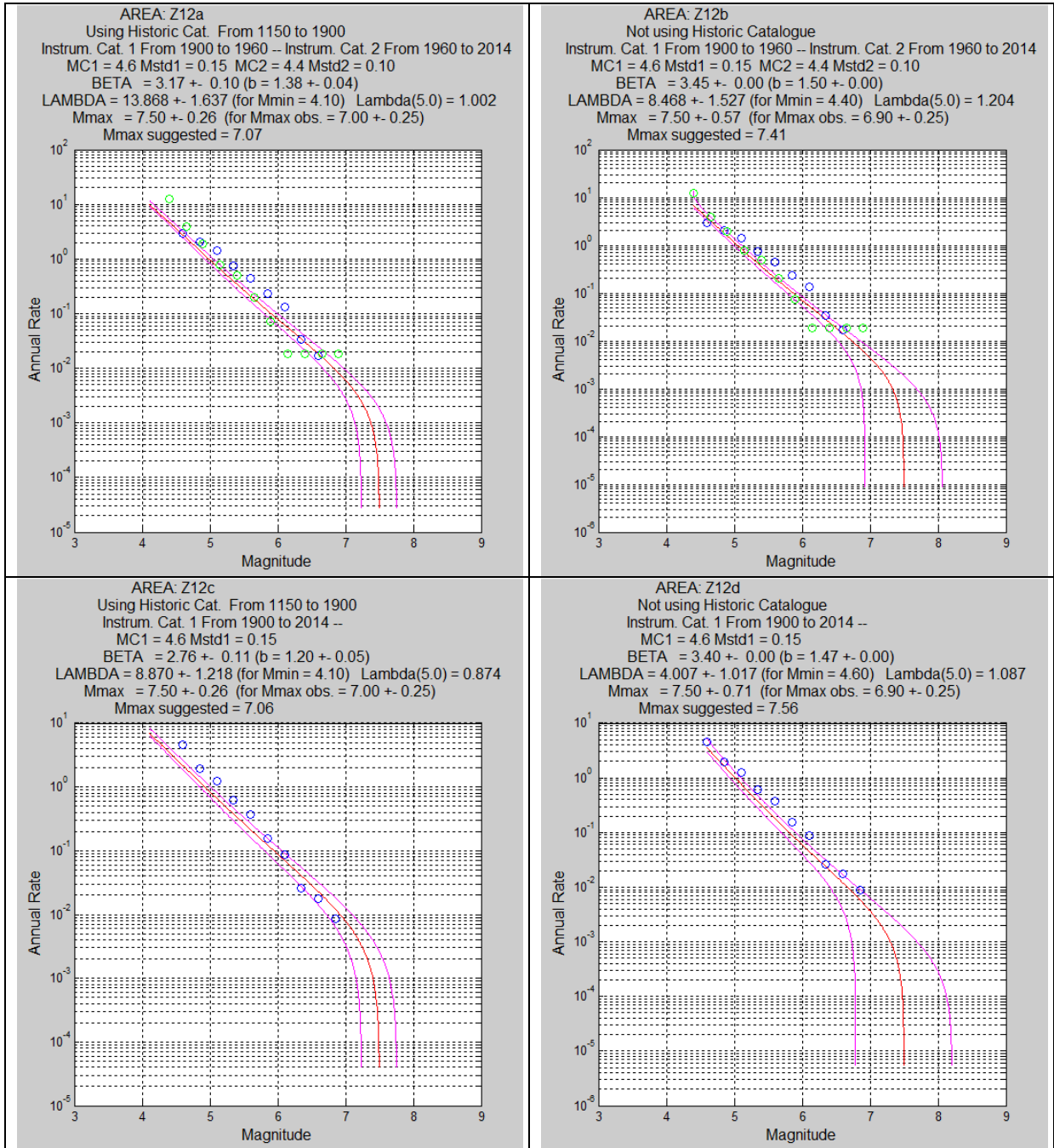


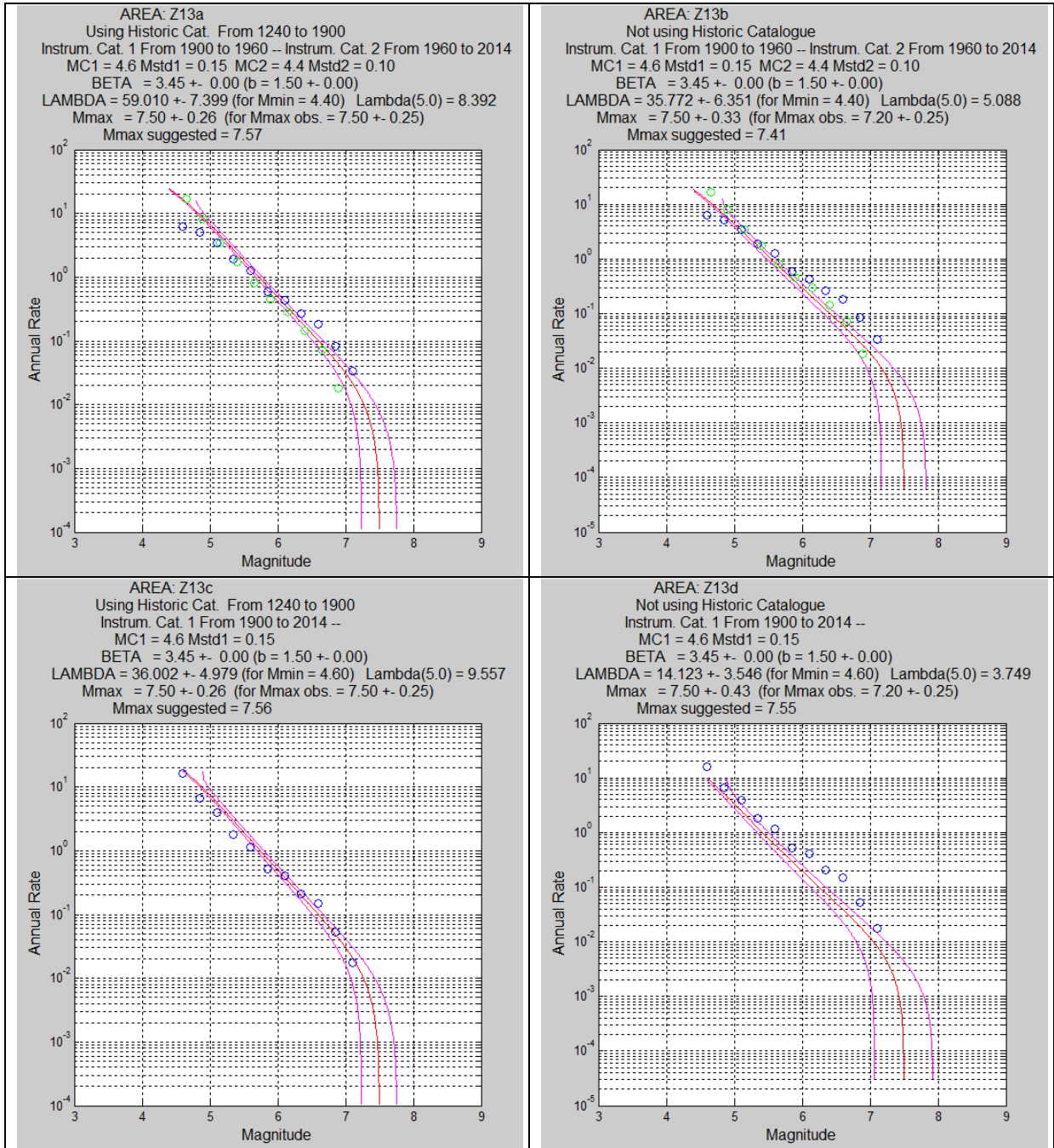


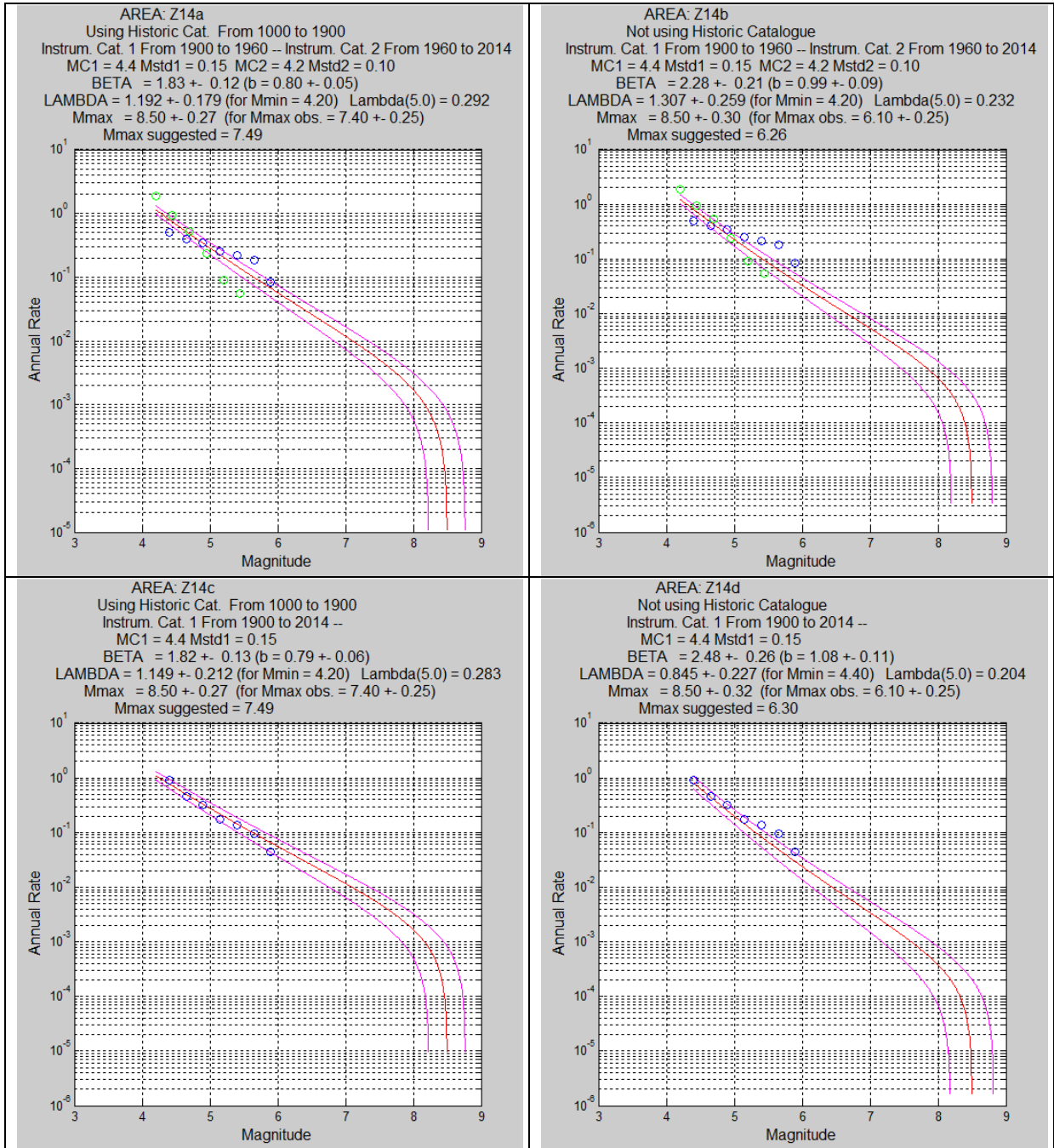


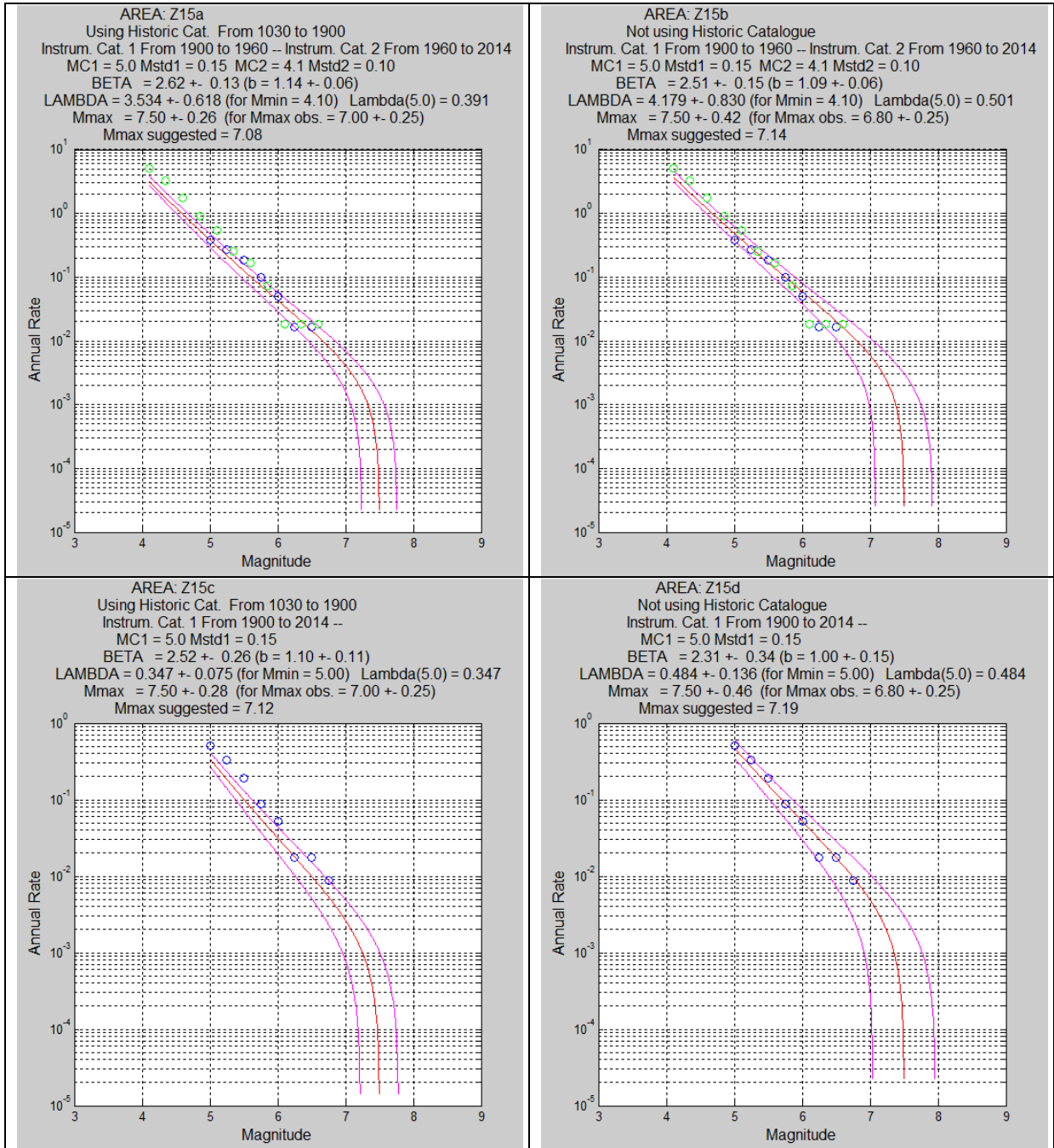


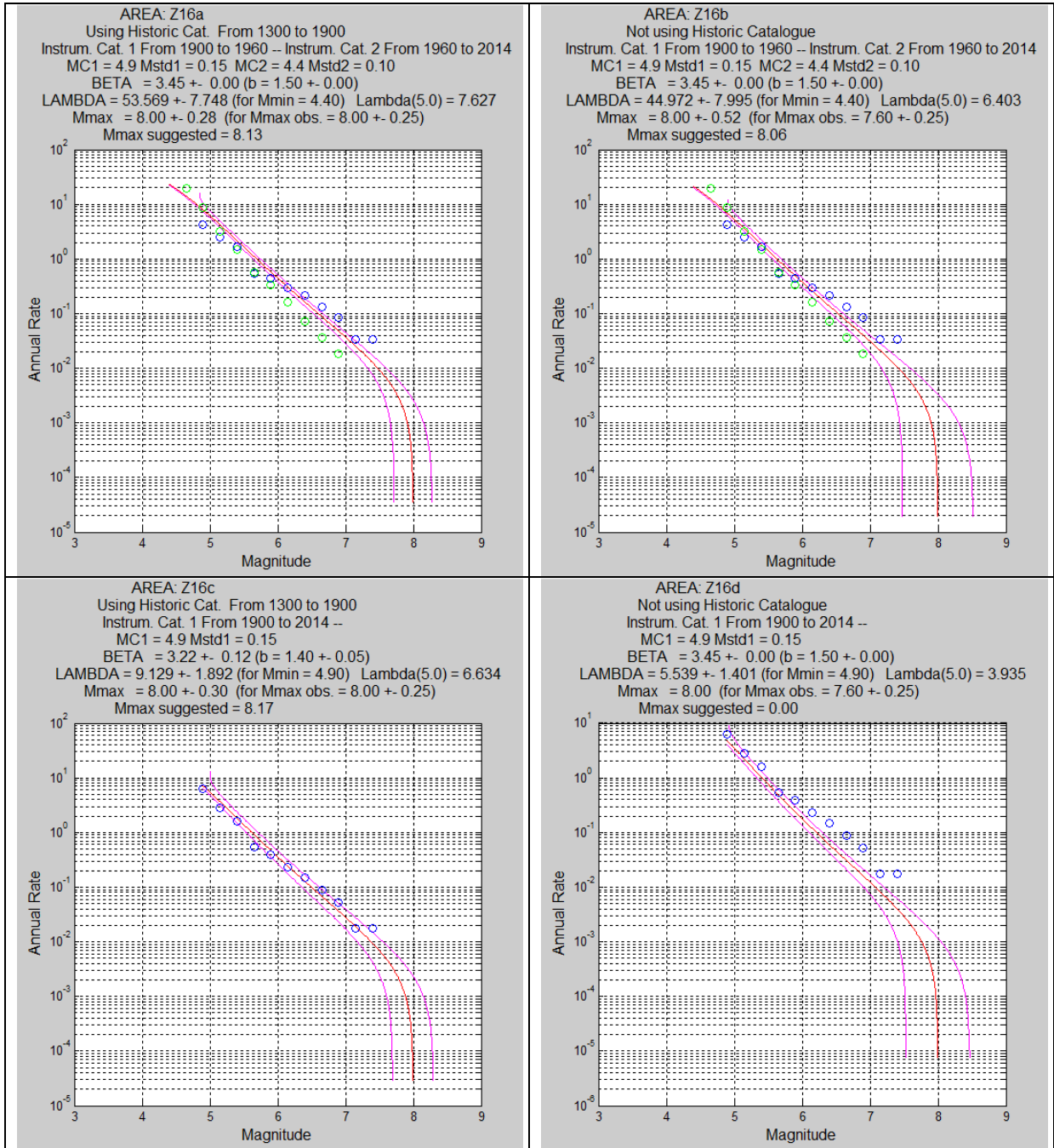


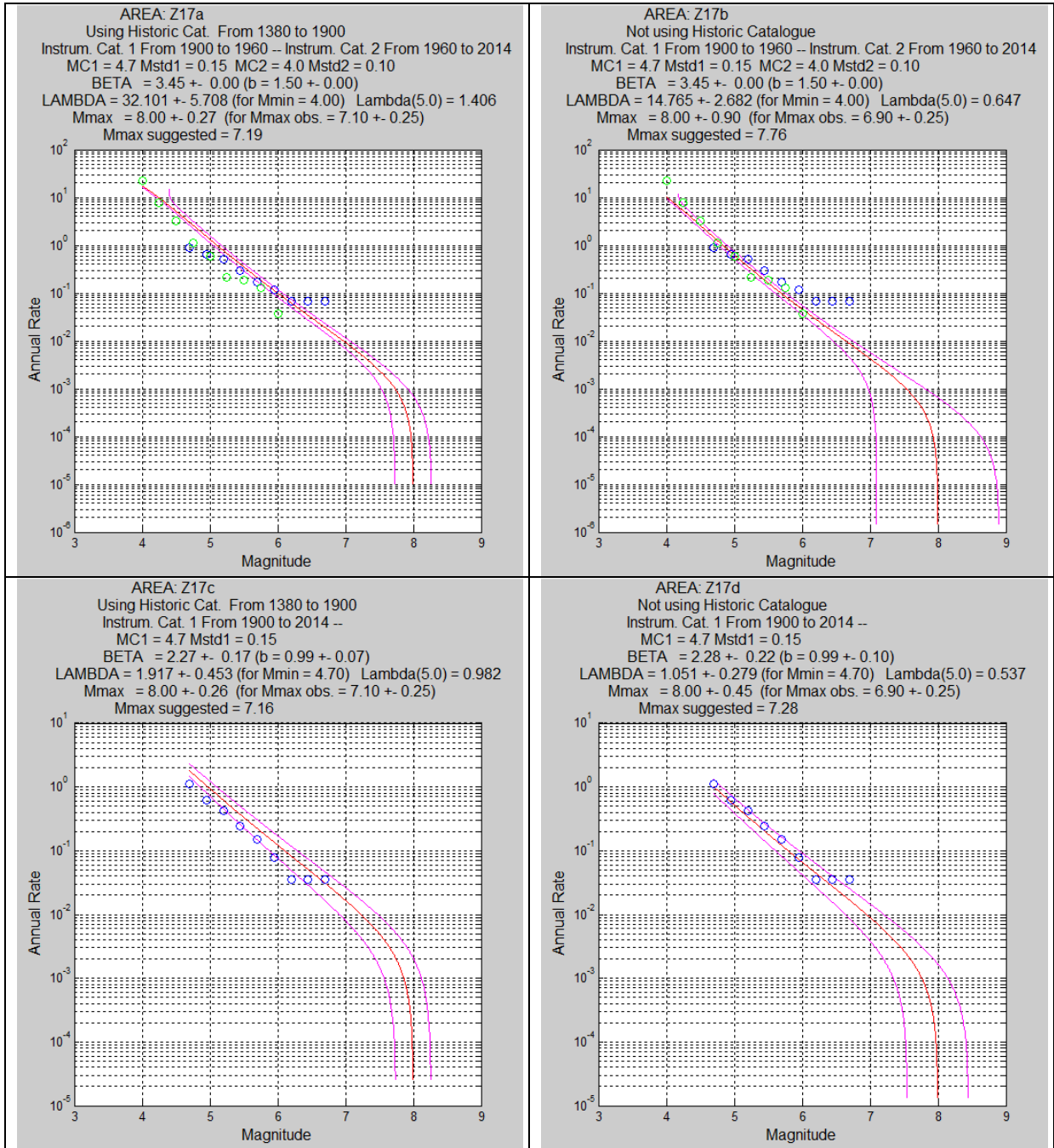


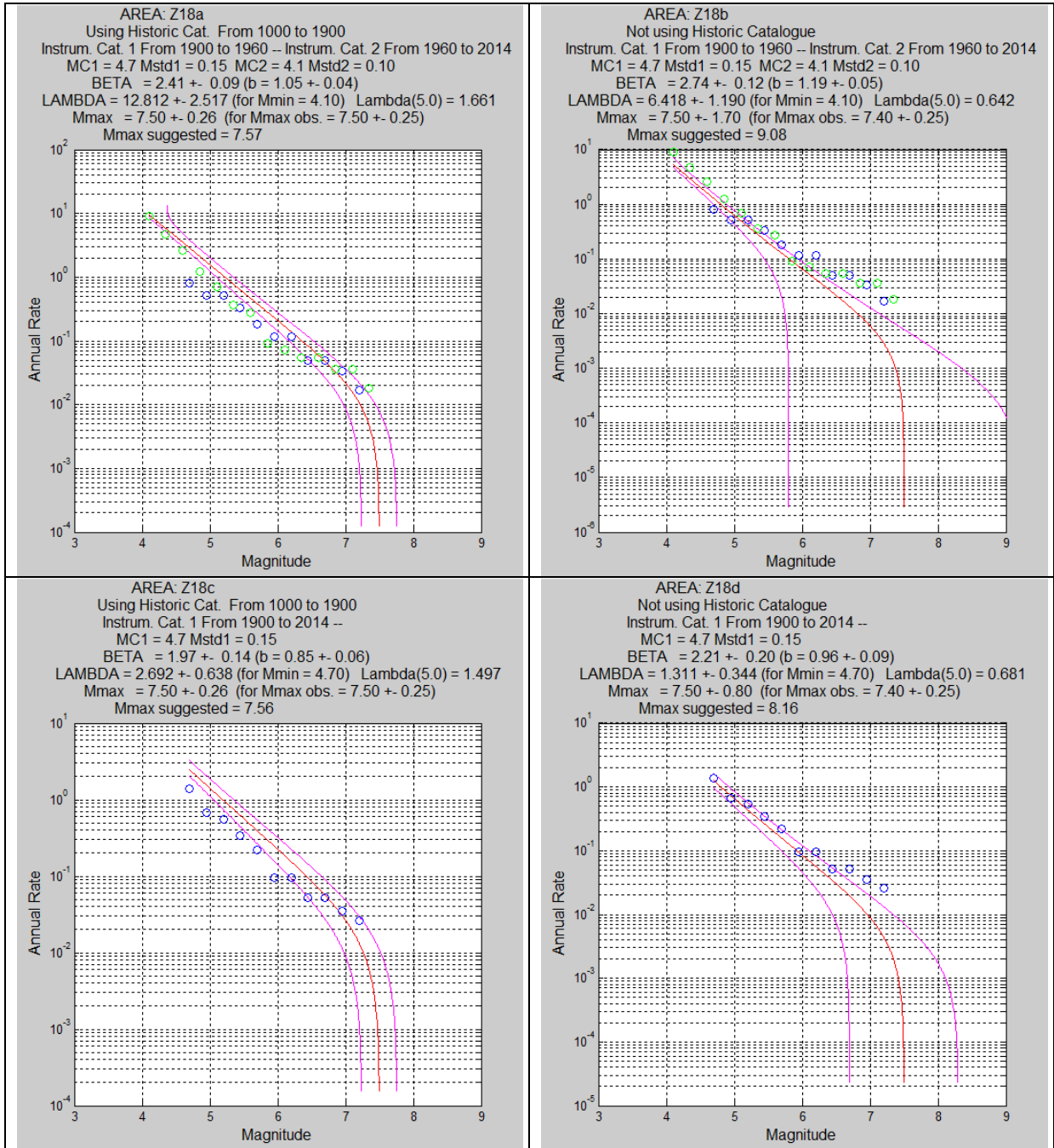


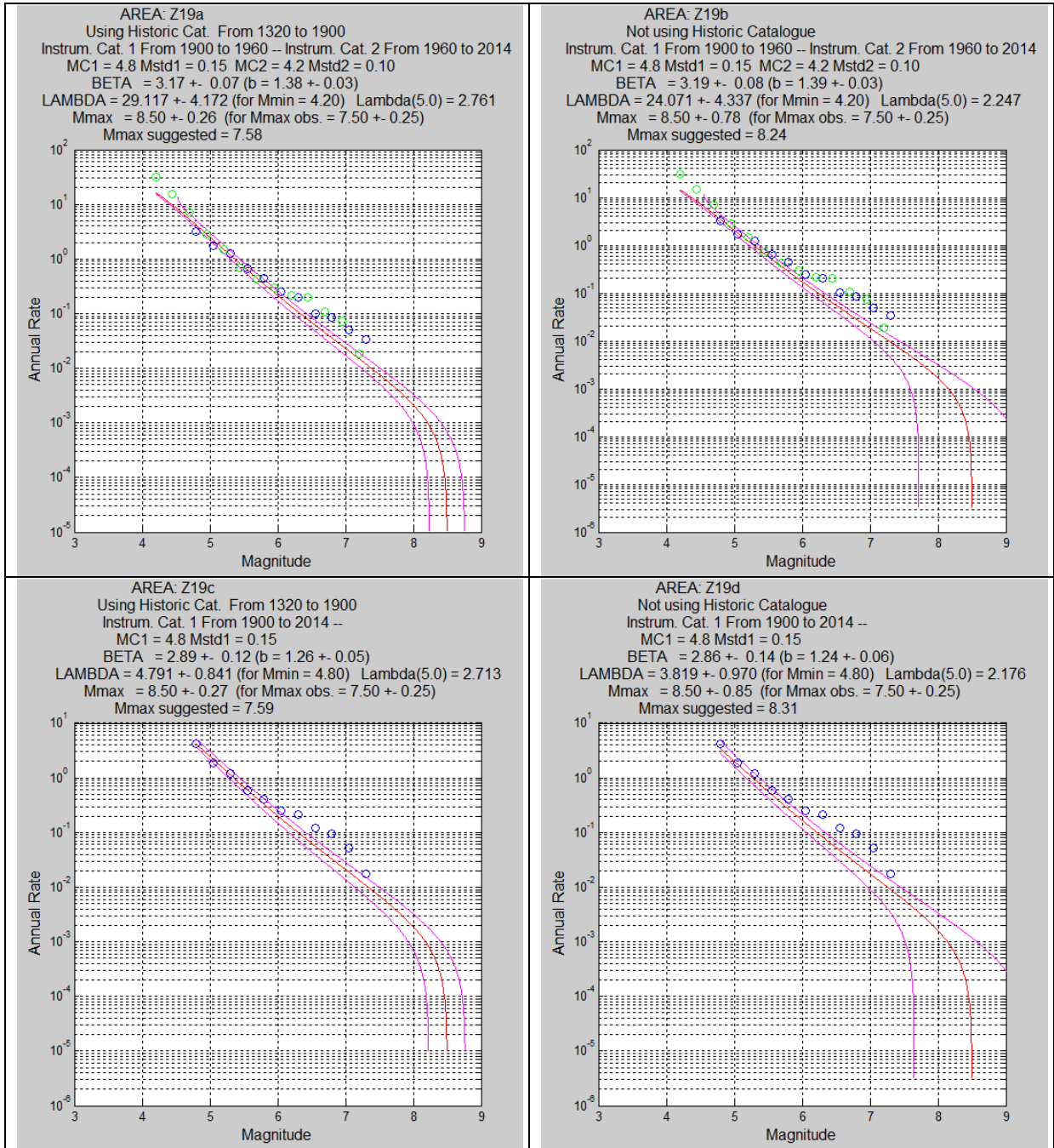


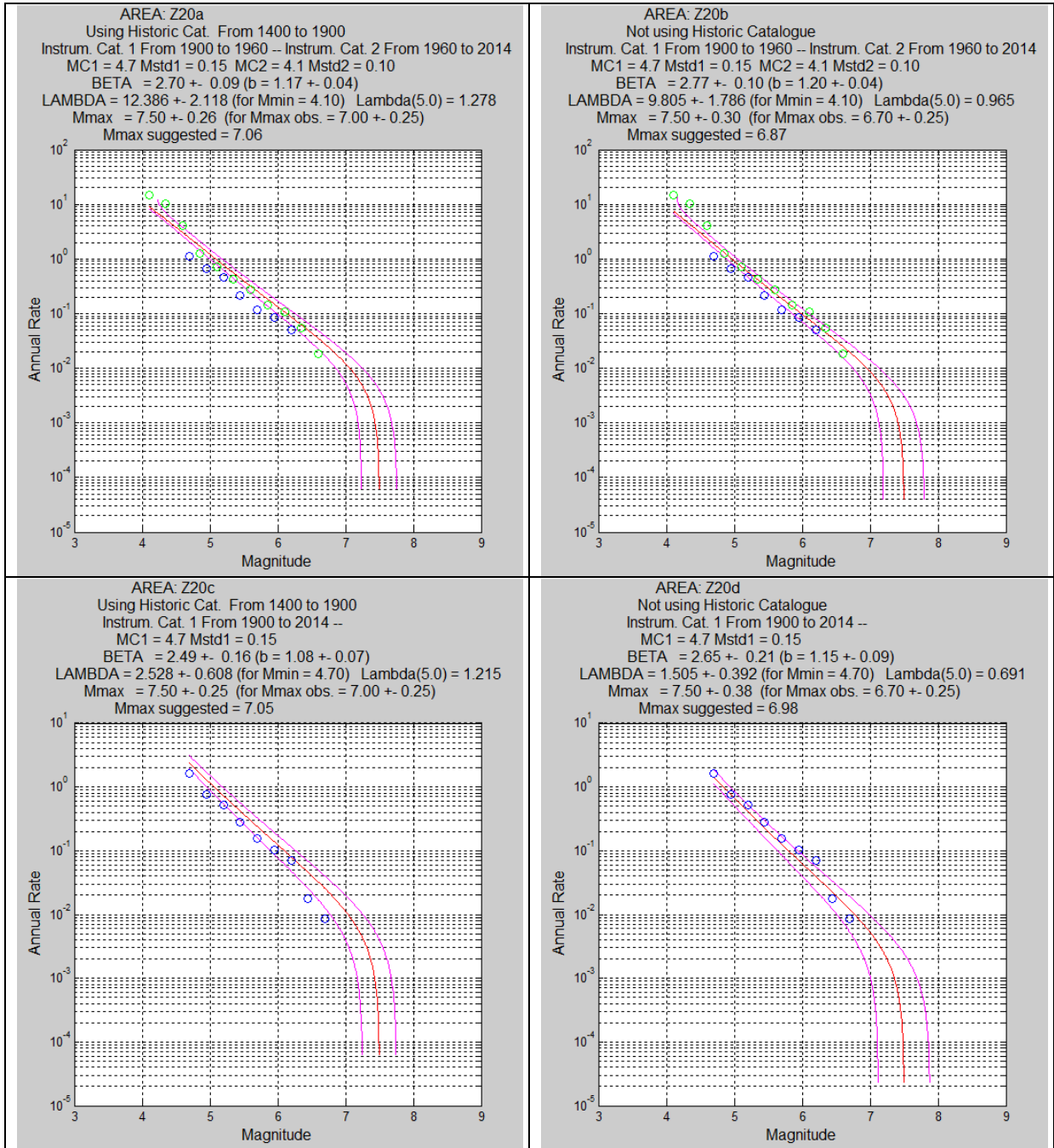


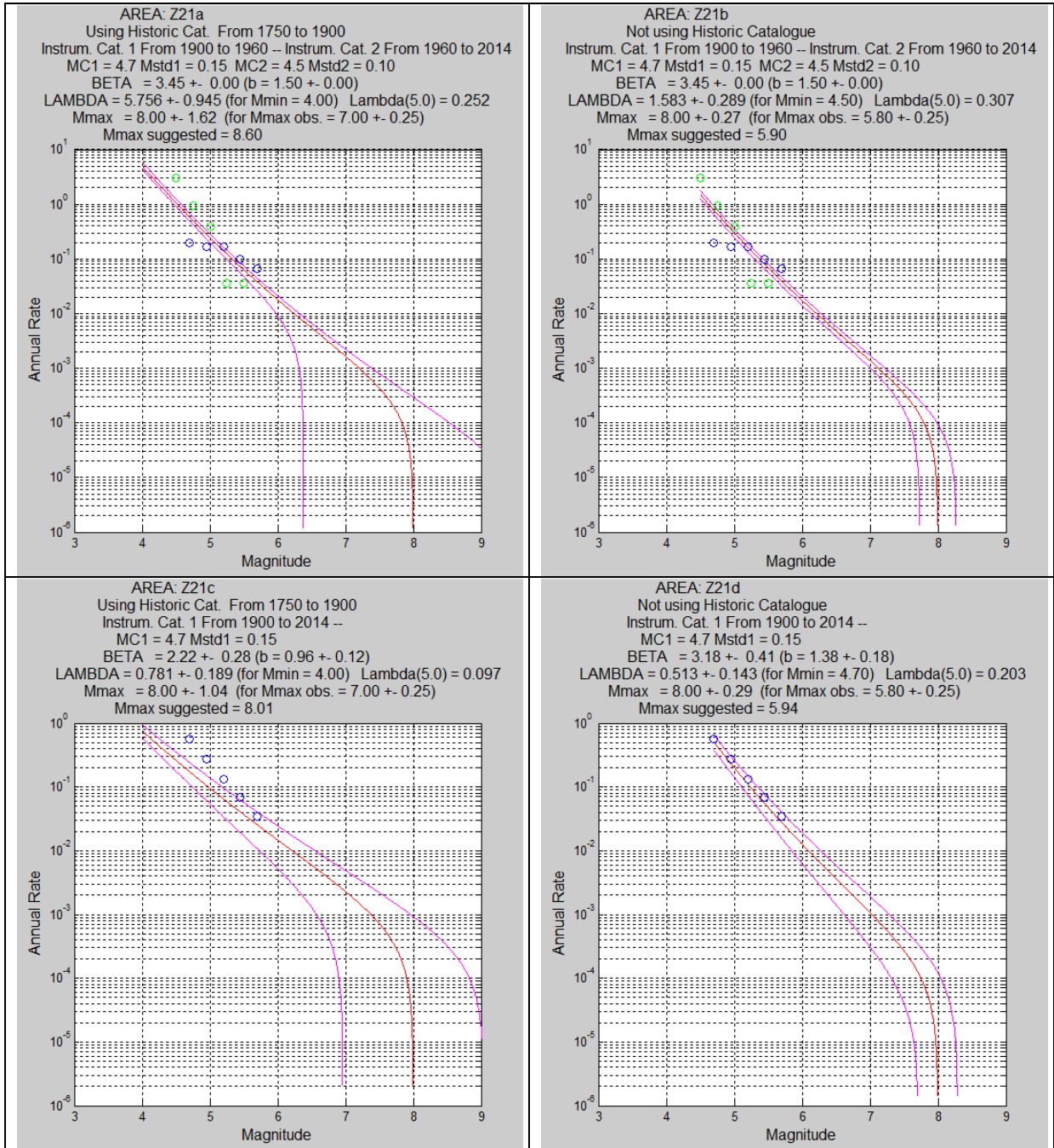


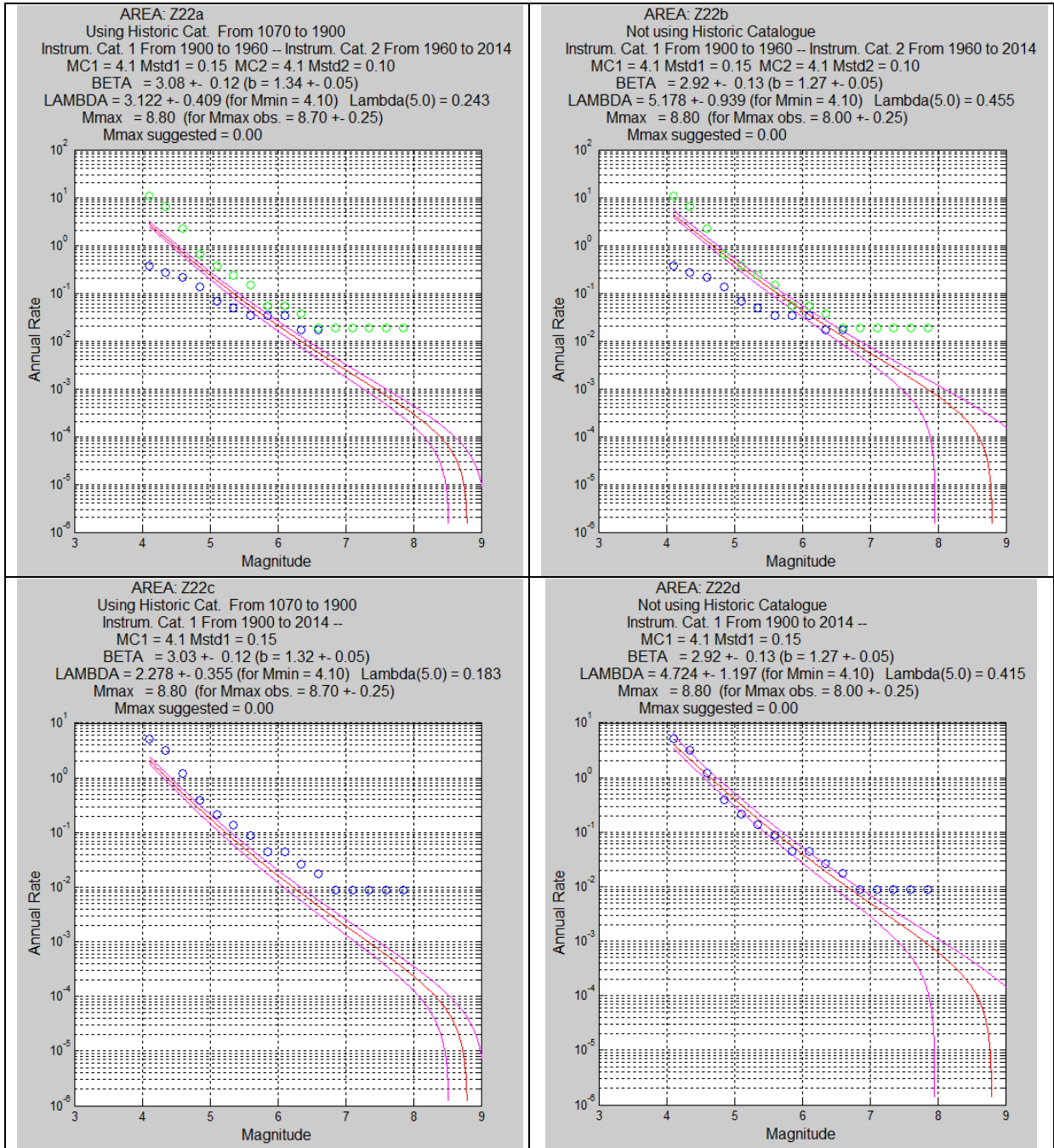


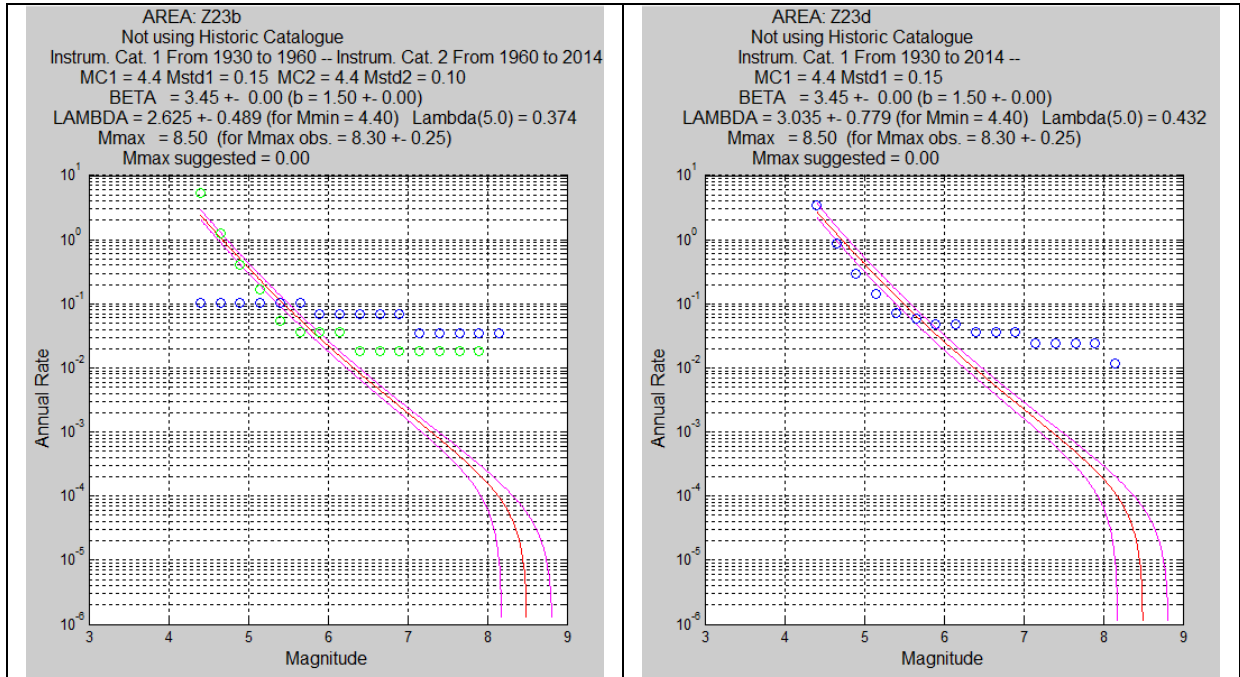












ANNEX 3

TSUNAMI INTENSITY SCALES

Tsunami intensity scale initially devised in 1927 by August Sieberg (1875-1945) and modified in 1962 by Nicholas Ambraseys

- 1. Very light.** Wave so weak as to be perceptible only on tide-gauge records.
- 2. Light.** Wave noticed by those living along the shore and familiar with the sea. On very flat shores generally noticed.
- 3. Rather strong.** Generally noticed. Flooding of gently sloping coasts. Light sailing vessels carried away on shore. Slight damage to light structures situated near the coasts. In estuaries reversal of the river flow some distance upstream.
- 4. Strong.** Flooding of the shore to some depth. Light scouring on man-made ground. Embankments and dikes damaged. Light structures near the coasts damaged. Solid structures on the coast injured. Bid sailing vessels and small ships drifted inland or carried out to sea. Coasts littered with floating debris.
- 5. Very strong.** General flooding of the shore to some depth. Quay-walls and solid structures near the sea damaged. Light structures destroyed. Severe scouring of cultivated land and littering of the coast with floating items and sea animals. With the exception of big ships all other type of vessels carried inland or out to sea. Big bores in estuary rivers. Harbor works damaged. People drowned. Wave accompanied by strong roar.
- 6. Disastrous.** Partial or complete destruction of manmade structures for some distance from the shore. Flooding of coasts to great depths. Big ships severely damaged. Trees uprooted or broken. Many casualties.

Tsunami intensity scale proposed by Papadopoulos and Imamura (2001)

I. Not felt.

II. Scarcely felt.

- a. Felt by few people onboard small vessels. Not observed on the coast.
- b. No effect.
- c. No damage.

III. Weak.

- a. Felt by most people onboard small vessels. Observed by a few people on the coast.
- b. No effect.
- c. No damage.

IV. Largely observed.

- a. Felt by all onboard small vessels and by few people onboard large vessels. Observed by most people on the coast.
- b. Few small vessels move slightly onshore.
- c. No damage.

V. Strong. (wave height 1 meter)

- a. Felt by all onboard large vessels and observed by all on the coast. Few people are frightened and run to higher ground.
- b. Many small vessels move strongly onshore, few of them crash into each other or overturn. Traces of sand layer are left behind on ground with favorable circumstances. Limited flooding of cultivated land.
- c. Limited flooding of outdoor facilities (such as gardens) of near-shore structures.

VI. Slightly damaging. (2 m)

- a. Many people are frightened and run to higher ground.
- b. Most small vessels move violently onshore, crash strongly into each other, or overturn.
- c. Damage and flooding in a few wooden structures. Most masonry buildings withstand.

VII. Damaging. (4 m)

- a. Many people are frightened and try to run to higher ground.

b. Many small vessels damaged. Few large vessels oscillate violently. Objects of variable size and stability overturn and drift. Sand layer and accumulations of pebbles are left behind. Few aquaculture rafts washed away.

c. Many wooden structures damaged, few are demolished or washed away. Damage of grade 1 and flooding in a few masonry buildings.

VIII. Heavily damaging. (4 m)

a. All people escape to higher ground, a few are washed away.

b. Most of the small vessels are damaged, many are washed away. Few large vessels are moved ashore or crash into each other. Big objects are drifted away. Erosion and littering of the beach. Extensive flooding. Slight damage in tsunami-control forests and stop drifts. Many aquaculture rafts washed away, few partially damaged.

c. Most wooden structures are washed away or demolished. Damage of grade 2 in a few masonry buildings. Most reinforced-concrete buildings sustain damage, in a few damage of grade 1 and flooding is observed.

IX. Destructive. (8 m)

a. Many people are washed away.

b. Most small vessels are destroyed or washed away. Many large vessels are moved violently ashore, few are destroyed. Extensive erosion and littering of the beach. Local ground subsidence. Partial destruction in tsunami-control forests and stop drifts. Most aquaculture rafts washed away, many partially damaged.

c. Damage of grade 3 in many masonry buildings, few reinforced-concrete buildings suffer from damage grade 2.

X. Very destructive. (8 m)

a. General panic. Most people are washed away.

b. Most large vessels are moved violently ashore, many are destroyed or collide with buildings. Small boulders from the sea bottom are moved inland. Cars overturned and drifted. Oil spills, fires start. Extensive ground subsidence.

c. Damage of grade 4 in many masonry buildings, few reinforced-concrete buildings suffer from damage grade 3. Artificial embankments collapse, port breakwaters damaged.

XI. Devastating. (16 m)

b. Lifelines interrupted. Extensive fires. Water backwash drifts cars and other objects into the sea. Big boulders from sea bottom are moved inland.

c. Damage of grade 5 in many masonry buildings. Few reinforced-concrete buildings suffer from damage grade 4, many suffer from damage grade 3.

XII. Completely devastating. (32 m)

c. Practically all masonry buildings demolished. Most reinforced-concrete buildings suffer from at least damage grade 3.